BIOFILM SENSING TOOL DEVELOPMENT FOR ENVIRONMENTAL MONITORING

by

Farhad Jalilian

BEng, Sharif University of Technology, 2015

A Thesis Submitted in Partial Fulfillment

of the Requirements for the Degree of

MASTER OF APPLIED SCIENCE

in the Department of Mechanical Engineering

Supervisory Committee

Supervisor

Dr. Caterina Valeo
(Department of Mechanical Engineering, University of Victoria)

Departmental Member

Dr. Mohsen Akbari
(Department of Mechanical Engineering, University of Victoria)

Abstract

In recent years, the treatment of stormwater and surface runoffs using innovatively created natural sites has gained increasing attention. These sites, that are vegetated multi-layered depressions on the ground, named as bioretention cells or rain gardens, are constructed with natural elements like soil, shrubs, grass, and trees. Such facilities are employed to treat stormwater quantitatively and qualitatively via various physical, chemical and biological pathways. The biological treatment of stormwater is carried out mostly by the dense bacterial communities that are existent around the plants of roots stationed in the rain gardens.

These dense bacterial communities, known as biofilms, play a significant role in the biological removal of contaminants through a process called bioremediation. The efficacy of bioremediation processes in bioretention cells is highly dependent on the successful formation and continued presence of root plant-associated bacterial biofilms, also known as rhizospheric biofilms. The availability of rhizospheric biofilms in bioretention cells, therefore, is an important determinant of the contaminant removal efficacy in bioretention cells. The bioremediation process efficacy can be improved by providing the biofilms with their ideal growth and environmental conditions. Being able to discover such conditions is the principal motivation behind the present thesis, the ultimate objective of it being to develop a sensor that monitors the growth of bacterial biofilm. There is, to date, no tool or sensor on the market that could estimate the amount of biomass available in bioretention cells. Gaining knowledge of the biomass availability can lead to further understanding of the ideal environmental and nutritional conditions for rhizospheric biofilms and their presence in subsurface environments.

Developing such a sensor required taking multiple steps, including the evaluation of the past and present methods of monitoring or studying biofilms, assessing the advantages and disadvantages of each method, and finding the best possible method with respect to the application of interest. When it comes to monitoring biofilms in the field or in situ, specific requirements are considered that narrows the choices down to a few methods. The vast majority of classic and innovative techniques of monitoring biofilms lack the required capabilities, such as non-invasiveness, cost-effectiveness and real-time measurements, to name a few. Impedance microbiology, as a technique that provenly has the capacity for in situ monitoring of microbial

metabolism, was chosen as the main premise behind the sensor prototype. The expected capabilities that were considered for the development of the sensor required the employment of a method that can specifically monitor biofilm in a real-time, non-invasive, non-destructive, rapid, simple-to-use, precise, affordable, repeatable, and automatic fashion. These considerations were taken into account within the instrumentation and the proof of concept phases of the monitoring system design and development.

After crafting the prototype, various phases were conducted including the programming, troubleshooting, as well as the testing and verification of the system using a biofilm-forming strain, Pseudomonas putida. Promising results were obtained as for the detection of the growth of bacterial samples via real and imaginary impedance monitoring. In addition, optical density measurements were taken from the samples in tandem with the impedance sensing experimentation. Optical density spectroscopy measurements, that were calibrated in terms of the number of cells per volume using hemocytometry, allowed for the estimation of the change in the number of cells per unit of volume respective to the alterations in the impedance properties. Therefore, the real-time biomass estimation of the bacterial samples became possible. The bacterial population estimation range was approximately 9.2×10^{6} up to 5×10^{8} cells per ml for Pseudomonas putida, but further testing and trials could improve and expand the estimation range. Overall, the test results demonstrate the capability of the monitoring system in detecting bacterial proliferation real-time of their growth with high sensitivity. The novelty demonstrated in this work includes but not limited to the affordable manufacturing of the monitoring system together with the calibration using high precision direct counting of biomass. With minor modifications, this sensor can further be improved in terms of different operational capabilities to become commercially available for the monitoring of biofilm in the field, not just in bioretention cells, but also in many other applications where bacterial proliferation is important to monitor, such as biofouling of equipment, food industry, medical and healthcare centers, etc.

Table of Contents

Table of Figures

Acknowledgment

First and foremost, I would like to thank my supervisor, Dr. Caterina Valeo, not just because of her priceless mentorship and profound guidance throughout this project, but also because of her trust in me through the tough situations I was in. Without her help and support, I would not have been in this position.

I would also like to thank Dr. Angus Chu, Dr. Mohsen Akbari and Dr. Rustom Bhiladvala for their insightful comments and perceptive remarks.

I would like to express my deepest gratitude to my family, my caring mother, supportive father, inspiring brother, and to the love of my life, Mahsa. I am grateful for them all and especially for my brother, Farhang, whose help and support has always been an invaluable gift for me.

Dedication

This thesis is dedicated to all the brave Iranians who have risked their lives in the fight for peace and freedom over the past 40 years of viciousness. Specifically, in deep condolence and lasting memory of those who lost their lives during the brutal suppression of the nation-wide protests in Iran in November of 2019. May your wishes all come true very soon.

Chapter 1 INTRODUCTION

1.1 Stormwater pollution and mitigation through bioretention cells

Stormwater is the excessive amount of rainfall or melted snow that does not sink into the ground and flows over the landscape surface to eventually find its way to a receiving water body. Impervious surfaces, which are prevalent in urban areas, generate large amounts of stormwater because they are compact surfaces with low permeability (such as roads and parking lots) and do not allow the rainfall to penetrate the subsurface (LeFevre, 2012). Stormwater flow captures and conveys contaminants and pollutants left on the surface between rain events. Increasing urbanization leads to increasing impervious surface area (Khan, December, 2010) and a wide variety of undesired contaminants are captured by stormwater in urban areas. According to Lefevre et al. (LeFevre et al, 2014), pesticides, pathogens, Total Suspended Solids (TSS), heavy metals, dissolved solids, petroleum hydrocarbons, and organic chemicals (Yu, 2015) can be present in urban stormwater runoff. Subsequently, urban storm water runoff has resulted in the degradation of the quality of receiving water bodies, and in turn, adversely affected human and ecological health (LeFevre et al, 2014).

Water quality is a significant component of stormwater management. Stormwater management involves flood prevention and increasing the quality of storm water runoff before it discharges into a receiving water body. Modern stormwater management includes Sustainable Urban Designs (SIDs) and Low Impact Development (LID), which integrates land use planning and engineering design to manage storm water runoff (LeFevre, 2012). Generally speaking, conservation of natural sites and utilizing them to increase water quality are the main goals of LID, which include retention ponds, green roofs (LeFevre et al, 2014) bioswales, permeable pavements, constructed wetlands, and bioretention cells (Yu, 2015).

One form of LID that is used to enhance stormwater quality is bioretention cells. Bioretention cells (also termed biofilters) are biological media filters that are utilized to improve water quality and temporarily store overwhelming stormwater volumes (Winston et al, 2016). Stormwater is directed into a bioretention cell, which is a shallow vegetated depression that has an engineered soil media (LeFevre et al, 2014). Bioretention cells improve water and urban runoff quality via various physical, chemical and biological processes that take place as water passes

through the filtration media (Khan, December, 2010). Figure 1-1 (a) shows a schematic of a typical design for a bioretention cell. Once the stormwater is percolating through the soil media, the toxicity of the runoff is decreased by capturing a various pollutants (Hsieh & Davis, 2005). The mulch layer provides an additional filtration barrier. Mulch and peat moss are often used in bioretention systems because of their high sorption capacity (Garbarini & Lion, 1986). After the percolation of stormwater is finished, the treated water can either trickle into the surrounding geologic environment or can be piped to other locations (Khan, December, 2010).

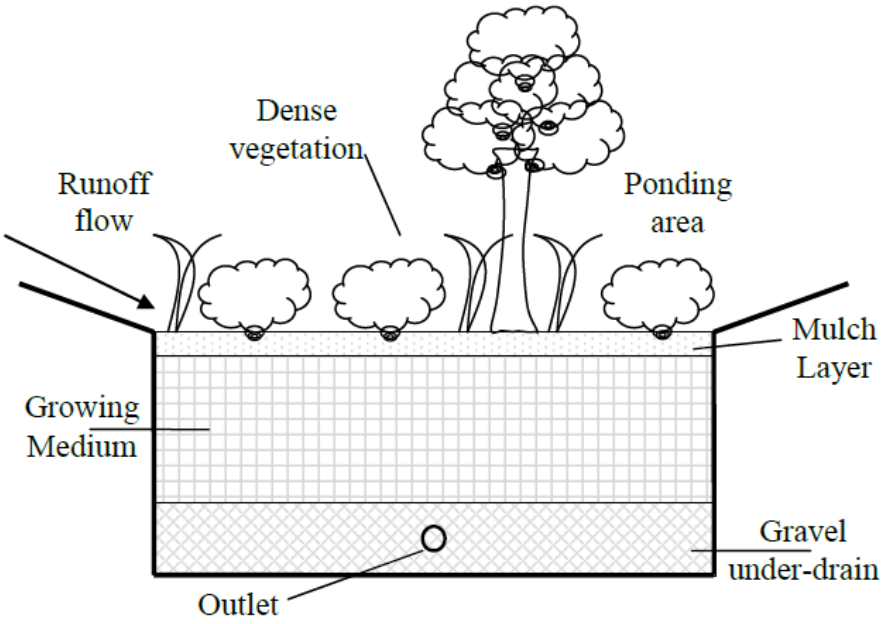

(a)

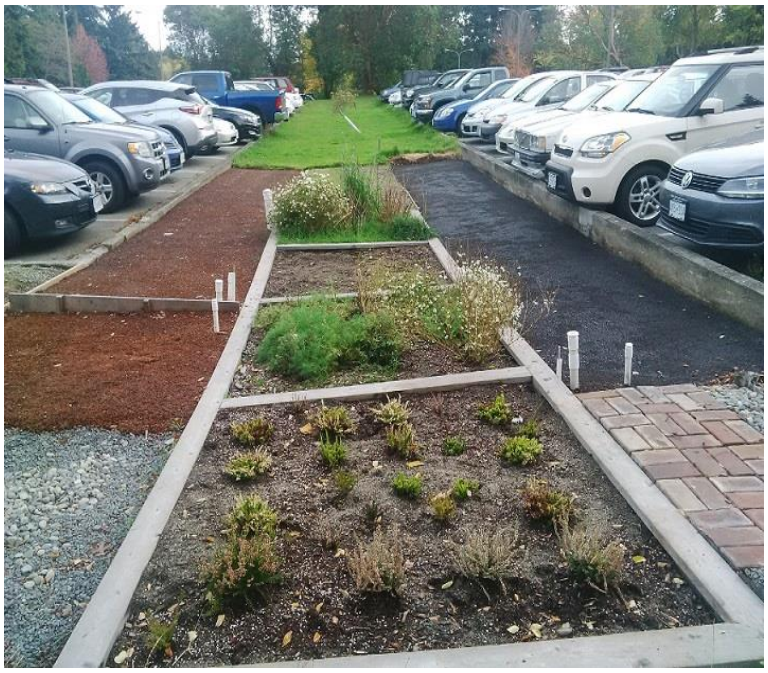

(b)

Figure 1-1. ***(a)*** *Schematic of bioretention cell showing the different elements and layers used in a typical bioretention cell, taken from (Khan, December, 2010).* ***(b)*** *A landscape of a bioretention cell located at the north end of parking lot number 6 of the University of Victoria, Victoria, BC*

In general, bioretention cells can be used for the purpose of a wide range of applications from high infiltration to pretreatment of urban runoff (Mihelcic et al, 2010). The biological processes of water and soil quality improvement and contaminant removal that takes place in bioretention cells is called bioremediation.

1.2 Key players in the bioremediation processes

Bioremediation is one of the waste management methods in which living cells are utilized to remove or neutralize waste materials and pollutants in soil and water. It can also be defined as the engineered utilization of the vegetated depressions on the ground, such as bioretention cells, to extract, remove, sequester, degrade, neutralize the pollutants from water, surface waters, ground waters, and soil (Ziarati & Alaedini, 2014). The process of bioremediation directly using specific types of plants in vegetated facilities is called phytoremediation. Phytoremediation is one form of bioremediation and is effective in contaminant removal processes. Scientists have identified more than 400 plant species potent of direct soil and water bioremediation (Lone et al, 2008). However, not just the plants themselves, but also the microbial communities that exist in the vicinity of the

roots of the plants – known as rhizospheric bacteria or rhizobacteria – have shown even a higher efficiency in removing pollutants. This is because the molecules and ion metabolites produced in the process are used by microbes as the nutrients required for their metabolic activities (Seneviratne et al, 2017) . This bioremediation process using the plant root-associated bacteria is called an *indirect bioremediation*, that is executed by the microbial processes in the rhizosphere. It is thought that when bacterial cells form a community, they become much more effective in bioremediation (Kalam et al, 2017). Among various species of microorganisms, certain types are capable of forming aggregates of bacterial cells, called biofilms. The key initiation mechanism for the formation of biofilms on surfaces like plant roots is chemotaxis, that allows single planktonic bacterial cells to form functional glue-like biofilms (Morgan et al, 2006).

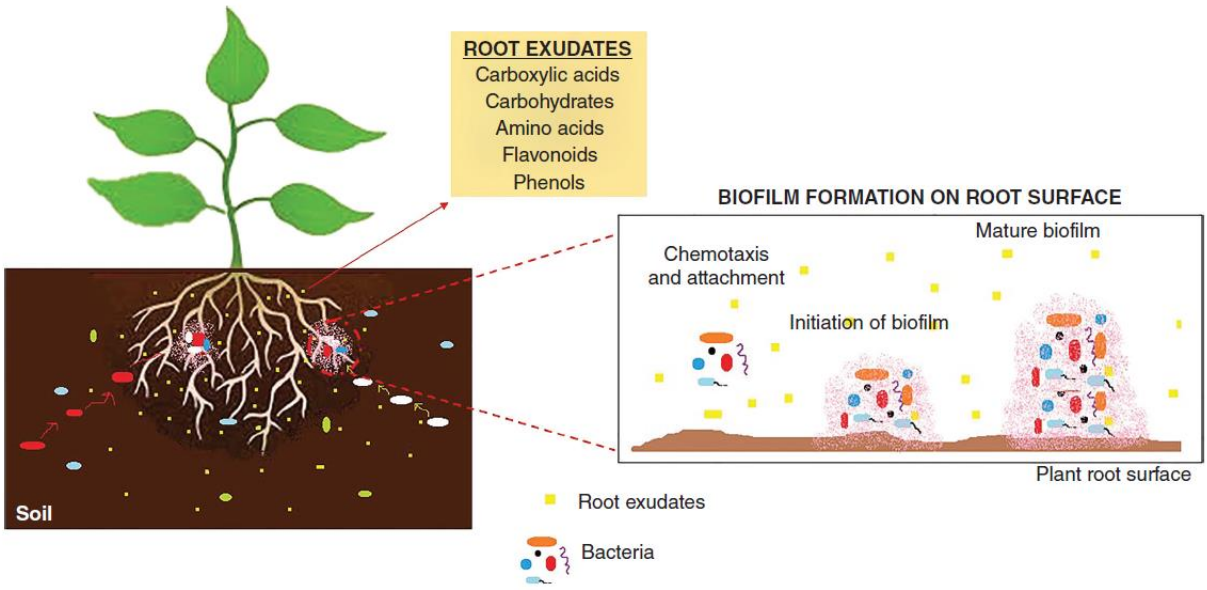

Figure 2-1. *A symbolic depiction of bacterial aggregation and attachment to the exudates and surfaces of the root plants via chemotaxis, taken from (Kalam et al, 2017).*

The formation of biofilms makes them resistant to environmental stress conditions (Ahmad et al, 2017; Kalam et al, 2017). Biofilms assist with the bioremediation not just by solubilizing and degrading contaminants, but also by improving the health and growth of their host plants (Kalam et al, 2017). Bacterial biofilms and their formation will be thoroughly discussed in section 1.2, but it is important to know that the proper employment of such biofilm-forming microorganisms in the field, that are responsible for a considerable portion of the water quality improvements, will further enhance the efficacy of contaminant removal. Plant growth-promoting rhizobacteria can

reduce the detrimental impact of toxic metals on the growth and health of the host plants in high heavy metal contaminated sites (Belimov et al, 2004). They can also decontaminate the soil from xenobiotic compounds, that are recalcitrant and carcinogenic even when present at low concentrations (Singh et al, 2006). Capable of removing heavy metals and xenobiotic compounds from the contaminated environments, biofilm-forming bacteria have shown promising bioremediation capabilities in a safe, cost-effective, and efficient way (Kalam et al, 2017). This displays the importance of studying the microorganisms and obtain information of the ideal environmental, physicochemical, and biological environments for their growth and proliferation, and therefore effective degradation of contaminants.

1.3 Biofilm formation and lifecycle

In the broader context of wastewater and stormwater runoff treatment technologies, formation and growth of biofilm are useful and effective means of treatment. For instance, in fluidized-bed, air-lift, and Moving Bed Biofilm Reactors (MMBRs) where maximum surface area of biofilm is desired to be reached, growth and inception of biofilm are of high significance. However, in most industries, such as manufacturing, medical industries, and petroleum, the formation of biofilms is not desired due to the risk of biofouling, corrosion, and infection (Mendoza Gonzalez & Kloc, 2012). In the present work, the focus is the biofilm that forms in water quality improvement facilities. In the next paragraphs, the overall formation process of biofilms is reviewed.

The structure and growth of biofilm, which in fact is crucial for treatment processes, is hugely dependent on plant root interactions. Plant roots release exudates that are nutrient-rich and play a crucial role in providing the biofilm a non-limiting environment for growth (Fujishige et al, 2006). The physical characteristics such as hydrophobicity and hydrophilicity, and roughness of the plant root that biofilm adheres to is of high significance in biofilm life cycle (Yu, 2015). The attention to plant-microorganism interaction in the biofilm that colonizes plant roots, also named as soil biofilm or rhizospheric biofilm, has increased recently. In this respect, scientists have tried to understand biofilm life-cycle using different experimental techniques. However, further work is much needed to obtain more information of the development of microbial biofilms in real field conditions.

De Carvlho and da Fonseca describe biofilm as a group of microorganisms that develop in damp environments (de Carvalho & da Fonseca, 2007). Biofilm can be formed as result of the aggregation of millions or single species of organic/ inorganic compounds that can range from decomposing materials to microorganisms (Decho & Gutierrez, 2017). According to Vlamakis et al. (2013), biofilms are assemblages of mircrooraginsms that are surrounded by an exopolymeric matrix and adhered to a surface (Vlamakis et al, 2013). The attachment of freely available bacterial cells to an inert surface such as plant root is the turning point where the planktonic life of bacteria turns to biofilm mode (Ansari et al, 2017). There are two types of biofilm growth: Planktonic and Sessile aggregates. The first type is biofilm in single cells, while the second type is a community of cells. The sessile aggregate of biofilm allows the community of cells to have greater capabilities in different aspects such as properties, behavior, and survival strategies (Donlan & Costerton, 2002).

Inception of bacterial biofilm can occur through two different mechanisms: The first mechanism takes place when biofilm is produced and the cells are held by strands, called Extracellular Polymeric Matrix (EPM) and form a complex structure with three-dimensional configuration that varies in size and shape (Dunne, 2002). The second mechanism is the growth of bacteria using quorum sensing. Quorum sensing is one of the key issues in bacterial studies and it is when cells communicate with each other by releasing, sensing, and responding to signal molecules that are diffusible (auto-inducer The cells and their neighbors respond to these auto-inducers and therefore, by the help of the concentration of auto-inducer, the bacteria is able to monitor population, change gene expression, etc. (Alfred B. Cunningham, 2008; Dunne, 2002).

The biofilm life cycle can be divided into five different phases. The first step is the initial attachment of organisms to a surface. Being in a close proximity is the first requirement for the adherence of the organism to a surface. Once the organism is close the surface, depending on whether the net forces are repulsive or attractive, adhesion occurs. It has been proved by Donlan et al. (2002) that as the surface roughness increases, the initial attachment increases because roughness enhances the surface area (Donlan, 2002). After the initial attachment, the organisms start quorum sensing and produce a complex EPM structure, which makes resilient bonds with the surface. It can now be said that a functional biofilm has been formed. This step is called irreversible attachment since the microorganisms are no longer able to move away from the surface. Next,

maturation step occurs, in which more mass and material is added to the biofilm as a result of the bulk flow around the surface, and the cells that are attached to the surface start to divide and proliferate. Since nutrients are required for biofilm to grow, and as well, waste removal is ongoing, bacterial growth potential is prone to be limited depending on biofilm structure and hydrodynamics. Therefore, limitation of nutrients leads to a detachment or dispersal phase, in which cells and masses of biofilm leave the colony to search for a better place for growth (Alfred B. Cunningham, 2008). Figure 1-2 illustrates different steps of biofilm life cycle.

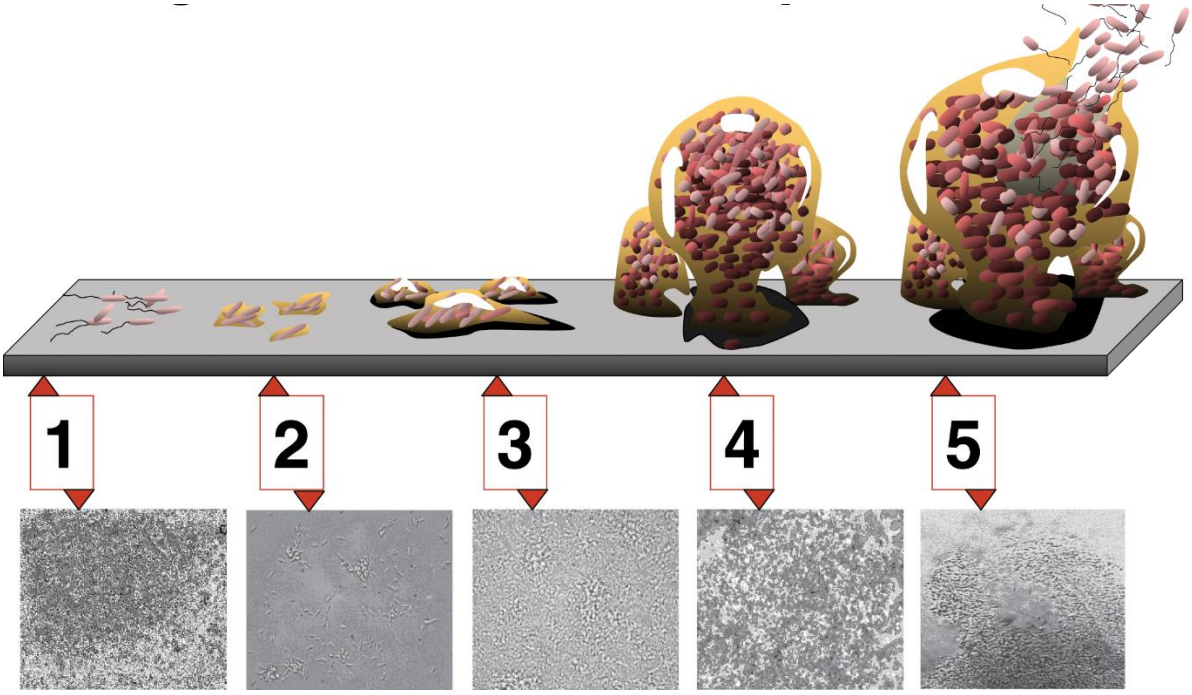

Figure 1-2*. Bacterial formation in biofilm life cycle. The life cycle consists of five phases: 1. Initial attachment 2. Irreversible attachment 3. Maturation I 4. Maturation II 5. Dispersal. The corresponding microscopic images of biofilms at different stages are also shown in black and white format. Taken from (Monroe, 2007)*

Figure 1-3 depicts the growth curve of biofilm. The first stage is the lag phase that is the time required for the initial attachment. The second phase is the acceleration phase, where EPM structures are formed as a result of quorum sensing. The third step is the exponential growth curve where maturation occurs. After growth phase, biofilm steps into stationary phase, in which the growth rate of bacterial cells is equal to the death rate of the cells. This stage is steady state in terms of the population of bacteria. Finally, the death phase occurs, where cells and masses detach and leave the colony (O'Toole & Ghannoum, 2004).

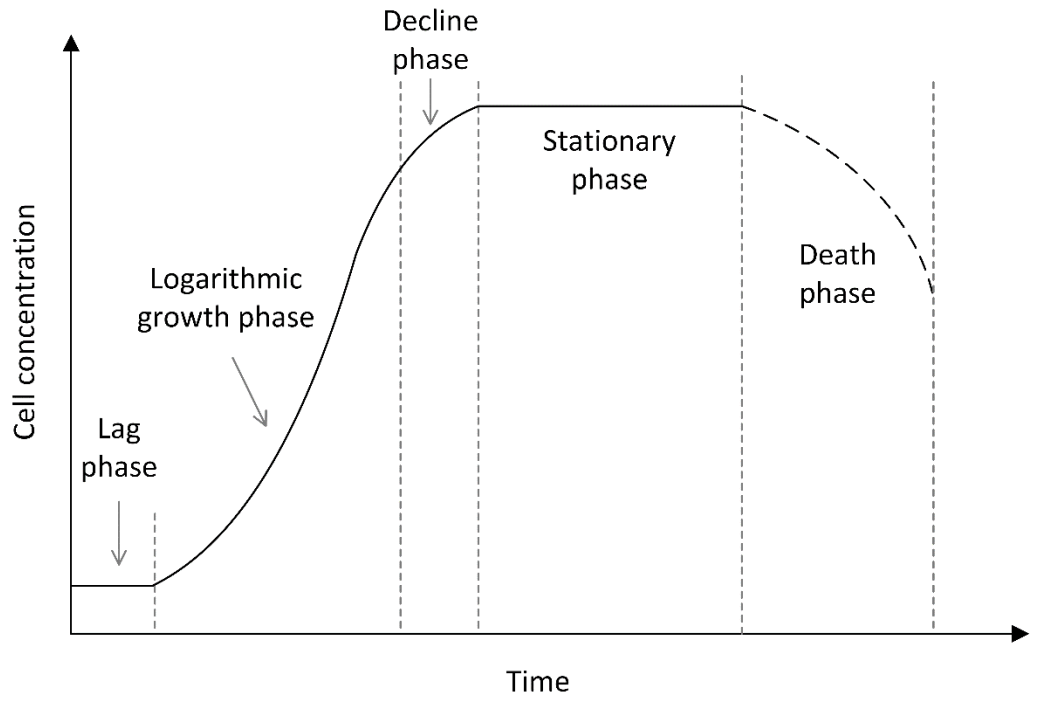

Figure 1-3. *A typical growth curve of biofilm consisting of five phases of the life cycle, starting with the lag phase, following by the logarithmic growth phase, decline and stationary phases, and eventually the death and dispersal phase.*

Further study is still required to understand and track the adhered bacteria to the surface of plant roots. For example, by using electron microscopic techniques, pictures of biofilm and their configuration can be obtained. Another advanced technology is confocal scanning laser microscopy, which allows live visualization of hydrated biofilm (Yu, 2015). However, further work and research are required to obtain more useful information about the interaction between biofilm and plant-root, and their development in order to increase the effectiveness of bioremediators, that is the ultimate objective of research like this. Despite the generation of many research data, there is a crucial lack of systematic data collection tools of subsurface biofilms. Many researchers have identified ways of studying such microbial communities, but more work is still required for the actual field implementation and data garnering.

1.4 Thesis Layout and Objectives

The general objectives of this study are to:

1. Provide a critical review on the possible monitoring methods of biofilm formation and availability together with the advantages and disadvantages of each method.
2. Provide literature evidence of the different monitoring methods that could potentially be employed for use in the field, and provide justification of choosing the best option for the case of bioremediation efficiency.
3. Implementing a tool or sensor based on the method of choice and testing of the method to see if literature evidence could be replicated.
4. Provide hands-on recommendations for future work based on the results obtained

The present thesis consists of 5 chapters and 6 appendices. The layout of the thesis is as followed:

- Chapter 2 provides an in-depth literature review of the different available methods of biofilm measurement and monitoring. A descriptive analysis of each method is provided.
- Chapter 3 includes the specific research objectives in more details and the problems that are going to be addressed within the scope of this thesis are summarized.
- Chapter 4 includes the journal paper that is drafted for submission. This paper thoroughly reviews the techniques used in the research work followed by the results obtained from the experiments. As well, the results of the tests replicated for further confidence are discussed.
- Chapter 5 discusses the conclusions and outcomes of the research work. It also suggests a set of recommendations compatible with the future work that could be conducted reach the ultimate objectives.
- Appendices: Appendix A consists of supplementary data that are resulted from preliminary testing of the monitoring sensor for further evidence of its capability. Also, the results of microscopic evaluations and plant root microscopy images are included in this section. Appendices B, C, D, and E provide elaboration on the step-by-step procedures developed for some of the laboratory scale work. In Appendix F, computer codes developed for the integration of the monitoring system are presented.

Chapter 2 LITERATURE REVIEW

2.1 Motivation for monitoring biofilms

Biofilm's significant role in wastewater biological treatment and water quality improvement is one of the cases where the formation of bacterial biofilm is regarded beneficial. However, there are many different fields and circumstances where the formation of biofilm is not desirable and once formed, the removal of the biofilm structure needs to be performed. Biocorrosion of pipes is one the most problematic issues in many industries and is caused by the formation of biofilms. According to Flemming et al. (Flemming et al, 1994), it was estimated that biofilm is responsible for 30% of the annual operating cost at a membrane water treatment plant In Orange County California. Food industry and healthcare services are among other areas where biofilm establishment in the systems is required to be prevented, preferably at an early stage. According to (Del Pozo & Patel, 2007), bacterial existence on the surface of the implanted biomaterials is the main cause of pathogenic infections. Difficult to eradicate, these biofilm formations are often immune and resistant to antimicrobial treatments. Therefore, being able to detect bacterial biofilm formation or to measure biomass availability is of great significance. Due to this reason, there is an extremely high amount of interest in developing tools or systems that are capable of serving such purposes. In the present chapter, a few of the most popular and successful discovered methods in monitoring of biofilms will be reviewed. The advantages and shortcomings of each method will be discussed. And lastly, the method of choice for the development of a sensor for the purpose of this research work will be introduced and reviewed in more details.

2.2 Classical and microscopic methods for measuring biofilms

Conventional methods of studying biofilms involve the enumeration and morphological observation of the microorganisms using microscopic techniques such as light, epifluorescence microscopy as well as Confocal Laser Scanning Microscopy (CLSM) and Scanning Electron Microscopy (SEM) (Schaule et al, 2000). Light microscopy and epifluorescence techniques are suitable for the biofilms with a thickness of less than 3-4 µm, because the multi-layered biofilm structures scatter the light emitted at the sample and disrupt the direct observation. 4',6-diamidino-2-phenylindole (DAPI) is one of the few staining dyes that has been used widely by researchers for biofilm studies. DAPI binds to the to double-stranded regions in DNA of the cells and makes

the visualization of dead and live adherent cells possible. (Hannig et al, 2007) reported great success in visualizing enamel biofilms using when using DAPI-staining combined with Fluorescence in situ hybridization (FISH) method. FISH, that utilizes rRNA-targeted probes for visualization, is the most common method of identifying the different microbes in a community of biofilm. The main reason why FISH is of high popularity among biofilm researchers is that it allows for the differentiation of the cells (Grohmann & Vaishampayan, 2017). FISH method's capability can be largely enhanced when combined with Confocal Laser Scanning Microscopy. CLSM, that is a subcategory of Laser Scanning Microscopy (LSM), allows for three-dimensional imaging of microbial structures. The main breakthrough that CLSM has brought to the field is that the biofilm samples can be imaged without fixation and while contained in their fully hydrated state, in situ (Neu et al, 2010). Point illumination and the elimination of out-of-focus light allows CLSM to trump the shortcomings of the conventional light microscopy, that is suitable for in-plane bacterial monitoring (Pamp et al, 2009). Despite tremendous success of CLSM-FISH in whole-cell monitoring of biofilms, accurate enumeration of bacterial population stays challenge, that requires the implementation of other techniques in tandem with CLSM-FISH (Pamp et al, 2009). Other technical limitations of CLSM include the need of fluorescence staining of the biofilm molecules and the inability in rendering biofilms with thickness of more than 150 μm. Novel technologies and sophisticated approaches have empowered CLSM to overcome the shortcomings.

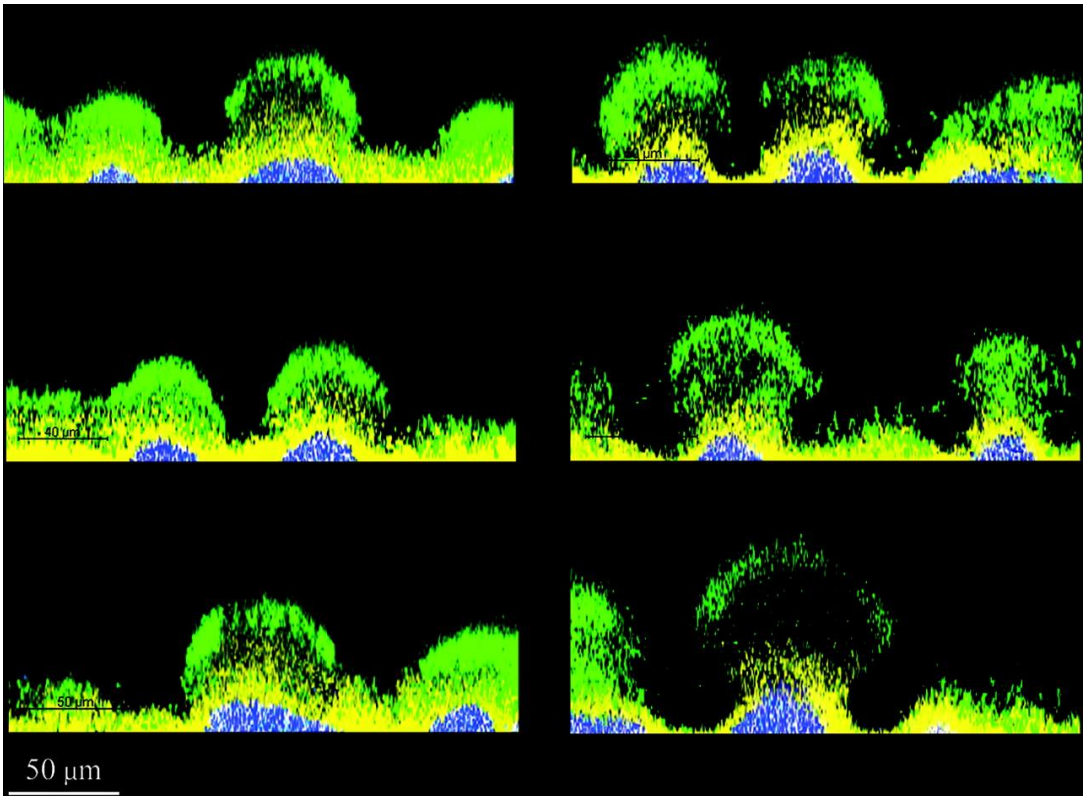

Figure 2-1. *Confocal laser scanning micrographs of biofilms formed of three different strains of Pseudomonas aeruginosa. The images in each column are taken from the same sample but from three different locations. The column on the left hand-side includes pictures at day 3 of inoculation and pictures on the right are taken on day 4, representing biofilm changes. Taken from (Pamp & Tolker-Nielsen, 2007)*

Transmission electron microscopy (TEM) and scanning electron microscopy (SEM) are the two subcategories of electron microscopy (EM), both of which have been used by researchers recently for three-dimensional analysis of biofilm structures. Electron microscopy functions based on the emission of a focused beam of electrons on the surface of the specimens and producing images of them based on the interactions of the electrons with the atoms of the specimens. the Rajeb et al. (Rajeb et al, 2009) employed SEM to illustrate the formation and expansion of microbial biofilm in near proximity of the sand grains packed in a lab-scale wastewater treatment percolation cylinder. Baum et al (2009) conducted a study on *Pseudomonas fluorescens* isolated from natural soil environment to find an estimation of the biofilm's chemical composition using light microscopy together with CLSM, TEM, and SEM altogether (Baum et al, 2009). These methods have drawbacks, including the need for sample penetration and sample dehydration, which can cause the loss of biofilm matrix. Extensive sample preparation and limited bacteria quantification are the other disadvantages of these techniques. One of the disadvantages of SEM

method is the need of high vacuum for the assessment of biological samples that not only requires the sample to be in the solid phase but could still create artefacts to the structure of the biofilms (Hannig et al, 2010). The high vacuum pressure environment is used between the electron optic column and the sample chamber to prevent the scattering of electrons on its way of travel to the specimen (Ominami, 2018).

Researchers have sometimes tried utilizing innovative strategies to achieve biofilm monitoring despite the inherent imperfections of the method used. Carla de Carvalho et al (de Carvalho & da Fonseca, 2007) , for example, have used a creative method to monitor biofilm *in situ* using an optical microscope. This method is based on the linear relation that the intensity of a pixel of biofilm has in x-y plane and the number of cells in z direction. They tried to investigate the biofilm 3D structure with brightfield transmitted and fluorescence light of an optical microscope. It is not possible to take 2D pictures of biofilm from different distances to create the 3D image. Nevertheless, when bright-filed light transmittance is used, the amount of cells in x-y plane changes with respect to the amount of light that passes through the sample in the z-axis (de Carvalho & da Fonseca, 2007). This principle is also used in determination of biomass concentration in the spectroscopy methods.

Environmental scanning electron microscopy (ESEM) is the modified version of SEM method, that eliminates the occurrence of mass loss and shrinkage owing to sample preparation procedures required for classical SEM (Delatolla et al, 2009). ESEM benefits from reduced sample preparation time compared to SEM which makes it far more capable of in situ of environment. However, factors such as beam radiation may adversely influence the integrity and viability conditions, even though ESEM benefits from reduced or variable pressure chambers instead of the high vacuum pressures used in SEM. (Bergmans et al, 2005). Cabala and Teper (2006) (Cabala & Teper, 2007) recommended ESEM as an efficient method in examining the crystallization of minerals in the rhizosphere environment. With the help of this method, they were able to gain understanding of the regional metalliferous pollution of a Zn-Pb mining area in Southern Poland by studying the metal depositions in the rhizosphere vicinity of the plants from the region. Reportedly, low image resolution due to lack of conductivity in hydrated samples (Luster et al, 2009) and (Azeredo et al, 2017).

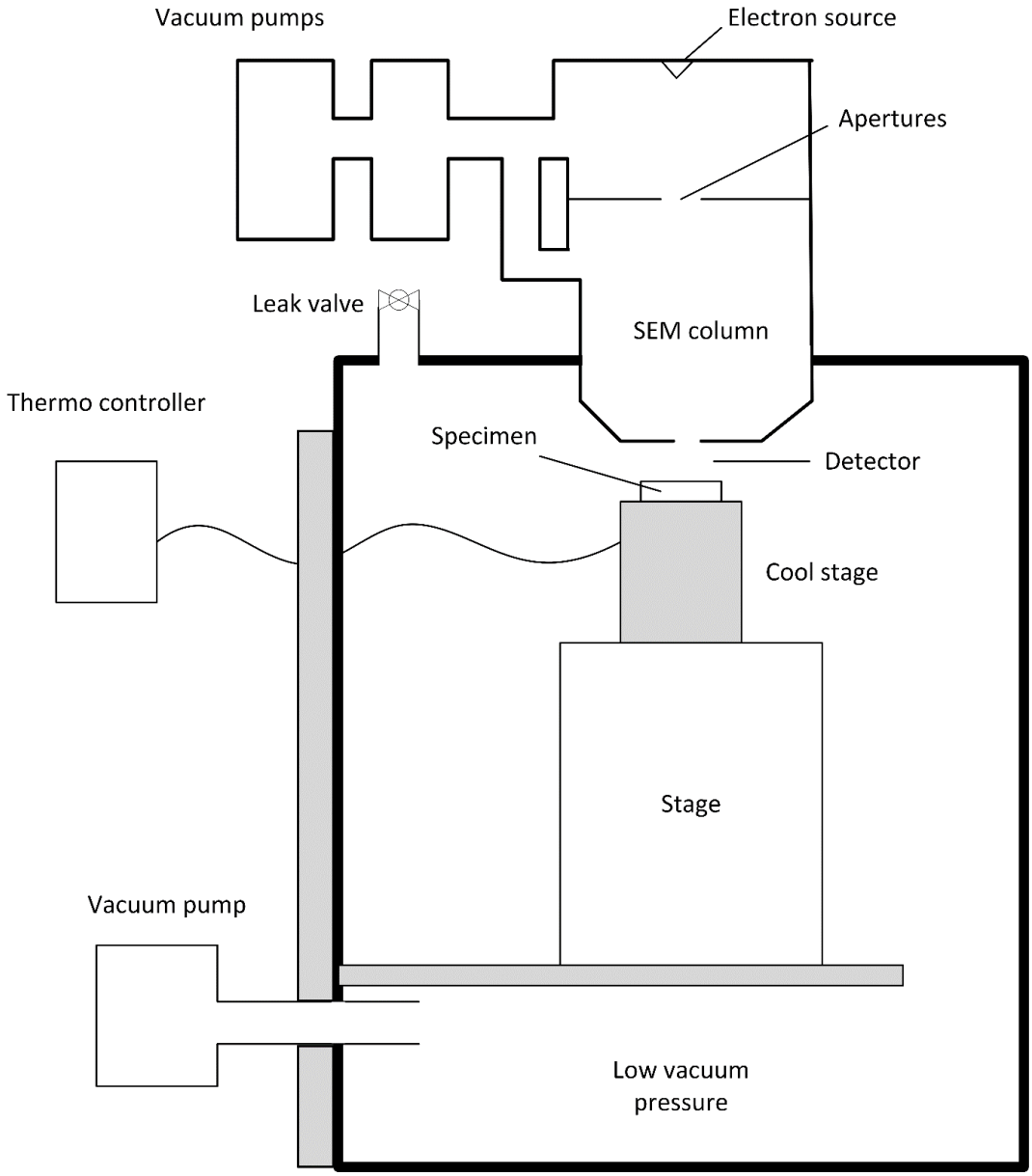

Figure 2-2. *Showing the schematic of a conventional ESEM. Redrawn with minor changes from (Ominami, 2018)*

It may be presented as a conclusion that microscopic methods could be used in combination with each other to fill the gaps and constraints of one another. ESEM, for example, can be used jointly with CLSM-FISH method to provide an estimation of the volume containing the total cell counts (determined by CLSM-FISH) per substratum (Delatolla et al, 2009). However, these techniques, although powerful, genuinely requires large lab spaces and roofed areas. CLSM systems, and microscopic techniques in general, lack being portable and applicable for field use, which is an extremely important matter to environmental monitoring including the rhizosphere

biofilms. As well, the equipment used for three-dimensional microscopy are in the category of highly expensive facilities and always require trained personnel to operate them. As partly touched upon in the previous sections and will be discussed later, the ultimate purpose of this research is to commission tools or systems that can monitor biofilm online, real-time, at low cost, and quantitatively for the engineering of the bioremediation systems. Therefore, the stationary microscopic techniques mentioned above, although powerful and effective, do not seem to have the flexibility to be used in such applications and are best suited for mostly qualitative assessments. It, however, is worth mentioning that they remain as the only means of observation and imaging of bacterial biofilms and should be used for the calibration and verification of alternative methods. In the next section, the alternative methods and system that function based on indirect measurements of bacterial biofilm will be reviewed.

2.3 In situ methods for measurement of biofilms

Traditional methods of studying biofilms are typically labor-intensive and time-consuming. Often, they require lengthy procedures and implementation by trained personnel. These techniques, that have been around for decades and are usually conducted by microscopes (Lawrence et al, 1991), require the removal of the samples form their own host environment. This is usually done by the exposition of testing surfaces called coupons that are removed from the environment of interest after a certain time and evaluated in the laboratory (Flemming et al, 1998). So, not only alterations and damage are possible to the biofilm, but also their results are not online and not representative of the metabolism of bacterial biofilms in their environment. This is the main motivation behind the efforts of scientists in developing methods and systems for the online or in situ monitoring of biofilm. Biofilms can form in a wide diversity of environments. Online monitoring of biofilms can be achieved using different methods depending on the environmental conditions of the host environment, and the chemical, biological, and physical properties of biofilm under investigation. Depending on the physical, chemical, and biological conditions of the environment of interest, methods of studying biofilm differ from one another, in a sense that the monitoring method used in one environment or application may not be as useful when utilized in a different application (Janknecht & Melo, 2003). To summarize the fundamental concept behind the different methods of monitoring biofilm, all the methods function based on a response signal acquired from the biofilm. These signals are a result of energy transfer, light scattering, heat

transfer, acoustic waves, electrical fields or electrical currents, and mechanical signals. The process of monitoring involves transmittance of input signals, modification of the input signals by the biofilm and its host environment, and detection of the output signals by the sensor. In fact, the biofilm leaves its characteristic footprints in the modified signal (output signal) (Janknecht & Melo, 2003). An ideal biofilm monitoring system is a system that can function non-destructive, continuous, online, and without intervention in the microbial community and should have fast, accurate, online feedback acquisition. In this chapter, some of the monitoring methods that have demonstrated promising performances in monitoring bacterial biofilms are going to be discussed.

Using the available discovered methods, researchers have been developing systems to achieve bacterial biofilm monitoring. The premises behind these systems include piezoelectric (Nivens et al, 1993), fiber optic (Zibaii et al, 2010), electrochemical (Dheilly et al, 2008), and thermometric (Reyes-Romero et al, 2014) techniques. This classification is based on the transducing element utilized in each method. These different categories are the basis of the transducing elements in theses so called biosensors. The advancement of technology and research have led to the evolution of these methods to different subcategories. In the scope of this thesis work, we review the advantages and disadvantages of each method and the cases of their field application, if any.

2.3.1 Piezoelectric

Microbial monitoring using piezoelectric systems works based on the effect of bacterial mass formation on the surface of the electrodes. It involves transmitting alternating current at the sample through metal electrodes formed on glass (quartz crystal) substrates to induce the oscillation of the electrodes. The formation of a mass of biofilm on the surface of the electrode increases the oscillating mass, and therefore decrease in the measured output frequency that can be monitored as a measure of biofilm formation compared to when no biofilm is available on the electrode surface. Quartz crystal microbalance (QCM) is one of the piezoelectric devices using the adhesion force of microbial biofilms (Azeredo et al, 2017). Several researchers such as Nivens et al. (Nivens et al, 1993) have developed QCM piezoelectric devices capable of monitoring biofilms. These devices provide real time and non-destructive biomass monitoring means. The main downside with this technique, however, include the necessity of biofilm adhesion onto the surface of the electrodes for the purpose of monitoring. This is a limitation of use especially when bacterial

in aqueous media, where existing unattached bacteria in the sample is of interest. This could also apply to biofilms that are loosely and non-rigid attached (Azeredo et al, 2017). The formation of biofilms occurs in a three-dimensional space where the extracellular matrix is form as a result of binding and aggregation, whereas the quartz crystal microbalance devices may not be capable of measuring the cells and matrices formed on top of the bound layer. Therefore, lacking depth resolution can be regarded as one of the important drawbacks of piezoelectric systems. It is also reported that the detection of biofilm is feasible when the biofilm is thin and does not have high bacterial concentrations. (Nivens et al, 1993) reported a detection limit of 3×10^5 cells.cm^{-2}, in that the bacteria under their test was *Pseudomonas cepacian.* In addition, as reported by Nivens et al. (1993), environment pressure and temperature in which the crystal was in affected the oscillation frequency. This indicates the need of attempts in using QCM in temperature and pressure-controlled environments or using techniques to compensate for such effects. This limitation can further be influential when monitoring of biofilms in the field is of interest. Other types of piezoelectric sensors are developed to detect different kinds of vibrations, but there is no evidence of their employment in the realm of biofilm monitoring (Janknecht & Melo, 2003).

2.3.2 Fiber Optic

Optical-based sensors are the other category of systems used to monitor biofilms, in that the differential of the turbidity, light scattering, light absorption, reflectance, refractive index, fluorescence, bioluminescence, and surface resonance, are the corresponding interaction between the biofilm and the radiated light (Fischer et al, 2016) and (Rodriguez-Mozaz et al, 2006).

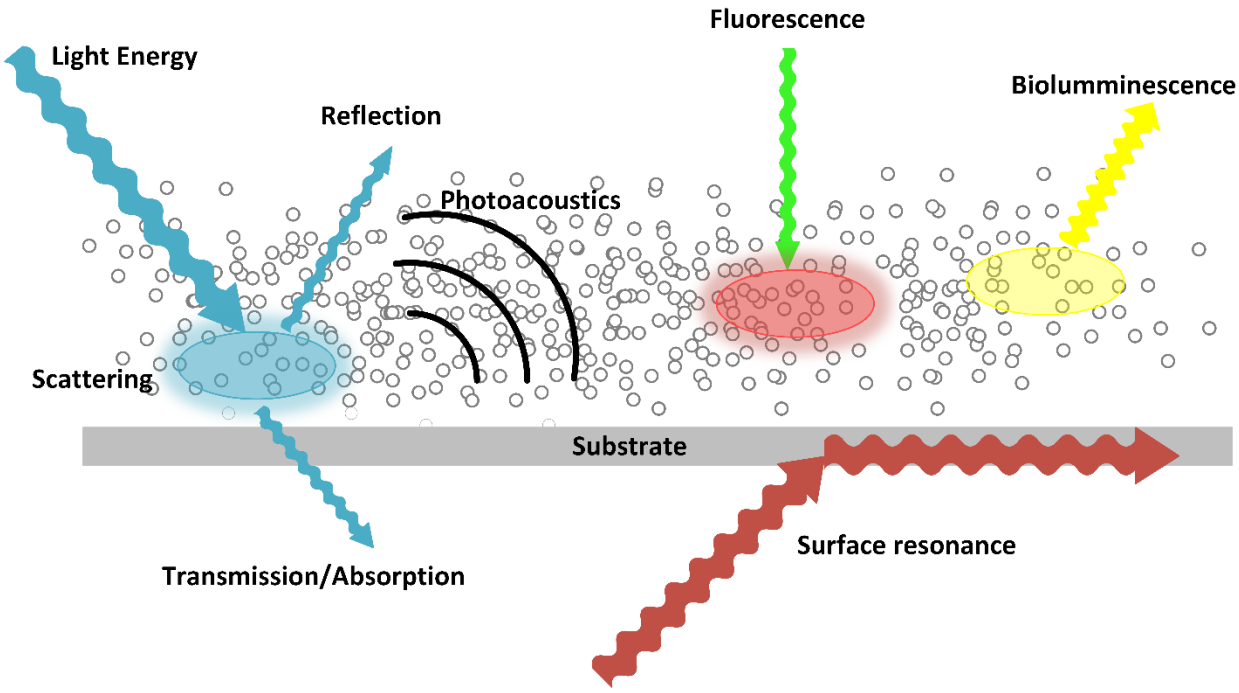

***Figure 2-3**. Various pathways of utilizing fiber optics in sensing biological samples. Redrawn with minor changes from (Fischer et al, 2016)*

Turbidity and surface sensitivity induced by the biofilms are the two of the measurands that are most commonly measured by optical sensors to for biofilm monitoring. Surface-sensitive sensors are developed to improve the signal-to-noise ratio or biofilm sensing efficiency and monolayers of biofilm by the means of evanescent field sensors (Fischer et al, 2016). About two decades ago, researchers proposed an optical fiber sensor (FOS) that was capable of monitoring the deposition of substances on the tip of the fiber (Flemming et al, 1998). But, the need of biofouling prevention sensors, motivated them to craft an FOS with a focus on monitoring biological existence in the groundwater piping system fed into a brewery. The sensor, which had a quartz polymer optical fiber head of 0.2 mm in diameter, successfully tracked biofilm growth after reaching 10^5 cells/cm^2 up to 10^{10} cells/cm^2.

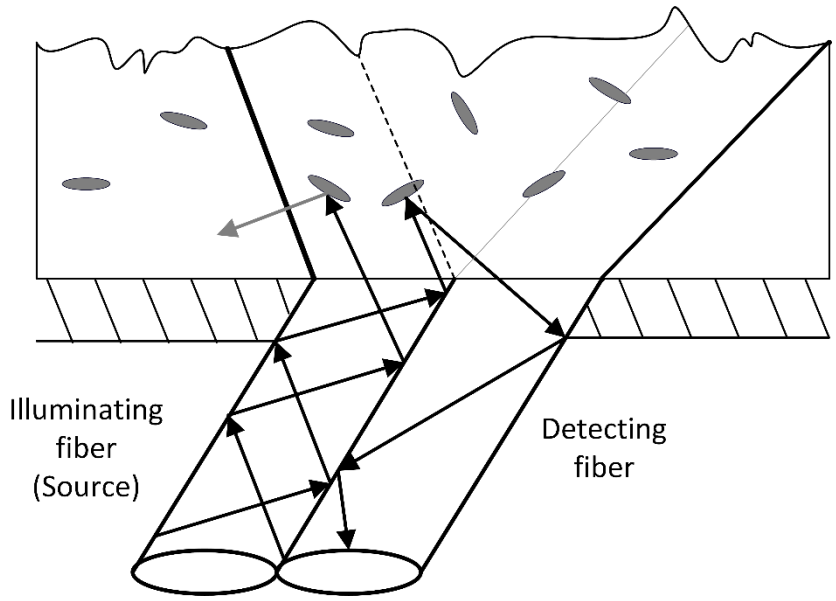

***Figure 2-4**. Scheme of FOS used by Tamachkairow and Flemming in the water pipe system at a brewery in Germany. Redrawn with minor changes from (Tamachkiarow & Flemming, 2003)*

Fischer et al. (2012) designed an optical fiber sensor that is suited for use in natural aquatic environments. The device works based on the intrinsic fluorescence properties of the biofilm protein. The working basis of this device is to first back-illuminate the biofilm that forms on a transparent substrate using a UV-LED, and then collect fluorescence by employing numerous optical fiber sensor. The intrinsic fluorescence of the amino acid tryptophan is excited at a specific wavelength and is detected at a different wavelength by using a numerically optimized sensor head that has a UV-LED light source and optical fiber bundles that collects fluorescence light. This system was proposed to be used in the Baltic Sea to monitor biofilm over a period of twenty-one days. Modeling and simulation of the system was done prior to the experimentations in order to have the optimized design (Fischer et al, 2012). The researchers reported a detection limit of 4×10^3 cells/cm^2. The main benefits of using this system is the low power consumption and low cost. Another advantage of this system is the fact that the LED is able to stop and start illumination in few milliseconds, which empowers the system to emit reproducible light intensities.

Ming et al (2013) designed an experimental setup of a fiber optic biochemical gas senor that is capable of "sniffing" the formaldehyde (FA) released in the process of formaldehyde detoxification using foliage plants (Ming et al, 2013). Using UV-LED illumination ($\lambda = 340$ nm) of nicotinamide adenine dinucleotide (NADH), that is a product of FA dehydrogenase reaction, they reported successful monitoring of FA concentrations of as low as 2.5 ppb up to 100 ppb (Ming

et al, 2013). This work may not directly be of interest for the measurement of plant-associated biofilms. However, it is valuable to know fiber optic sensors may be used as a reliable method when measuring the degassing of biofilms is the purpose of the future studies.

There is, to date, no report of the successful usage of fiber optic sensor in the subsurface and soil environments. As well, the geologic environments are genuinely opaque media that contain abiotic and grain-like substances that could potentially disrupt the process of illumination and detection in such sensors. Other downside related to the utilization of optical fiber is that they are not suitable for the monitoring of thicker biofilms (Janknecht & Melo, 2003).

2.3.3 Thermometric biofilm sensing

In the field of biosensing, thermometric transducers measure the amount of heat induce by biological existence with a thermistor that is sensitive to heat (Ertürk & Mattiasson, 2017). Same as piezoelectric sensing of biofilm, the premise behind the thermometric method is the creation of intensification or reduction on the output signal caused by the attachment of bacterial biofilm on the controlled surface. The deposition of bacterial biofilm on the surface causes an additional resistance against the flux of heat between known temperatures of the both sides of the surface (Janknecht & Melo, 2003). Figure 2-5 shows the scheme of a conventional thermometric biofilm monitoring system, in which cold and hot water flow through vessels channels that have thermocouples both immersed in them and embedded in the walls of the channels. The differential flux of heat induced by the adhesion of biofilm on the surface of the channels' walls is measured and interpreted as the thickness of the adherent biofilm.

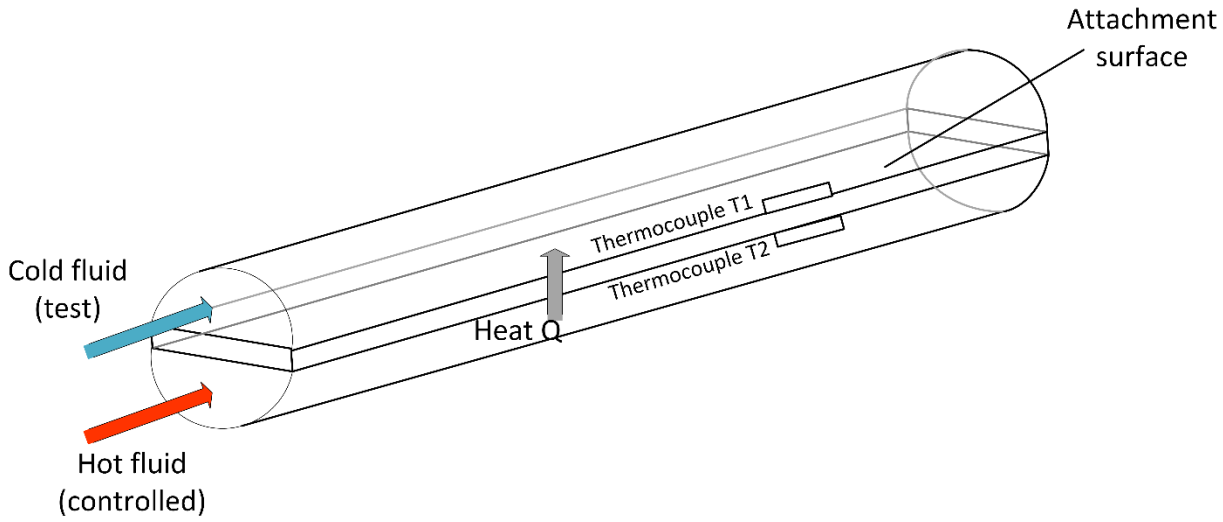

Figure 2-5. *Heat transfer monitoring device of biofilm adhesion. Redrawn with minor changes from (Janknecht & Melo, 2003)*

Reyes-Romero et al (2014) designed a novel thermometric sensor that utilizes AC signals in creating oscillating heat through the heater that is in contact with the surface, upon which the biofilm grows. A temperature probe is also placed in contact with the surface to measure the dynamic thermal fluctuations of the growth medium as a measure of biofilm formation (Reyes-Romero et al, 2014). Even though they have obtained varying signals as a result of bacteria proliferation and their effort in simulating the thermophysical properties of biofilm, there is lack of quantitative assessment or verification of the capability of the system. As well, no specific measure of the effectiveness of the device in terms of biofilm thickness or bacterial population is reported.

In general, a disadvantage of thermometric sensors, when the field use is of interest, is the additional instrumentation required solely for the purpose of keeping the environmental temperatures not necessarily constant, but less dynamic than natural changes to allow for the biofilm formation heat effectuation reaching a sensible signal-to-noise-ratio. According to Janknecht and Melo (2003), this technique does not have enough sensitivity to monitor the initial attachment of bacteria and probably cannot detect the adhesion first layer(s) of biofilm.

2.3.4 Electrochemical sensing of biofilm

Metabolism of bacteria occurs through a series of biochemical reactions such as converting large molecules into smaller ones and releasing the energy as well as utilizing organic and inorganic compounds for their maintenance and growth (Jr., 1996). According to Brosel-Oliu et al

(2015), the conversion process of large substrates into smaller charged and ionic metabolites leads to a change in the ionic composition of the cells that can be measured via electrochemical methods as a measure of bacterial metabolism or growth (Brosel-Oliu et al, 2015). This is the reason why electrochemical biosensing has become the focus of many biofilm-related sensing research and development recently. Rapid responses, relatively easy-to-interpret data collection, and high sensitivity are just a few of the reported strengths of this method in comparison with other methods. There are multiple fashions of obtaining electrical signals from a specimen of biofilm. Electrochemical biosensing, like other online methods, works based on the idea of tracking the alterations of the output signal with respect to a controlled input. Amperometric, potentiometric, conductometric, impedimetric biosensing are the different classes of electrochemical sensing of biological existence.

Amperometric biosensors function based on the electron current generated by the oxidation-reduction reaction of species in contact with the surface of the working electrodes while keeping the reference electrode at a fixed potential (Lei et al, 2006). Aperometry is widely used in environmental monitoring, especially for the determination of biochemical oxygen demand (BOD) of water samples. However, the downside is the need for the available oxidizing and reducing agents in the circuit, which are usually not present when dealing with biofilms. Conductometry is a fast and relatively simple method that is used not only in the field biosensing but also in many industrial applications. It is based on the electrical conductivity of the analyte solution that is basically the inversed value of its electrical resistance. Despite the rapid and easiness of use, conductometry is not a selective method for biofilms, in a sense that the changes in the analyte in terms of organic and/or inorganic content that can cause alterations in the electrical conductivity might also be interpreted as biofilm emergence or removal.

Potentiometric methods that are based on the measurement of the potential difference between a working electrode and reference electrode separated by a membrane, suffer from the weakness as of amperometric systems when it comes to measuring biofilms. In addition, potentiometry requires a very stable and accurate reference electrode that is genuinely a challenge to maintain (Su et al, 2011). Therefore, these three methods do not seem to be applicable for use in biofilm monitoring, especially in subsurface environments where the space is limited and the

use of potentiometric electrodes are near to impossible, as the miniaturization of such electrodes are cumbersome.

Impedimetric biosensing, on the other hand, has gained an overwhelming amount of interest in the fields related to studying biological species in general and bacterial biofilm, specifically. In fact, the applicability of this method has led to the advent of the field of impedance microbiology (IM). Impedance microbiology is the field of implementing impedance spectroscopy on microbiological species. As is deduced from the name, this method involves measuring the impedimetric features of bacterial samples as a measure of their growth and availability in the system. Electrical impedance is the resistance of the circuit against the flow of current when certain voltage is applied. Impedance, however, is a more general term than resistance that we know of resistors. Impedance consists of not only the resistance of a resistor in the circuit, but also the resistance from any capacitance and inductance features available in the system, if there are any. This stems from the fact that in certain conditions, other than resistors, capacitors and inductors can display resistance against the flow of current. Therefore, resistance, capacitance, and inductance could create impedance that includes as many as at least one and up to all these three features at the same time. If the voltage applied is through a direct current (DC), an inductor of the system behaves like a normal wire and does not display any inductive resistance, and a capacitor in the system acts like an open circuit such that the resistance of it is infinite. But when the voltage applied to the circuit is through an alternating current (AC), any resistor, capacitor, and inductor available in the system display some measurable impedance.

2.3.4.1 Impedance biosensing

Living cells are composed of a closed, insulating membrane that is filled with liquid plasma and shows dielectric properties (Janknecht & Melo, 2003). Such structure allows them to behave like electrical capacitors, that are built to store electrical charge when an electric current is applied to them (Xu et al, 2016). When cells are exposed to an electric field, the ions available in plasma tend to move towards the cell membrane creating a movement of ions which also induces a change in the electric filed. These changes can be measured by controlled signals transduced from signal source through the electrodes in contact with the biofilm. As well, extracellular electron transport (EET) that is a well-known process of microorganisms in transporting electrons between the intracellular metabolic processes and the extracellular electron donors or acceptors, generates

alterations in the electron transport and therefore resistance of the system under measurement (Yates et al, 2018). Hence, other than capacitance, microbiota activity and proliferation are expected to be measurable through the tracking of the resistance. There are, however, no practical or theoretical evidence of microbial activity involving the creation of inductive properties in the system. Therefore, the impedimetric (Z) sensing of biofilms involves the measurement of resistance (R) and capacitance (C) of the biological samples of interest via the AC sinusoidal excitement of them. Impedance is the ratio of voltage applied over the flow of current. For AC signals, the ratio of the voltage over current is a number consisting of a real and an imaginary part. Impedance is displayed as:

$$Z = \underbrace{R}_{\text{real}} + \underbrace{jX}_{\text{imaginary}} \tag{2-1}$$

where Z is the impedance, R is the resistance (and the real component of impedance), j is $\sqrt{-1}$, X is the reactance, and jX is the imaginary component of impedance. Reactance is the component of impedance related to the storage of charge in a conductive medium that comes in two forms: capacitance and inductance (Chroma Systems Solutions, 2019). As discussed above and due to the unavailability of inductance in microbial samples, reactance is interpreted as capacitance. Capacitance therefore is calculated via the following equation:

$$C = \frac{1}{\omega . f} \tag{2-2}$$

where f is the frequency of the input signal in unit of Hertz (Hz) and ω is a term dependent of the frequency of the input signal as such:

$$\omega = 2 . \pi . f \tag{2-3}$$

When a given circuit is composed of pure resistance, the voltage and current signals fall and rise at the same time even though their magnitude can be different. The voltage and current in such situations are known to be “in phase” with each other or their phase difference or shift (φ) is zero. Due to the sinusoidal behavior of AC signals over time, the voltage and current are governed by the following equations:

$$V = V_{max} . \sin(\omega t) \tag{2-4}$$

$$I = I_{max} . \sin(\omega t + \varphi) \tag{2-5}$$

where φ is the angle by which the current is leading from the voltage signal. In a purely capacitive circuit, the current leads the voltage by $-\frac{\pi}{2}$ or -90°. In circuits where the resistance and capacitance are equal values, the resulting phase shift is $-\frac{\pi}{4}$ or -45°.

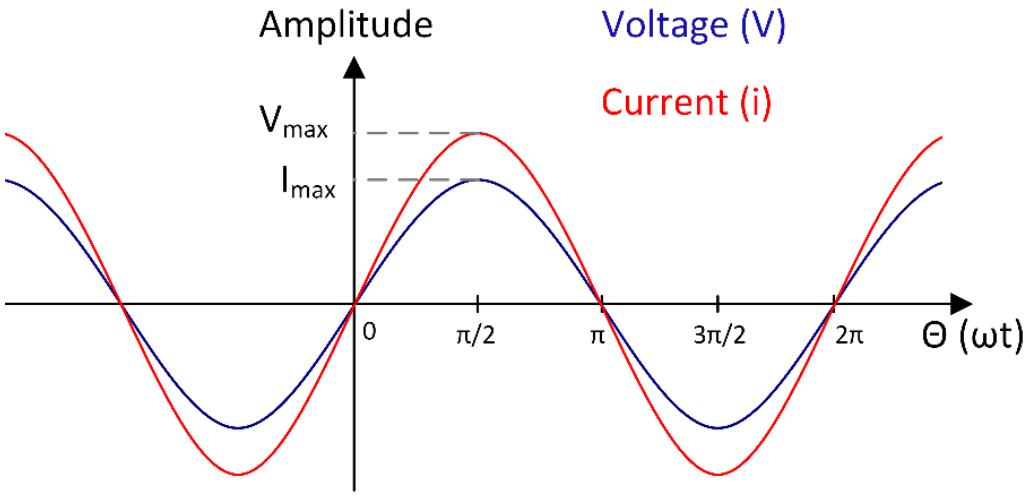

(a)

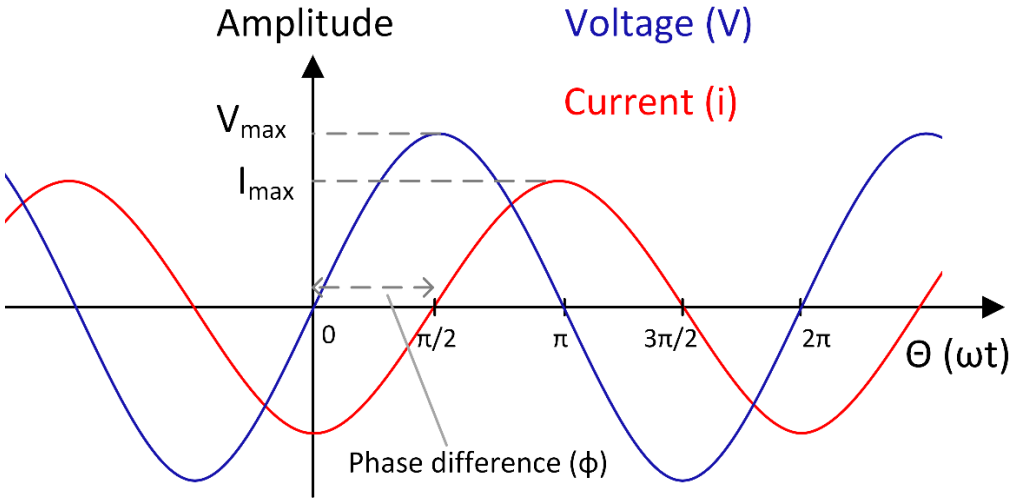

(b)

Figure 2-6*. Sinusoidal forms of the transmitted AC signal voltage to the RC elements and the impressed AC current.* ***(a)*** *Shows the in-phase voltage and current signals that occurs in the presence of pure resistance and the absence of capacitance in the system.* ***(b)*** *Shows the specific out-of-phase case of voltage and current signals that occurs in the presence of pure capacitance and the absence of resistance in the system.*

When resistance and capacitance are both present in the system, the circuit is regarded as an RC circuit, which creates a phase angle of some amount between -90° and 0°. The RC circuit can also be described with the impedance triangle (Electronics-Tutorials, 2014).

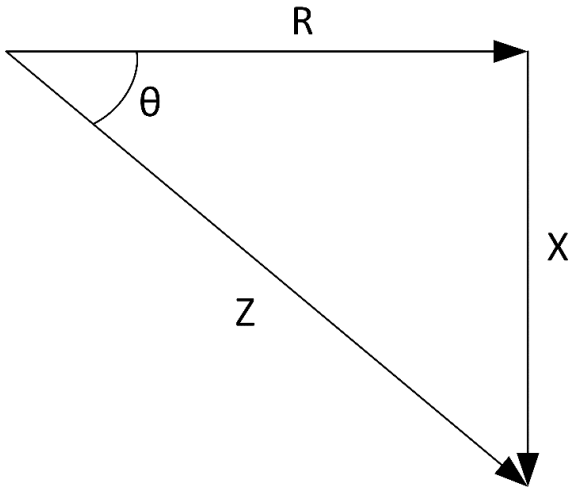

Figure 2-7. *The vector form of impedance components. Showing that impedance is a vector summation of capacitance and resistance*

The impedance (Z) can be described as:

$$Z = \sqrt{R^2 + X^2} \tag{2-6}$$

And the phase angle is governed by the following equation:

$$\theta = Arctan(\frac{X}{R}) \tag{2-7}$$

There are other presentation forms for the impedance, such as phasor format, but they all deliver the same concept.

There have been eminently numerous research works based on the idea of impedance microbiology. From food safety monitoring (Grossi et al, 2010) to point-of-care diagnosis of clinical diseases (Pal et al, 2016), impedance microbiology has been the main premise behind the monitoring systems developed. Nonetheless, since this research is conducted for the studying of plant root-associated biofilms, the emphasis is put on the instances of impedance spectroscopy application in such environments. Even though there has been no report of direct impedance sensing of biofilm colonizing the plant roots, there have been multiple research works focused on the biofilm formed in the subsurface environments. Frequency-domain induced polarization (FDIP), that is vastly used in mining, hydrogeological, oil-gas, and environmental (Vanhala & Soininen, 1995) studies for the assessment of geologic media, is conducted based on polarizing of

the media using AC signals, similar concept as impedance spectroscopy. In some instances, such as the work done by Revil et al. (2017) on brine-saturated clayey soils, the word "induced polarization" is used as an alternative name for complex conductivity, that is just a different name for AC impedance spectroscopy (Revil et al, 2017). In the section below, research work published on subsurface environments, that is perhaps the closest evidence relevant to the monitoring of biofilm produced in rain gardens, will be reviewed.

2.3.4.2 Impedance monitoring of biofilm formation in geologic media

A major advantage of impedance spectroscopy is that minimal sample preparation is sufficient or the continuous monitoring of the samples without having to physically exploit samples and interrupt the host environment (Xu et al, 2020). Recent advances in the field of environmental electrochemical monitoring, has shown the potential of frequency-domain induced polarization in providing the means of plant-root structure and characterization measurements based on the biogeophysical responses that can be acquired from plant root cells (Ehosioke et al, 2018).

Davis et al. (2006) studied the dynamic changes of impedimetric properties of biostimulated sand-packed columns. They crafted two 30-cm-long experimental columns filled with sand grains, and placed two electrode coils 16 cm distant from each other inside along the length of the columns for current injection. The columns were fed with different fluids circulated throughout the entire length of the columns using a peristaltic pump. This was done to encourage different biological and physicochemical environments and compare the different impedimetric properties. A mixture of nutrients and diesel fuel circulates in one column (unstimulated), and a mixture of nutrients, diesel fuel, and bacterial culture circulates in the other (biostimulated). Diesel fuel was added to the cylinders in order to simulate oil well conditions. Using a dynamic signal analyzer, AC signals would be transduced to the electrodes and the conductivity magnitude (mathematically reverse of impedance) and the phase shift were measured over 60 days and the real and imaginary components of conductivity (reverse of impedance) in columns were calculated.

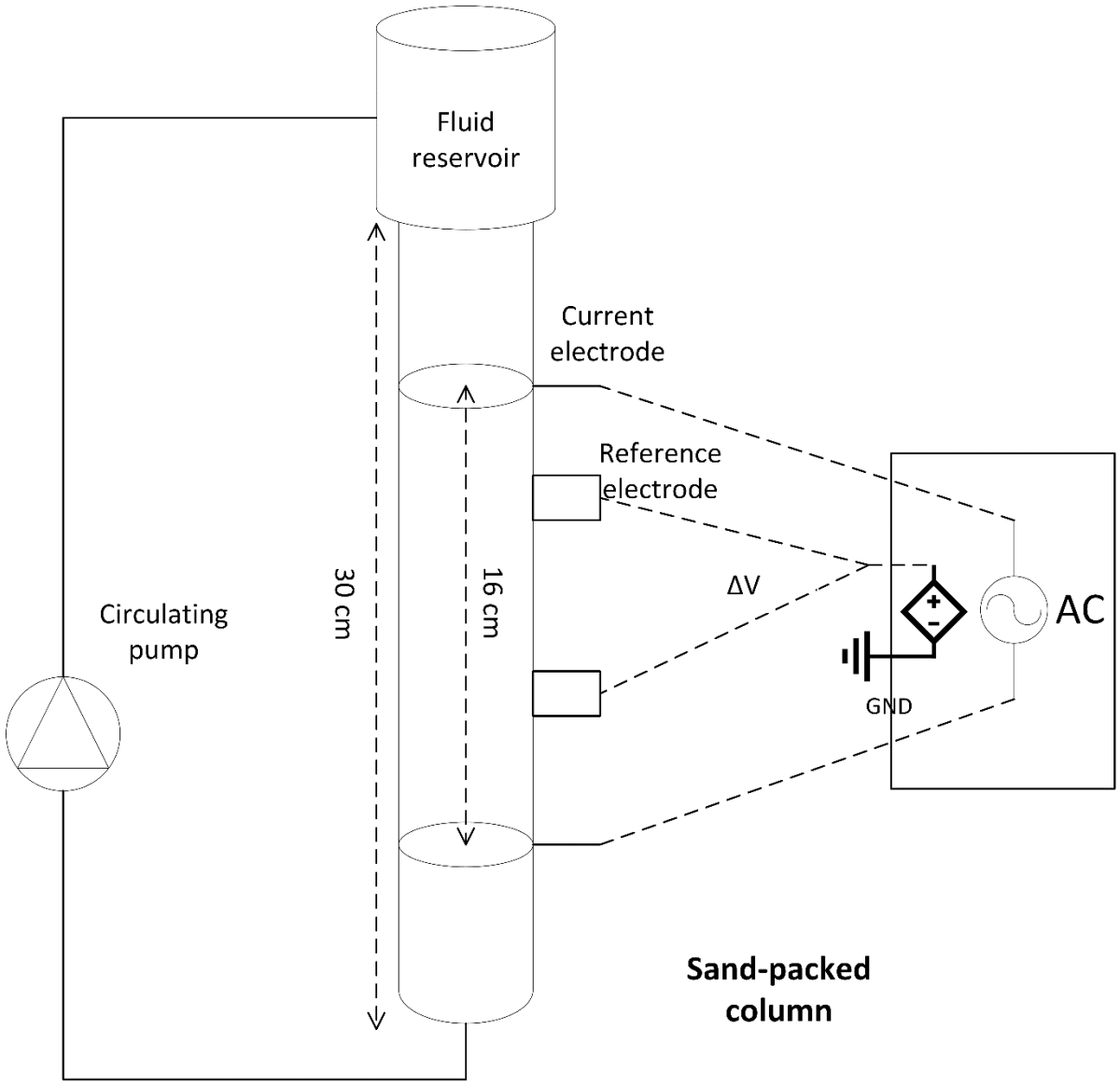

Figure 2-8. *Schematic diagram of the experimental setup used for the studying of biofilm grown on sand grains using impedance spectroscopy. Redrawn with minor changes from (Davis et al, 2006)*

ESEM imaging was also conducted to confirm the microbial growth in any of the columns. They noticed an increase of 280% in the imaginary impedance of the biostimulated column from day 0 to day 23. The change in the same parameter for the unstimulated was relatively small. The real part of impedance increased by 28% and 18% in the biostimulated and unstimulated columns, respectively. ESEM imaging of the columns on day 23 showed an increase of 230% increase in cell number in the biostimulated column, which is in close correspondence with the increase in the measured imaginary impedance. Therefore, the observed rise in the imaginary conductivity is inferred to be due the aggregation of the bacterial cells and/or the adherence of biofilm to the sand

grains. The ESEM images of sand grains from the unstimulated column did not lead to a corresponding relationship with the small impedimetric changes in this column. The researchers also noticed a decrease in the amount of imaginary conductivity after day 23 until day 60 in the biostimulated column, that is proposedly due to the cell detachments and lysis occurred in this period probably because of nutrient deficiency. The authors conclude that the imaginary component of impedance, can be interpreted as complex conductivity or capacitive impedance, can be utilized as a solid indicator of microbial growth and formation. Davis et al. also propose that this method can be used for the investigation of integrity of biofilms in the process of contaminants remediation (Davis et al, 2006). Overall, a similar idea as the sand-packed cylinder method has a vast potential to be used in a bioretention cell. One major downside to this specific way of implementing impedance spectroscopy is the extremely long testing period, 23 days under stimulated conditions. This is due to the fact that the system is only sensitive to substantial biological changes and a vast amount of biofilm formation is needed for the system to react to. In other words, the signal-to-noise ratio or biofilm monitoring efficiency is considered low. To overcome this shortcoming, miniaturization of the system is required to allow for higher sensitivities to biofilm growth and availability. Paredes et al. (2014) also suggested that the smaller the area of the electrodes, the less biological existence required to cause influence (Paredes et al, 2014a). The advances in technologies such nanofabrication and lithography have made the miniaturization of electrodes used in impedance biosensing possible, to extent where most of the bacteria-related impedance sensing is done via micro-scale electrodes known as interdigitated arrays (IDA) or interdigitated microelectrodes (IDE). The application of such electrodes will be thoroughly reviewed in the next chapter. Other than miniaturization, rapid advancements in the means of signal transduction, computing software, and device automation and control has contributed greatly to the betterment of biosensing technology (Rodriguez-Mozaz et al, 2006). In the present work, we try to take advantage from these techniques the best we can.

2.3 Concluding remarks and gaps in knowledge

To conclude, being able to monitor biofilm real-time of its development allows for the tracking of possible changes in the system as they occur. This is beneficial both when the static growth in the host in the host environment is of interest and also when the effect of certain chemical agents on the formation and proliferation of biofilm is of interest (Reyes-Romero et al, 2014), both of which

could lead to crucial improvements in the engineering of the bioretention cells and therefore, the efficacy of water quality improvements.

The functional requirements for the ideal monitoring system of interest for biofilm monitoring in situ of the bioremediation facilities include real-time, non-invasive, non-destructive, online, quantitative, portable, autonomous with sufficiently long testing uptime and signal acquisition as well as large substrate surfaces, and affordable tracking. These themselves omit the microscopic methods as an option for the rapid, portable or online monitoring of biofilms in the field. Other than these factors, it is best that the system could sense the bacteria population from a wide range of concentrations. Thermal and piezoelectric sensors typically require the formation of biofilm layers in the order of tens of micrometer to show a response, and therefore, they are not an option for the early detection of bacterial biofilms that is highly crucial in many different applications (Turolla et al, 2019). Low detection limits of the optical sensors and their function variations related to the environment do not make them dependable for use in geologic media. On the other hand, impedance biosensing has shown a vast potential in having the advantages of the online monitoring methods together with unique features, such as flexibility and customizability based on the application, high sensitivity, extensive evidence of field use, and potential of low-cost and portable implementation. Therefore, in the research work herein, impedance biosensing is chosen as the main method behind developing a sensor for use in monitoring environmental biofilm. Microscopic and optical density methods were also used as the second wing for the proposed prototype to allow for verification and calibration of the sensor. To the best of our knowledge, there is currently no available tool for capable of monitoring the biomass available in the bioretention cells.

Rodriguez-Mozaz et al assert that in spite of the past huge improvements in the biosensor technology, there still exists the challenge of developing more reliable devices. (Rodriguez-Mozaz et al, 2006). Despite vast efforts and the advances in the field of biosensor development, there still exists flaws that need to be addressed, that are the motivations behind the studies such as the present one. First and foremost is the fact that no sensor that is commercially available and can be used in an industrial-scale and for field use is available to the best of our knowledge. The few available systems are compatible with lab-scale use. In addition, unclear verification methods, sensitivity and detection thresholds enquire the need for further implementation and development

of a well-calibrated biosensing system. As well, a system is required for the research group to be able to study the effect of environmental conditions on the growth and metabolism of different biofilm-forming microorganisms to better engineer the bioretention cells.

Chapter 3 RESEARCH OBJECTIVES

The objective of this research is to design and craft an inexpensive monitoring system for bacterial biofilm. According to the literature review, frequency-domain induced polarization method, also known as complex conductivity or impedance spectroscopy, has the potential to be a suitable monitoring method for geologic media. Therefore, the aim is to design an impedimetric monitoring system that monitors biofilm formation and growth in real time.

To reach the objective of developing such a tool, lab-scale implementation and testing is required by following the steps below:

(i) crafting a lab-scale testing sensor;
(ii) debugging and integrating the system for online and autonomous measurements;
(iii) verifying whether the theories and results in the literature could be reproduced through testing and redesign the future experiments for optimal outcomes;
(iv) verification of the impedance result using an alternative method in tandem with impedance measurements;
(v) calibration of the impedance measurements in terms of the actual bacterial cells per unit of volume.

Due to the complexities of conducting the abovementioned steps directly in the field, we decided to carry them out in lab-scale on controlled samples that are repeatable. As well, field use without lab-scale and pilot-scale verification could bring up serious uncertainties about the robustness of each and every one of the steps mentioned above. Therefore, rather than trying to execute the impedance experimentation on the biofilm of plant roots and in uncontrolled environments, bacterial samples in known growth media were used. Upon the successful implementation of lab-scale impedance biosensing setup, field use would be approachable as the next phase. In Chapter 4, the details of the methods used are explained in depth.

The parameters that can be measured using this system will be characterized and the relation between the electrical capacitance/resistance and biofilm growth will be analyzed. By conducting the experiments, we will try to answer the question of how the impedimetric sensing

process can be affected by biofilm establishment and development. The results will then be augmented by carrying optical density spectroscopy and optical microscopy.

The last objective is to determine the challenges for *in situ* monitoring of biofilm using this method and whether this system can be utilized in macro-scale bioretention cells. If so, possible optimizations and development will be recommended for future studies, and other applications of such system will be addressed.

Chapter 4 AFFORDABLE REAL-TIME BACTERIAL GROWTH MONITORING AND BIOMASS ESTIMATION

The draft article presented here is for submission to the journal *Sensors.*

4.1 Abstract

An affordable and fully automated sensor for monitoring of biomass availability in the context of water quality improvement through vegetated bioretention systems was developed. Impedance microbiology was chosen as the primary method for designing a sensor that could monitor the growth of bacteria in a growth medium. The impedance properties of *Pseudomonas Putida* samples over the course of experiments were monitored under AC signals of 100 mV peak-to-peak and sweeping frequencies of 20 Hz to 300 kHz. The capacitance of the samples was recognized as the most sensitive impedimetric parameter with an average magnitude alteration of 37.1% due to bacterial growth. For verification, simultaneous to the impedance testing, optical density measurements calibrated by direct hemocytometry counts were taken of similar samples. The experiments resulted in the development of exponential and double exponential relationships that estimate the biomass available in the medium based on the change in capacitance. The detection range of the system for the tested strain is as wide as ~9.2×10^6 cells/ml up to ~5×10^8 cells/ml, depending on the accuracy of interest. This sensor provides rapid, real-time, and non-invasive monitoring capability.

4.2 Introduction

Stormwater generated from precipitation and surface runoff can not only lead to localized flooding, but to contamination of receiving waters due to the pollutants collected in the runoff (Khan, December, 2010). Modern stormwater management involves sustainable urban designs (SUDs) and low impact development options (LIDs) that integrate land use planning and engineering design (LeFevre, 2012) to manage stormwater runoff sustainably. Conserving the pre-developed characteristics of natural sites and utilizing them to increase water quality are the main goals of LID, which include retention ponds, green roofs (LeFevre et al, 2014) bioswales, permeable pavements, constructed wetlands, and bioretention cells (Yu, 2015). Bioretention cells, also referred to as bio-infiltration cells, vegetated biofilters, or rain gardens, are one type of LID that has been proven to decrease stormwater runoff quantity and increase stormwater quality from

urban areas. Bioremediation is a waste management method in which microorganisms play a critical role in removing or neutralizing waste materials and pollutants in bioretention cells.

Biofilms provide a huge potential to remove waste by natural conversion of toxic contaminants into harmless by-products and has opened a field called biofilm-based treatment (Mendoza Gonzalez & Kloc, 2012). One of the most promising applications of biofilms is their use in bioretention cells, in which biofilm emerges and grows on and around the vegetation root area referred to as the rhizosphere. Soil biofilm treats water by changing its configuration, composition and gene expression to consume pollutants and organic materials as their food source (Alfred B. Cunningham, 2008). Biofilm can form as result of the aggregation of millions or single species of organic/ inorganic compounds that can range from decomposing materials to microorganisms (LeFevre et al, 2014). According to Carpentier and Cerf (Carpentier & Cerf, 1993), a biofilm is a community of microbes implanted within an organic polymer matrix that adheres to a surface. Therefore, the three main components that are required for biofilm to form are microbes, an organic matrix, and a viable surface. Biofilm are the environment by which microbes adhere to the surface of almost every solid, such as river rocks, medical devices, etc. (O'Toole & Ghannoum, 2004). Bacterial biofilms have recently been gaining attention within a wide range of subjects, such as healthcare, environmental engineering, industrial biofouling, etc. Whether the biofilms are deemed disadvantageous or beneficial in each topic of interest, further understanding of their growth and metabolism is required to control the biofilm and achieve desirable improvements. There is a lack of understanding of the bioremediation process in field applications of bioretention cells. Consequently, design guidelines optimizing bioremediation in rain gardens is lacking. This is also partly due to the fact, that there are few tools if any that can properly assess the bioremediative state of a rain garden. Being able to monitor the growth of bacterial biomass in these treatment systems could lead to improvements in treatment efficacy and design, but to the authors' knowledge, there are no reliable methods for monitoring biofilm and biomass in rain gardens today.

There have been various approaches in studying the biofilm communities, and each method has advantages and drawbacks. According to Lewandowski and Beyenal (Lewandowski & Beyenal, 2003), monitoring biofilms helps us to gain a good understanding of biological processes within biofilm structure. However, clarity is need on what parameters need to be measured and

how these parameters can describe the biofilm system sufficiently for the end-user of that application. Monitoring biofilm can be achieved using different methods depending on the environmental conditions of the host environment, and the chemical, biological, and physical properties of the biofilm under investigation. But in general, the common fundamental concept behind these different methods for monitoring biofilm is that they all function using a response signal acquired from the biofilm. These signals are a result of energy transfer, heat transfer, acoustic waves, electrical fields or electrical currents. The process of monitoring involves transmittance of input signals, modification of the input signals by the biofilm and its host environment, and detection of the output signals by the sensor. In fact, the biofilm leaves its characteristic footprints in the modified signal (output signal) (Janknecht & Melo, 2003). Environmental conditions such as pH, temperature, and nutrient can control the attachment of bacterial cells to a surface. These conditions can prevent or facilitate biofilm formation. Therefore, an ideal biofilm monitoring system is a system that can function in situ, non-destructively, continuously, online, and without intervention in the microbial community. Since biofilm formation starts with the adherence of planktonic cells to an inert surface then followed by reproduction, biofilm monitoring tools are often designed to detect bacterial growth and proliferation in a growth media.

Various methods have been developed for reliable biofilm monitoring or evaluation. In addition to microscopic visualization techniques (Lawrence et al, 1991) used in many studies (2D microscopy (de Carvalho & da Fonseca, 2007), scanning electron microscopy (SEM), transmission electron microscopy (TEM) and confocal laser scanning microscopy (CLSM) (Baum et al, 2009), other techniques include piezoelectric (Nivens et al, 1993), optical and fiber optic sensing (Fischer et al, 2012),(Fischer et al, 2016), electrochemical (Cristiani et al, 2008), acoustic (Davis et al, 2010), and thermometric (Reyes-Romero et al, 2014). Although many of these methods have proven to provide good results, their complexity and limitations have narrowed their applicability to just a few specific uses. In the case of rain garden biomass monitoring, the sensing system needs to have specific characteristics to be able to function in field applications. For example, it must have immunity to fluctuations in humidity and temperature. Overall, a desirable monitoring system should provide affordable, fast, accurate, and online feedback acquisition.

Impedance Microbiology (IM) is the conduction of electrochemical impedance spectroscopy on microorganisms. The working principle of IM is on the changes that the microbial metabolism induces in the electrical properties of the growth media. IM uses the alterations in impedance and complex conductivity of the biological sample, and allows for rapid, non-invasive, real-time, and easy-to-use bacterial growth monitoring. Impedance sensing of biological samples has been around for a few decades but has recently gained increased attention due the advancements in technologies for fast, affordable, and automated implementation and testing. Sorrells et al. (Sorrells, 1981)]utilized the impedance measurements for the fast detection of bacterial content in grains of cereal in less than 12 hours. Firstengberg-Eden and Kelin (Firstenberg-Eden & Klein, 1983) attempted to determine the level of coliforms using rapid impedimetric measurements in raw meat samples and compare them with the long-established plate count method. Impedance measurements were employed by Gnan et al. (Gnan & Luedecke, 1982) and Hardy et al. (Hardy et al, 1977) as alternate methods for bacterial measurements in raw milk and frozen vegetables samples, respectively. Pompei et al. (Pompei et al, 2012) evaluated the detection of lactobacilli concentration in beer by using impedance measurements. Using the same method, the study of *Escherichia coli* and total coliforms were conducted by Colquhoun et al. (Colquhoun et al, 1995) and Strauss et al. (Strauss et al, 1984), respectively, in the context of water and wastewater quality. Tubia et al. (Tubía et al, 2018) utilized an impedance-based spectroscopy technique to detect yeast spoilage. Sammer et al. (Sammer et al, 2019) determined the available biomass of aquatic worms in situ using impedance spectroscopy technique. IM has also been used ins studies on subsurface environments. Ntarlagiannis et al. and Davis et al. (Davis et al, 2006; Ntarlagiannis et al, 2005b) used low frequency polarization of bacterial cells in sand-packed cylinders. In the realm of impedimetric biological sensing, capacitance has also gained increasing interest recently, leading to the emergence of capacitive biosensing that is a sub-category of impedance biosensing. According to Gizem Erturk (Ertürk & Mattiasson, 2017), the detection of various biological cells and components, such as proteins, nucleotides, microbial cells, pesticides, and herbicides, etc. has become feasible with capacitive biosensors.

The goal of this research is to develop a tool or sensor that could be utilized for the monitoring of bacterial biofilm and provide an estimation of biomass availability in the context of water quality improvement from bioretention cells treating stormwater. As such, no available system that is affordable and provides the right type of information for design purposes exists. Such a tool

could be used by municipalities to determine the function of their rain gardens in terms of remediation for water quality and to what degree; whether maintenance is required or design changes to remain sustainable. The development involves (i) conceptualizing, (ii) testing, (iii) verifying, and (iv) calibrating in order to provide practical information about the growth of bacterial biofilm from the beginning of proliferation stage through the stationary phase when bacterial population has reached a maximum.

4.3 Methodology

Given the literature on existing systems, IM was chosen as the basis for this sensor.

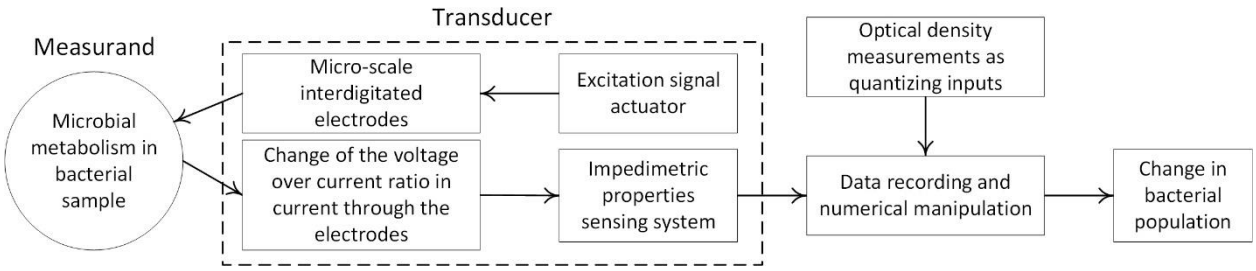

Figure 4-1. *Block diagram of the impedance-based sensing system of bacterial population growth*

4.3.1 Bacterial strain under the test

The main strategy in choosing a bacterial strain is to conduct the experiment on a strain that can form biofilm structures. It is also important that the species can grow in a subsurface environment and rhizospheric areas. A few different strains were investigated as candidates of this choice, such as *Streptomyces Viridosporus* (ATCC 39115) that is isolated from soil and is capable of biofilm formation. Other common biofilm formers are *Pseudomonas Putida*, *Pseudomonas Fluorescens*, *Rhizobium Leguminosarum*, and *Sinorhizobium Melitoti*. *Bacillus Subtilis*, *Sinorhizobium Meliloti* (*Ensifer Meliloti*), and *Pseudomonas Aeruginosa* are other candidates because of their ability in forming biofilms. The next factor is the ease of growth for these species, that can be as easy as inoculation in Luria-Bertani (LB) broth, used for *Pseudomonas Putida*, or using a composition of a few different growth nutrients such as yeast extract, mannitol, agar, soil extract, such as that for *Rhizobium Leguminosarum*. Considering the reasons mentioned above and the risk level of working with these strains, *Pseudomonas Putida* was chosen as the bacterial strain of interest for the experiments. This risk level I strain can be grown in Luria-Bertani broth medium at 30°C.

Isolated *Pseudomonas Putida* were grown on petri dishes containing tryptic soy agar at 30°C overnight. Once the colonies are formed on the agar medium, they are ready to be transferred to the liquid growth medium. A smear of the bacterial colonies formed on the agar plates were extracted using a sterilized inoculation loop and placed in sterilized LB broth. LB broth (Lennox), powder from Sigma Aldrich (ref: L32022-250G) was used for the preparation of bacterial solutions for testing.

The strain of *Pseudomonas Putida* was introduced to sterilized LB broth medium for culturing overnight at 30°C. After one day, bacterial cells in the LB broth were grown and the solution was cloudy and ready for serial dilution. This steady-state batch was used to create 6 samples that were serially diluted 1:10 with fresh LB broth, forming samples of a wide range of bacteria concentration (10^1, 10^2, 10^3, 10^4, 10^5, and 10^6 times diluted) that were ready for impedance testing. Part of each exact sample was set aside for optical spectrophotometry measurements. 275 µl of each sample (6 dilutions and the steady-state sample) was decanted onto the wells of the E-plate for impedance measurements. The impedance measurements on bacterial samples were performed at room temperature.

4.3.2 Impedance measurement device (The testing AC signal conditions):

Various factors must be accounted for in selecting an appropriate impedance testing platform for the application involved. The testing frequency range, the testing voltage, the price of the device, the data and command inquiry as well as communication capabilities are important factors. The frequency range needed for impedance microbiology is important because the wavelength of the AC signals should be long enough to allow the bacterial metabolism to create a sensible impact on the overall impedance properties. The voltage applied to the biological samples is important because of two main reasons: (i) if the voltage applied is too low, the measurement circuit, that is supposed to measure the electrical properties of the samples with the current passing through the sample, would not be sufficiently sensible for an accurate measurement; and (ii) if the voltage applied to the samples is too high, it can lead to inaccurate measurements as well as potentially strong electrification of bacterial cells resulting in die-off. In fact, electrification with high voltage electrical impulses is a technique that has recently been used to remove or reduce the presence bacterial biofilm colonies and facilitate wound healing. This technique is also called electroceutical treatment and could use voltages as high as 6V over a long period of time to eradicate biofilms

(Devendra H. Dusane 2019). In the current research, it stands to reason that the high-voltage electrification of the samples should be avoided, and the electrical measurements are conducted with the aim of providing a platform that monitors bacterial population as their growth takes place. One of the objectives of the experiments is to find an optimized frequency in terms of sensitivity to bacterial growth. Since this requires the measurements to be conducted at various frequencies, the impedance measurement device should be able to switch between frequencies and be configurable. This is the main difference between impedance analyzers and LCR meters, that measure L (inductance), C (capacitance), and R (resistance). The former can sweep the frequency within a range, but LCR meters are capable of measuring the electrical properties of interest at frequencies with discrete values (Ashworth, 2017). For this specific reason, impedance analyzers are generally more expensive than LCR meters. This limitation of the LCR meters, however, would not be critical to this study if multiple frequency set points can be configured in a set of measurements.

The parameters that are measured by the LCR meter are resistance (R), and reactance (X), which can be utilized to calculate various impedimetric properties such as capacitance (C) (in this case could also be called imaginary impedance), absolute impedance magnitude (|Z|), resistance (R) (real part of impedance) and phase angle (θ). There are, therefore, a few different ways of displaying the data. Real and imaginary impedance, on their own, are representative of pure resistance and pure capacitance properties of the samples, respectively. The effect that microbial metabolism has on the electrical properties of the growth medium is typically comprised of an RC circuit combination. Based on the parameters measured by the LCR meter, the impedimetric parameters were calculated using

$$\theta = \mathrm{Arctan}\left(\frac{X}{R}\right) \tag{4-1}$$

$$|\mathrm{C}| = \frac{1}{2\pi \mathrm{f} \mathrm{X}} \tag{4-2}$$

$$|\mathrm{Z}| = \sqrt{(\mathrm{R}^2 + \mathrm{X}^2)} \tag{4-3}$$

where f is the frequency at which R (resistance) and X (reactance) are measured. The relationship used for calculating the parameter's variation (v) of magnitude during the growth phase is governed by the following equation:

$$v = \frac{X_i - X_e}{X_i} \times 100 \quad (4\text{-}4)$$

where X_i is the impedimetric property of interest of the sample before the logarithmic reproduction and X_e is the same parameter at any later time of interest.

Previous research that performed impedance microbiology provided useful information for the approximate properties of impedance. Grossi et al. (Grossi et al, 2010) were able to test and verify a portable sensor that detects bacteria at a frequency of 200 Hz and 10 mv peak-to-peak voltage in liquid and semi-liquid samples. This sensor detects the total bacterial concentration, at a threshold of 10^7 cells/ml within 3 to 12 hours of inoculation and was successful in detecting the occasional and specific bacteria in ice-cream samples. Radke and Alocilja (Radke & Alocilja, 2004) developed a biosensor using immobilized antibodies on a MEMS electrode using a frequency range of 100 Hz up to 100 kHz and at 100 mV. Paredes et al. (Paredes et al, 2014b) performed impedance-based tests within a range of between 10 Hz and up to 100 kHz. Higher frequencies have such short wavelengths that do not allow the microbial metabolism to cause alterations in the impedance phase and magnitude. Other researchers have suggested a similar frequency range (Davis et al, 2006). Yang (Yang, 2008) in a study on detecting bacterial cells in suspensions using electro impedance spectroscopy, used a frequency range of 1 Hz to 100 kHz. Generally, therefore, the impedance spectroscopy of bacterial cells does not require significantly high frequency wavelengths, and can be achieved by using low frequency excitations. As well, operating the system at low excitation frequencies and voltages would minimize the power consumption of the testing unit, which is advantageous.

Other than the frequency range and voltages that determine the choice of a proper impedance measurement device, the affordability of the device is important because the intention is to create a device that can be used widely by engineers and technicians working in municipal services. Devices such as potentiostats (Cristiani et al, 2008),(Torres et al, 2008) dynamic signal analyzers (Davis et al, 2010), (Davis et al, 2006; Ntarlagiannis et al, 2005b), (Ntarlagiannis et al, 2005a) and impedance analyzers (Paredes et al, 2014b), (Vasiljevic et al), (Paredes et al, 2014a), (Paredes et al, 2013), (Paredes et al, 2012), (Mallén-Alberdi et al, 2016), (Wang et al, 2015), (Varshney & Li, 2008) have been used by many researchers for the purpose of impedance spectroscopy. However, in this study, the authors selected a much more affordable device, an LCR meter, and worked

toward programming it in such a way as provide similar benefits to high-end potentiostats and impedance analyzers.

4.3.3 The use of IDA in impedance microbiology

As far as the monitoring of bacteria using impedance sensing is concerned, the use of interdigitated arrays (IDA) is highly popular. Whether or not there are immobilized antibodies on the electrodes, the key aspect is the size of the electrodes, in a sense that it provides high sensitivity to the micro-scale changes in electron transport. IDAs, also known as IDEs (interdigitated electrodes), are structured as comb-like conductive traces of transducers, such as gold and platinum, that are typically comprised of a working electrode and a reference electrode and are coated on the surface of glass, silicone, or hard plastic substrate. The two electrodes are fabricated in a way that the parallel fingers of the combs of the two electrodes are interleaved from one finger to another, and stay at a miniscule distance but are not in contact. The IDAs have the advantage of providing low ohmic drop and therefore, easier achievement of a steady-state current response [46]. The spacing between the fingers, the length and the width of the fingers, the height of the traces, and the overall active area of the electrodes are among the most important parameters for the IDEs, when it comes to the optimization of the signal-to-noise ratio (S/N) based on the application of interest (Min & Baeumner, 2004), (Varshney & Li, 2009). As documented by Van Gerwen et al. (Van Gerwen et al, 1998), the smaller the spacing and the width, the higher the sensitivity to the electrochemical changes in between the microbands of the electrodes. Using impedance sensing with an IDA microelectrode, Yang et al. (Yang et al, 2004) provided successful evidence of the detection of *Escherichia coli* O157:H7 bacteria. Immobilization of antibodies was used on to the indium-tin oxide IDA for this study to increase selectivity. The IDA used for this research had 25 pairs of fingers that were coated on glass substrate and were 15 μm wide (digit width) and 15 μm apart from each other (interdigit width). Kim et al. (Kim et al, 2012) manufactured an IDA by depositing gold patterns of microbands on silicon wafers to achieve the rapid detection of bacterial attachment. The configuration of the microelectrodes used for this study was similar to the well-known comb-like structure with 50 pairs of mirobands that were 10 μm wide and 10 μm distant from each other. In another study, MacKay et al. (MacKay et al, 2017), nanofabricated a set of microarrays of gold nanoparticles that had only a gap of 2 μm between the electrode digits with the microband width of 4 μm. Turolla et al. (Turolla et al, 2019) evaluated the possibility of using 10 μm-spaced coplanar microelectrodes in impedance sensing of slime

formation in pipes and tanks. Thus, impedance spectroscopy on biological samples requires electrodes with comparable dimensions as that of the cells of interest. In the case of bacterial cells, that are generally smaller than human and cells, the width and spacing of the microelectrodes used in previous research are in the range of 1-20 μm (Varshney & Li, 2009).

4.3.4 Transducer of the device concept

After comparing many LCR meters in terms of the frequency range, the voltage range, the programmability, the basic accuracy, the measurement capabilities, and the price, Keysight E4980AL/032/201 made by Keysight Technologies, Santa Rosa, CA was chosen to be used as the measurement device.

As far as the sensing electrodes are concerned, after thorough evaluation of the possibility of manufacturing or using interdigitated electrodes on the market, 16-well E-Plates (E-Plate 16) made by ACEA Biosciences Inc., San Diego, CA was chosen as the sensing microelectrode. This product, as depicted in Figure 4-2 (a), is composed of a well plate (16 wells) that have gold traces deposited in the bottom of each well. The dimensions of the electrodes are within the constraints of this study. Additionally, the fact that the well plates would enable one to hold up to 16 different samples simultaneously is advantageous, although only 6 of the wells were used for testing.

(a)

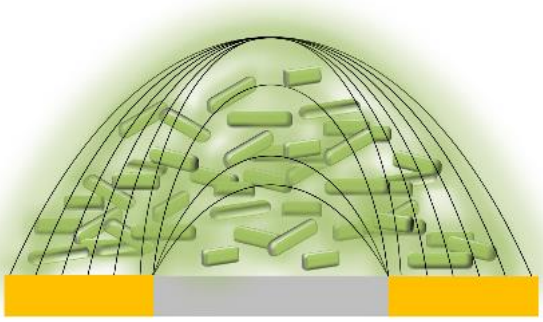

(b)

***Figure 4-2**. **(a)** Shows the 16 E-plate that has 16 wells with pairs of gold microelectrodes fabricated at the bottom of each well. **(b)** Cross-sectional scheme of the electric field that forms as a result of the microbial metabolism in the area near the surface of the electrodes.*

4.3.5 Automation of measurements

One of the most fundamental and distinguished objectives of this research was to be able to conduct automated measurements of several biological samples without the need of human intervention or supervision over the course of measurements. Automated measurements, in this context, would briefly mean that the setup conducts impedance measurements of 8 different biological samples (through 8 wells of the E-Plate), and sweep from low to high excitation frequency when a certain channel is isolated for the measurement. In other words, the experiments would require continuous measurement of the impedance of an array of channels under sequentially varying frequencies. In this respect, it is necessary to build a platform that is capable of multiplexing and switching channels on a continuous and orderly basis. The working mechanism of the setup would be based on assigning specific tasks to each component and providing proper communication means between the components to facilitate the integration of the system. In a nutshell, the controls of switching to channels, transducing AC signals as well as the control of the measurement functions, and lastly, data inquiry and storage are the major pieces of the system's functioning mechanisms.

ADG708 and its Evaluation Board (EVAL-16TSSOPEBZ) made by Analog Devices Inc. were used in the circuit as the switching component. ADG708 is an 8:1 switching system-on-chip (SoC) that determines to switch to one of the 8 outputs (S1 to S8) controlled by the 3-bit binary address codes (A0, A1, A2) that it receives (Inc., 2019). This chip was chosen because of its low on resistance, low current leakage, low power consumption and portability. GW Instek GPD-

4303S power supply was used to provide power to the multiplexer. A microcontroller chip and its development kit (nRF52832 and nRF52-DK) both made by Nordic Semiconductors, Trondheim, Norway were used as a controlling unit for the transmission of the digital signals required for the multiplexer to switch between channels. Using SEGGER Embedded Studio for ARM V4.10 as editor and compiler/linker/debugger, a code was developed in C programming language for the microcontroller to control the multiplexer.

The microcontroller is controlled by a series of codes that sequentially commands the change in the digital signals sent to the multiplexing switch, and the multiplexer forwards several digital outputs into a single line. The command center for the testing setup is a laptop (Dell Lattitude 3480) that is connected to the microcontroller and the LCR meter and sends commands to both components by means of universal serial bus USB ports. A "master" software was therefore needed to help with the integration of the instruments into one coherent system and decrease the complexities in controlling the devices. This master code was implemented in Python using SCPI (Standard Commands for Programmable Instruments) commands to send measurement settings and inquiries to the LCR meter, to inquire and save the test data, and to tell the microcontroller to switch to the next channel. The microcontroller receives a serial input from the laptop. Based on that, it creates a route between one of the inputs (S1 to S8) to a single output. This enables the python program to exercise control between one of the wells and the LCR meter. A delay was incorporated in the code to yield enough time for the LCR meter to finish the measurements on the well before the microcontroller closes the next channel for measurement.

The function of the system starts with a command sent by the command center to the microcontroller, asking the multiplexer to switch to the first channel. When the channel is closed, the command center commands the LCR meter to start sweeping AC signals from low to high frequencies using values defined in the program and measure the R-X values of the sample under the test. The R-X values are the real and imaginary components of the impedance, that can later be used to calculate the resistance and capacitance properties of the sample as well as the phase shift between the applied and the measured signal. The measurement by the LCR meter has two parameters, the voltage and the frequency. In order to have a better understanding of the impedance changes in the biological samples, the measurements were done at various frequencies as low as 20 Hz up to as high as 300 kHz, and the AC signal voltage is set to 100 mV peak to peak. One of the system's channels was used to capture any glitches or disturbances in the system by

maintaining it connected to a RC element of known resistance and capacitance of 30 Ω and 474 nF, respectively. The magnitude of the RC element was chosen based on the comparativeness with the typical magnitude of the resistance and capacitance previously observed in the preliminary impedance analysis on the bacterial samples.

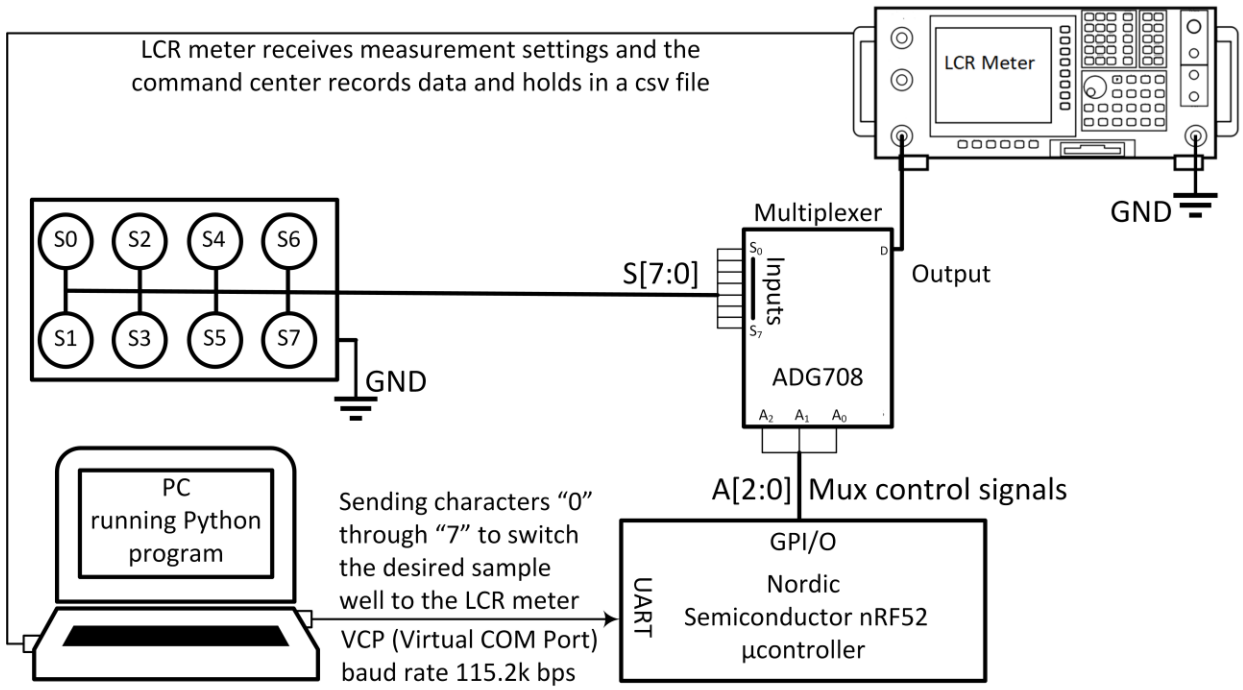

(a)

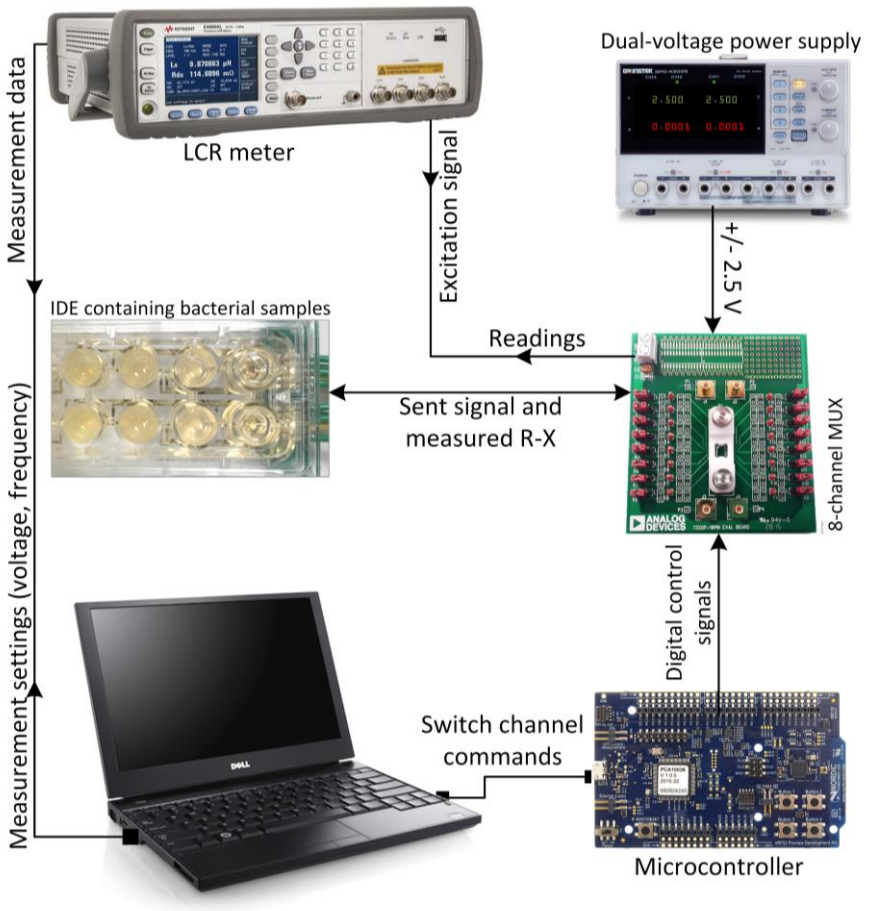

(b)

Figure 4-3. (a) *Drawing of the bacterial growth monitoring system together with a summary of the communication mechanism between the different components. The system is fully automated and is controlled by the command center.* ***(b)*** *Depicts a schematic of the main electrical components that compose the system. The setup is made up of affordable elements.*

4.3.6 Equivalent circuit models

Bacterial detection and analysis using impedance-based techniques could be classified into two different approaches: faradaic and non-faradaic. In the faradaic approach, an interface is required for the transfer of charges from the species under the test to the electrodes, which requires the employment of redox-active species (Daniels & Pourmand, 2007). Since there exists no redox species in our setup, this study was based on a non-faradaic approach of impedance measurements.

For non-faradaic impedance measurements, there are several models that could be used to fit the impedance data. The models are comprised of hypothetical resistances and capacitances (RC circuit) that are formed based on the conductivity of the medium and the electrodes (Brosel-Oliu

et al, 2015). Generally speaking, the resistance and capacitance of the growth medium (electrolyte) as well as the resistance and capacitance of the bacterial biofilm are the main elements in most of the suggested models. With the occurrence of biochemical reaction at the surface of the transducer (electrode), a double-layer capacitance could be formed that is basically induced by the formation of ionic species, as a result of microbial metabolism. As an existing element in the RC equivalent circuit models, many researchers suggested the double-layer capacitance (Paredes et al, 2014b), (Kim et al, 2012). Resistance and capacitance of bacteria could either be in parallel or in series with the solution resistance and the DLC.

In summary, the device concept is designed and programmed to send low voltage alternating current (AC) signals to a series of an interdigitated gold electrodes (IDE). The excitation device sweeps from low to high frequencies to find the frequency at which the impedance is the most sensitive to growth. Alterations in the electrical properties are studied, verified, and calibrated with the microscopic hemocytometry and optical density spectroscopy.

4.3.7 Hemocytometry and optical density measurements

In-tandem verification of impedance sensing leading to the estimation of bacterial concentration is a necessary part of the proposed devices proof of concept. Electron scanning electron microscopy (ESEM) (Mallén-Alberdi et al, 2016) and atomic force microscopy (Turolla et al, 2019) were often used as confirmation methods for impedance measurements in the literature but these require expensive facilities. Pal et al. (Pal et al, 2016) used optical density at 600 nm and surface plating techniques to substantiate their impedance sensing results. Optical density spectrophotometry at 600 nm are vastly used in applications involved with the growth of bacteria in culture (Brian C. Matlock). However, surface plating is a time-consuming method and should be performed by trained personnel (Wang et al, 2015).

Hemocytometry, on the other hand, is one of the most reproducible methods for the direct counting of different bacteria types (Schad). Hemocytometry provides a highly accurate count of bacteria, while spectrophotometry is an indirect measurement of bacterial concentration but a much more rapid method. Ideally, therefore, optical spectrophotometry that is calibrated by hemocytometry would be conducted on the samples from similar batches as are under the impedance testing. This affordable approach, that does not require high-end microscopes and 3D imaging facilities, would help to gain a good understanding of the bacterial cell concentration in

each sample at a given time and to correlate them with the impedance spectroscopy results. In principle, hemocytometry is utilized as a leverage to calibrate the optical absorbance measurements. The purpose of this calibration was to eliminate the need for conducting hemocytometry, which is a labor-intensive and time-consuming task, in the long-term.

In order to quantify the absorbance measurements and correlate them to the concentrations by giving values of cell counts to the them, a set of hemocytometry tests was conducted on the samples with known optical absorbance. Hemocytometry allows the direct count of the number of cells per a known volume of sample. SMART® Spectro 2 spectrophotometer made by Lamotte, Chestertown, MD was utilized for all the optical density measurements and Petroff Hausser Counting Chamber (ref: 3900) made by Hausser Scientific, Horsham, PA that has a cell depth of only 10 microns was used for all hemocytometry measurements. The spectrophotometer was calibrated and used to estimate the bacterial population in similar samples that were tested simultaneously under impedance sensing. Hence, the samples were selected for spectrophotometry based on their potential to represent varying amounts of growth and bacterial populations. This could also be an adequate choice of testing strategy in terms of validating the repetitiveness of the technique.

4.4. Results and Discussions

4.4.1 The impedance changes at fixed frequency as response to bacterial growth over time

The results of a test that was conducted on the steady-state (saturated) sample, and 6 bacterial samples that were diluted serially are presented here in three different ways. First, the impedance results of different samples at a fixed frequency over time are compared. Secondly, the impedance results of different samples under the sweep of frequency are explained. Lastly, the relative variations of impedance parameters will be interpreted as the biomass change to provide a clearer explanation of the capabilities of the impedance sensing setup.

Measuring the impedance responses of bacterial samples demonstrated a sudden change in terms of real and imaginary impedances after a few hours of inoculation. The sudden changes occurred in all the samples one after another. The sample with the highest initial number of bacteria, approximately 2.444×10^7 cells/ml, showed changes in impedance properties before every other sample. This sample was diluted 10-fold from the steady-state batch and had an optical density absorbance value of 0.14 at the beginning of the experiment. Subsequently, other samples

started to show impedance changes one after another in the sequence from the initial concentration that began the experiment. Therefore, the sample that started with the least number of bacteria (approximately 2.4×10^2 cells/ml) was the last one that showed the sudden impedance changes, as shown in Figure 4-4. This figure includes the variations of impedimetric parameters of samples over time. All these parameters are normalized over their initial values at time zero to allow for the elimination of bias available in the measurement system.

As the impedance sensing was being conducted, both the measured resistance and reactance showed alterations in their values during the logarithmic growth phase of bacterial samples, which is confirmed by simultaneous hemocytometry and optical density measurements. Alterations in phase angle, capacitance and impedance magnitude are expected and thus, the overall impedance magnitude that encompasses both the resistance and capacitance changes may provide a more comprehensive understanding. These sudden alterations were noticed at all frequencies, but the results are presented at frequency of 1,000 Hz, that is low enough to reflect variations in impedance values. The impedimetric properties of the steady-state sample (saturated sample) stayed relatively constant throughout the experiment.

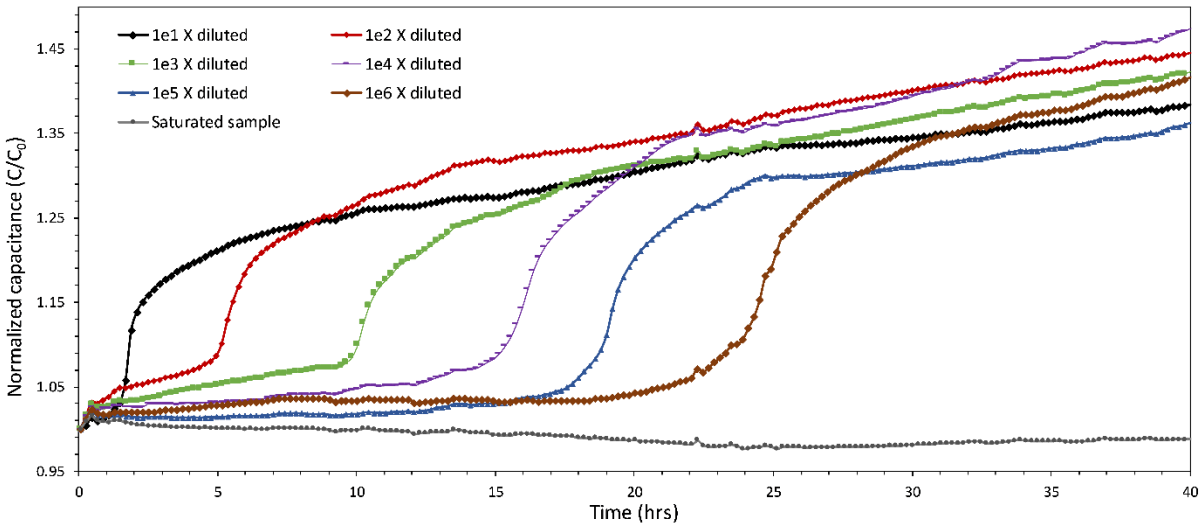

(a)

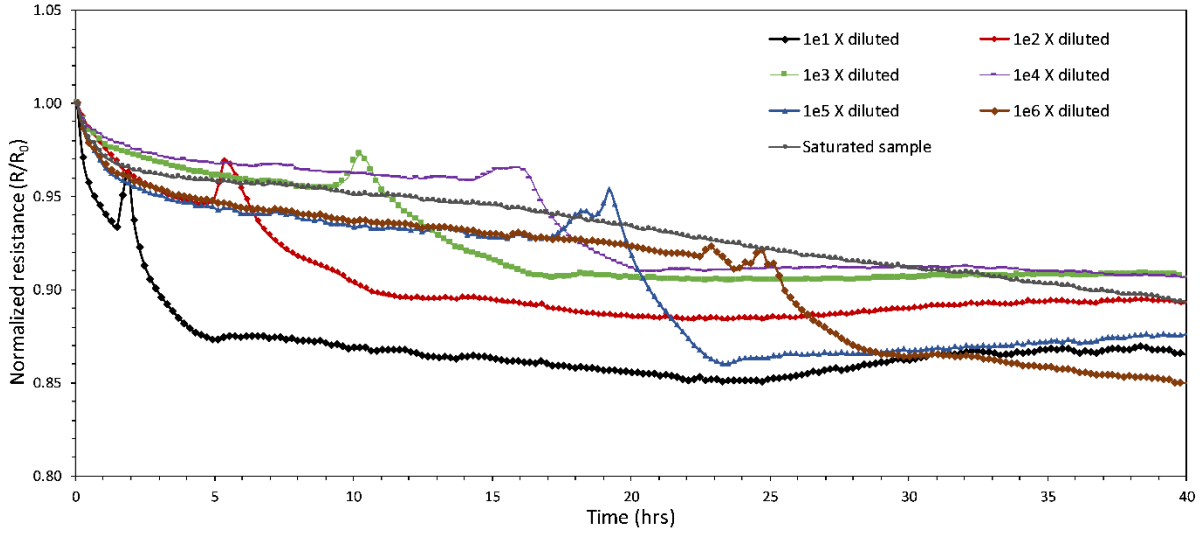
1e1 X diluted
1e2 X diluted
1e3 X diluted
1e4 X diluted
1e5 X diluted
1e6 X diluted
Saturated sample
Normalized resistance (R/R0)
Time (hrs)

(b)

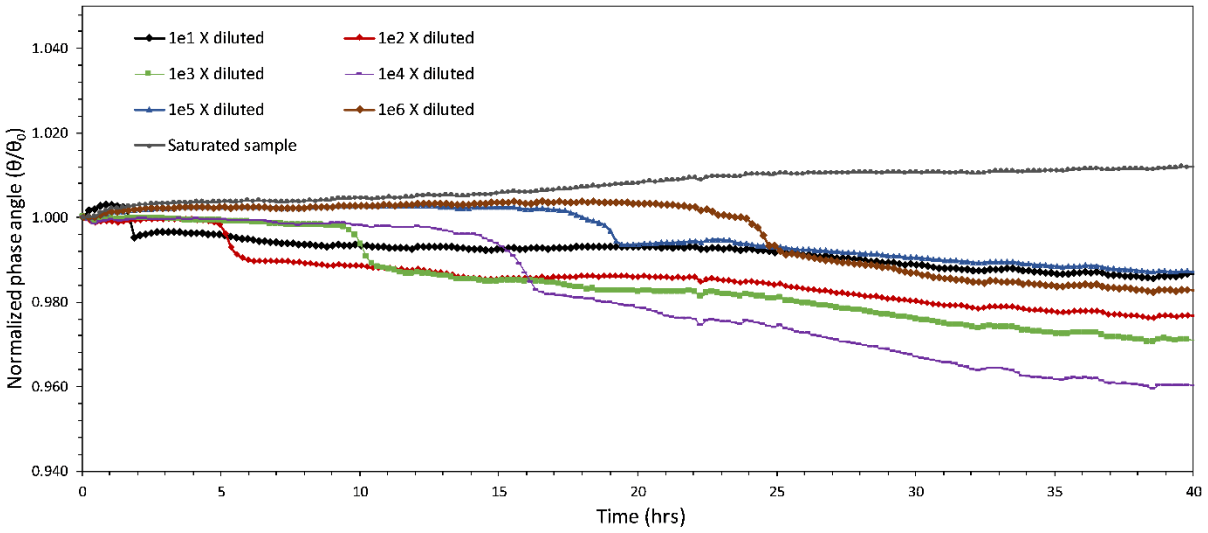
1e1 X diluted
1e2 X diluted
1e3 X diluted
1e4 X diluted
1e5 X diluted
1e6 X diluted
Saturated sample
Normalized phase angle (θ/θ0)
Time (hrs)

(c)

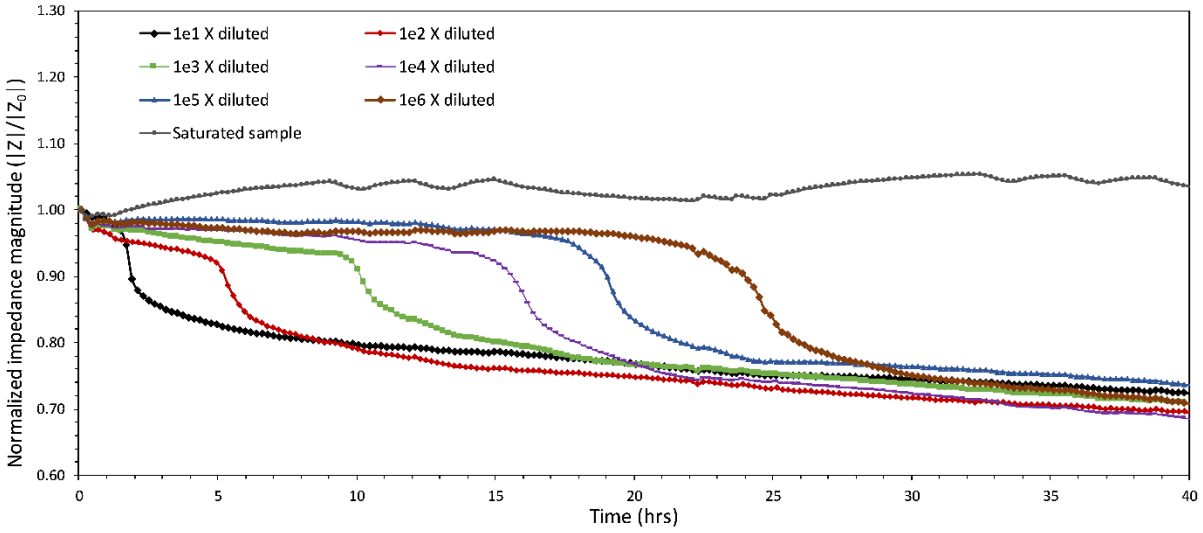

(d)

Figure 4-4. *Monitoring of the impedance values over time for all the 7 samples at 1,000 Hz.* ***(a)*** *Capacitance of the samples start to increase rapidly one after another in the order of their initial concentration. Data points are obtained approximately every 12.2 minutes.* ***(b)*** *The resistances of the samples do not represent a definitive trend, even though there is some decrease in observations simultaneous to the capacitance changes.* ***(c)*** *Some increase occurs in the values of phase angle calculated for each sample, but no more than 2% of their initial value.* ***(d)*** *The impedance magnitudes of the samples start to plunge one after another in the order of their dilution.*

As bacteria start to proliferate, the impedance changes occur in a way that the resistance decreases slightly together with some other irregularly trended variations, and the capacitance increases sharply at the same time as shown in Figure 4-4 (b) and (a), respectively. The overall impedance magnitude, that reflects and includes the changes in the magnitude of both real and imaginary impedance also showed a sudden decrease, Figure 4-4 (d). As suggested by Wang et al. (Wang et al, 2015), the decrease in resistance that occurred at the same time as the reproduction of bacteria is probably due to the formation of a bridge bacterial clusters between the electrodes, facilitating the electron transfer among them. Even though there exists a decrease in resistance during the growth phase, the existence of random spikes makes this parameter unreliable to be representative of growth evaluation.

The measurements indicate that the normalized phase angle hover in the range of 0.96 to 1 (Figure 4-4 (c)), which also indicates the combinatory existence of both capacitive and resistive properties of the biological samples. Among all representation forms, the capacitance and impedance magnitude seem to provide a more definitive demonstration. To prove this theory, the variation from baseline was calculated for each parameter using Equation 4-4. Calculating the

variation of the impedimetric parameters of all samples for before and after the growth showed an average of 37.1%, 33.5%, 14.4%, and 1.6% variation for capacitance, impedance magnitude, resistance, and phase angle, respectively. This demonstrates that the capacitance is the most sensitive to the metabolic changes, even though impedance magnitude could provide a more inclusive value comprising of both resistance and capacitance. Capacitance, therefore, is the more potent parameter for the monitoring of growth.

4.4.2 Sweep of frequency at different times

The results of the frequency sweep from 20 Hz to 300 kHz for the sample, the one that was diluted 1,000 times from the steady-state batch, are presented here; and the results from the rest of the samples are added as error bars. The 1,000 times diluted sample was chosen because of its moderate representation of samples of lower and higher initial concentrations. The green, red, and the blue markers, in Figure 4-5 (a-d) represent the values of impedimetric parameters at different times of the experiment normalized by their values at time zero, in that when the proliferation has not started (green), the proliferation has started (red), and the proliferation is finished (blue). By comparing the results of frequency sweeps for a given sample, it is clear that the variations could be differentiated much more easily at lower frequencies than at higher frequencies. This is also in agreement with the results that were obtained by other research (Paredes et al, 2014b), (Paredes et al, 2013), (Paredes et al, 2012). Over time, the resistance of the sample decreases compared to when the exponential growth has not started, indicating that the growth of bacteria further facilitates the electron transport in the system. At the same time, however, the ability of the system to store the electric charge applied by the excitation signal is increased. In Figure 4-5 (a), it can be observed that the capacitance values over the progression of time and therefore bacterial growth are much more distinguishable compared to other impedimetric parameters. In fact, for a given sample, capacitance is the only impedimetric property that shows distinction between the measurements at various states of time and across the whole frequency range, Figure 4-5 (a).

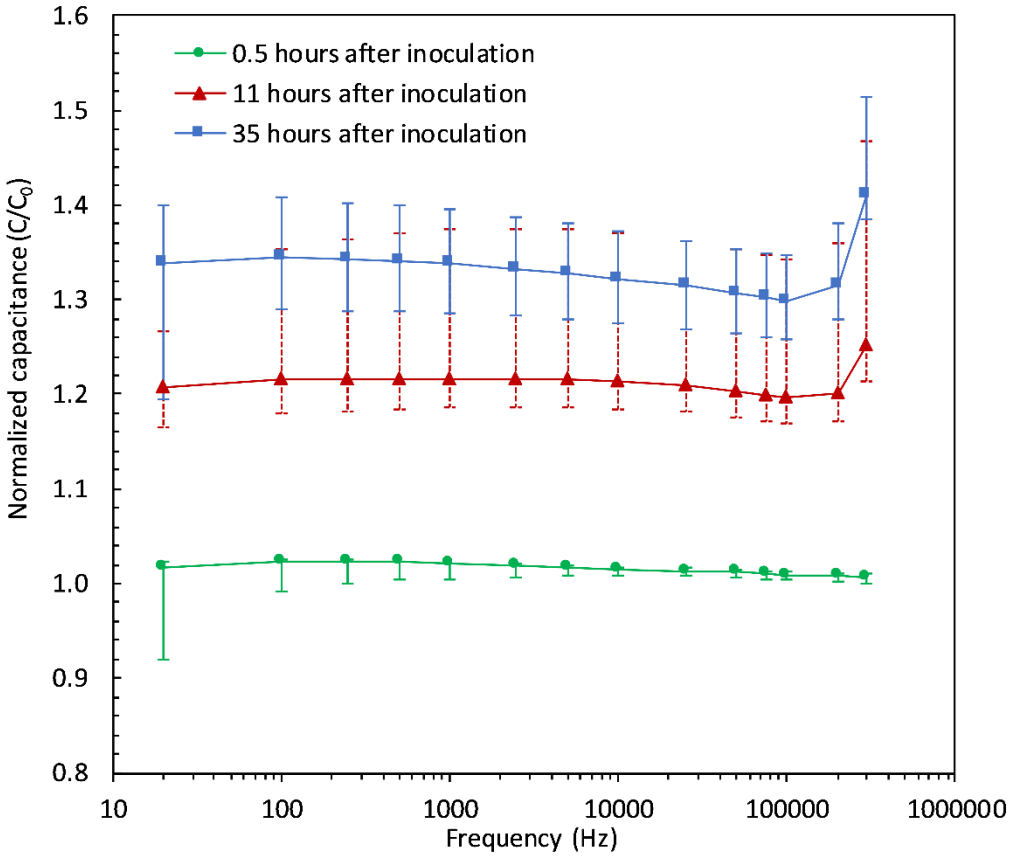
0.5 hours after inoculation
11 hours after inoculation
35 hours after inoculation
Normalized capacitance (C/C0)
1.6
1.5
1.4
1.3
1.2
1.1
1.0
0.9
0.8
10
100
1000
10000
100000
1000000
Frequency (Hz)

(a)

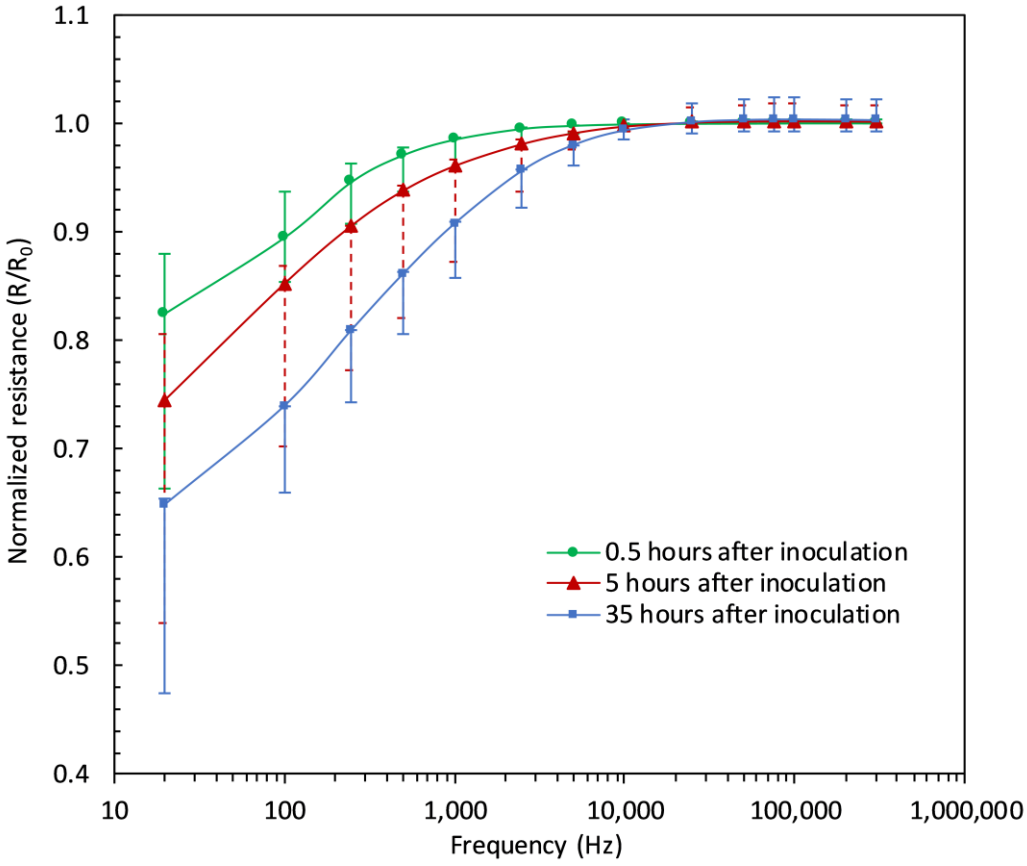
1.1
1.0
0.9
0.8
0.7
0.6
0.5
0.4
Normalized resistance (R/R0)
10
100
1,000
10,000
100,000
1,000,000
Frequency (Hz)
0.5 hours after inoculation
5 hours after inoculation
35 hours after inoculation

(b)

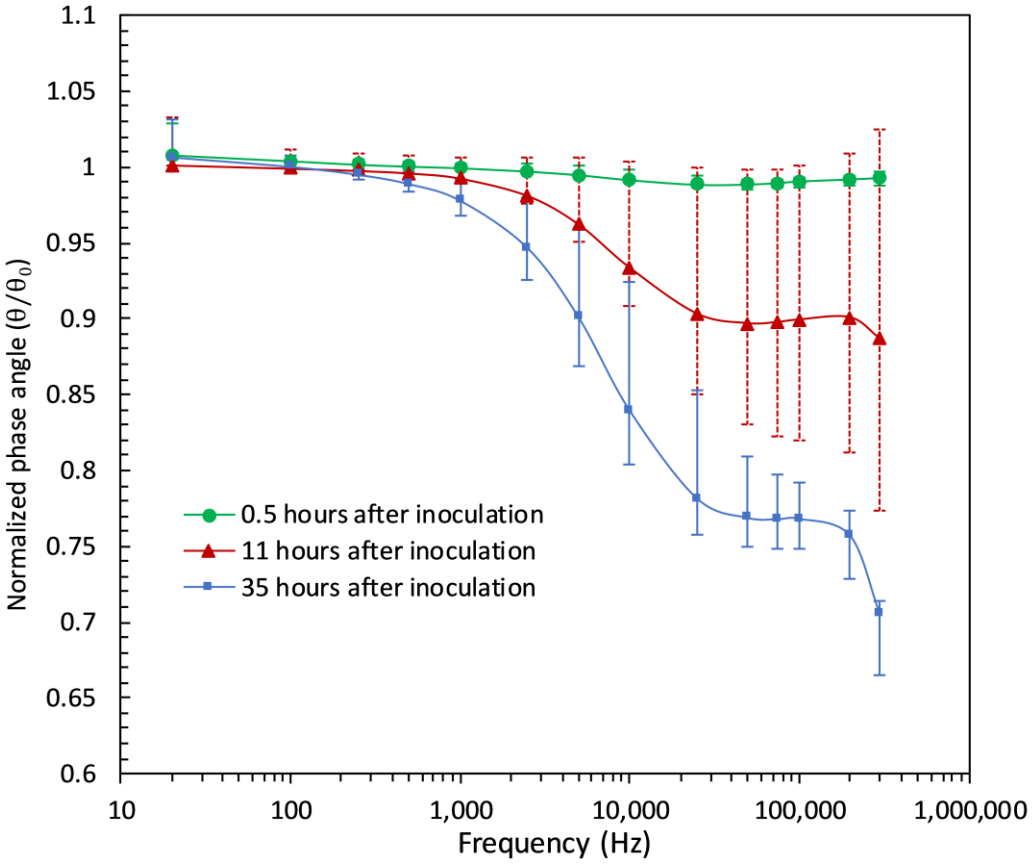
1.1
1.05
1
0.95
0.9
0.85
0.8
0.75
0.7
0.65
0.6
Normalized phase angle (θ/θ0)
10
100
1,000
10,000
100,000
1,000,000
Frequency (Hz)
0.5 hours after inoculation
11 hours after inoculation
35 hours after inoculation

(c)

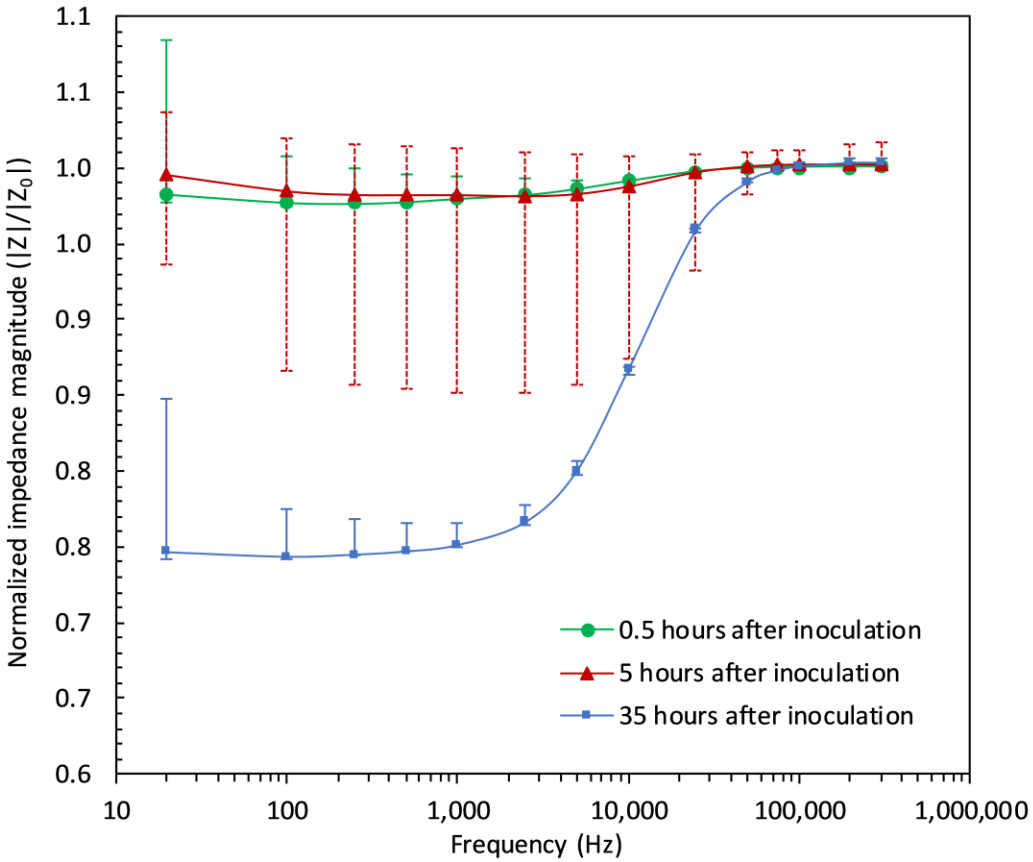

(d)

Figure 4-5. *Magnitude of impedimetric parameters for the 10^3 times diluted sample over the sweep of frequency from 20 Hz to 300 kHz at before, during, and after bacterial reproduction. Results of other samples are plotted as error bars covering the minimum and maximum values of the parameters among samples at each frequency point.* ***(a)*** *Capacitance frequency sweep results. There exists a clear distinction between magnitudes of capacitive property of the sample over time, in that values before, during and after the exponential growth show different magnitudes at all points, especially under low and mid-range frequencies.* ***(b)*** *Resistance frequency sweep results. Slight change is noticeable in the resistive property of the sample from before the proliferation to after the proliferation.* ***(c)*** *Phase angle data under the sweep of frequency. The distinction between the magnitudes are noticeable only at lower frequencies.* ***(d)*** *Impedance frequency sweep data showing a decrease of impedance magnitude at low frequencies after the proliferation is finished.*

4.4.3 Equivalent circuit model for biological changes

Six models are evaluated in fitting the impedimetric experimental data. Python Zfit application was used to conduct data fitting of impedance measurements and to find the RC elements suggested by each model. Nelder-Mead downhill simplex method was used to find the best fits by converging RC values to experimental data by keeping the squared-error minimized. Dellis and Carpentier (Dellis & Carpentier, 1993) also reported high accuracy and capability of the Nelder

Mead method in fitting the impedance spectroscopy data. The goodness of fit (ξ) that was used to compare between the models is the average percentage difference of the impedance magnitude calculated by the suggested RC values from each model ($|Z_{model}|$) from the experimental model ($|Z_{exp}|$), in that:

$$\xi\,(\%) = \left|\frac{|Z|_{exp} - |Z|_{model}}{|Z|_{exp}}\right| \times 100 \qquad (4\text{-}5)$$

The effort here was to evaluate which model could best describe the data obtained from the samples. A model that is suggested by Liu et al. (Liu et al, 2018) infers that the adherence of bacterial cells to the surface of the microelectrodes and their echxistence in the growth medium induces an RC circuit consisting of double-layer capacitances (C_{dl}), solution resistance (R_s), and bacterial resistance (R_S) and capacitance (C_b). As proven by Kim et al. (Kim et al, 2011), double-layer capacitance is a key existing element in explaining the impedance spectroscopy data of adhesion and maturation of bacterial biofilm. This theoretical model fits the data of our experiment with minimal error.

Theoretically, if we imagine a certain value for the double-layer capacitance at the beginning of the test and before the growth, the increase could be explained by a parallel capacitance model. In the world of circuits, the addition of a new capacitor to the circuit, in this case capacitance of bacteria (C_b), would only cause an increase to the overall capacitance if it is added in parallel to the existing capacitor(s), in this case the capacitance of the solution (C_{dl}). Other than the parallel arrangements of the bacteria and double-layer capacitors, the increase in capacitance could be justified by assuming the capacitance of the growth medium and capacitance of bacteria as a whole (C_T), and that the bacterial growth enhances the total capacitance property of the sample.

Table 4-1. *Potential equivalent circuit models together with their schematic and their success in fitting the impedance data obtained by sweeping of frequency.*

Equivalent circuit model schematic	Equivalent model	Model error (%) from experimental impedance magnitude (ξ)

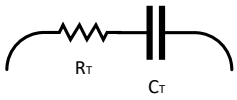	Model 1 - Inspired by (Paredes et al, 2014a), (Varshney & Li, 2008), (Turolla et al, 2019). This model fits our data. $Z = R_T + \frac{1}{C_T wj}$	4.3
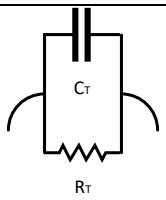	Model 2 - This model does not fit our frequency sweep data. $Z = \frac{R_T}{1 + C_T wj}$	1365.4
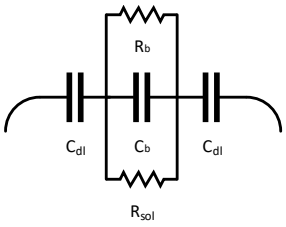	Model 3 - suggested by Parades et al. (Paredes et al, 2014b). This model did not fit the data of our experiment. $Z = \frac{R_b R_{sol}}{2 + R_b R_{sol} C_b wj} + \frac{2}{C_{dl} wj}$	914.6
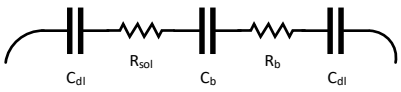	Model 4 - also suggested by Paredes et al. (Paredes et al, 2014b). This model fits our data. $Z = R_b + R_{sol} + \frac{2C_b + C_{dl}}{C_{dl} C_b wj}$	4.2
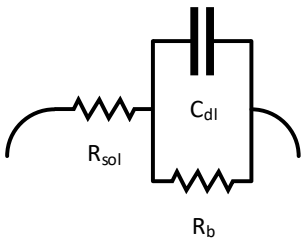	Model 5 - known as Randles equivalent circuit. This model did not fit our frequency sweeping data. Inspired by (Kim et al, 2012), (Kim et al, 2011), (Radhakrishnan et al, 2014) for the rapid detection of bacteria on IDA. They assumed what we call the resistance of bacteria the resistance against the charge transfer. And a constant phase element was allocated to the overall capacitance of the sample. $Z = R_{sol} + \frac{R_b}{1 + R_b C_{dl} wj}$	42.5

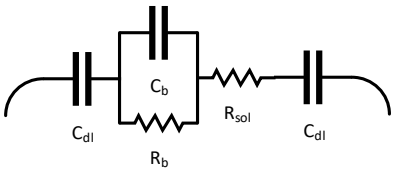	Model 6 - suggested by Liu et al. (Liu et al, 2018). This model also fits our data. $Z = R_{sol} + \frac{R_b}{1 + C_b wj} + \frac{2}{C_{dl} wj}$	5.1

As summarized in Table 4-1, there is more than one model that could provide a fit to the experimental data in estimating the impedance magnitude with an error of 5% or less. One could however argue that the presence of microbial biofilm, that has a convoluted structure, could be of such high complexity in terms of equivalent electrical circuit in micro level that could not be explained with any 1D, 2D, or even 3D equivalent models. The microbial metabolism contains such high randomness that a realistic equivalent RC circuit could be impacted by each and every bacterial cell that on its own has interaction with other cells and electrode areas. Thus, finding an absolute value for the resistance and capacitance of bacteria that is defined in a segregated way from the resistance and capacitance of the growth media and the overall system, may not be ideal. That is why we suggest that, in non-faradaic studies, exploring different equivalent RC circuits would be more realistic if the resistance and capacitance of bacteria and growth media, whether serial or parallel, are looked at as a whole (C_T , R_T), and the deviations are calculated accordingly. The impedance sensing data could not be fit to a parallel model, and therefore, a serried combination is presented.

***Table 4-2**. The values obtained by curve fitting using model 1 (serried CT and RT) are summarized in this table. The capacitance increase over time is also to the extent of the experimental data. As well, resistance alterations are not considerable.*

	10 times diluted sample - Average data fitting error from experimental data 4.7%				10,000 times diluted sample - Average data fitting error from experimental data: 3.8%			
Time (hrs)	Calculated R_T (Ω)	Deviation from baseline (%)	Calculated C_T (nano Farad)	Deviation from baseline (%)	Calculated R_T (Ω)	Deviation from baseline (%)	Calculated C_T (nano Farad)	Deviation from baseline (%)
0	40.83	-	162	-	121.1	-	153	-
5	41.63	2.0	190	17.1	120.9	-0.2	151	-1.3
10	41.76	2.3	196	20.9	120.6	-0.4	153	0.0
15	42.12	3.2	198	22.0	120.7	-0.3	158	2.9
20	41.35	1.3	209	28.7	120.5	-0.5	197	28.5
25	41.24	1.0	214	32.0	120.6	-0.4	205	33.6

30	41.75	2.3	210	29.7	120.6	-0.4	206	34.5
	100 times diluted sample - Average data fitting error from experimental data 4.1%				100,000 times diluted sample - Average data fitting error from experimental data: 4.7%			
Time (hrs)	Calculated R_T (Ω)	Deviation from baseline (%)	Calculated C_T (nano Farad)	Deviation from baseline (%)	Calculated R_T (Ω)	Deviation from baseline (%)	Calculated C_T (nano Farad)	Deviation from baseline (%)
0	70.56	-	152	-	40.66	-	156	-
5	71.04	0.7	159	4.3	41.14	1.2	152	-2.8
10	71.25	1.0	182	19.8	40.99	0.8	151	-2.9
15	71.63	1.5	188	23.7	41.08	1.0	152	-2.4
20	71.11	0.8	199	30.8	40.46	-0.5	184	18.2
25	71.13	0.8	204	34.3	40.52	-0.3	199	27.5
30	71.59	1.5	203	33.1	41.1	1.1	196	26.0
	1,000 times diluted sample - Average data fitting error from experimental data 4.0%				1,000,000 times diluted sample - Average data fitting error from experimental data: 4.4%			
Time (hrs)	Calculated R_T (Ω)	Deviation from baseline (%)	Calculated C_T (nano Farad)	Deviation from baseline (%)	Calculated R_T (Ω)	Deviation from baseline (%)	Calculated C_T (nano Farad)	Deviation from baseline (%)
0	97.91	-	153	-	69.23	-	156	-
5	98.00	0.1	153	-0.1	69.47	0.3	153	-2.1
10	98.16	0.3	159	4.4	69.39	0.2	152	-2.2
15	98.43	0.5	180	18.0	69.46	0.3	151	-3.0
20	98.21	0.3	196	28.1	68.87	-0.5	159	2.1
25	98.29	0.4	200	30.8	68.95	-0.4	183	17.1
30	98.38	0.5	199	30.4	65.54	-5.3	199	27.7

In Table 4-2, the absolute values found by convergence of the Nelder Mead method on model 1 is presented for all the samples. The resistance does not show reliable variation. However, the capacitance of the system shows continuous sudden improvement as time progresses. Even though mathematically describing the growth of bacteria is valuable, what is considered more important in the context of this research is to be able to estimate the biomass real-time of the changes occurring with the capacitance magnitudes.

4.4.4 Optical absorptance curve

After thorough analysis and comparison of direct counting results, it was found that the bacterial population (P) would be described most accurately by an exponential relationship against the optical absorbance values, in that:

$$P\left(\frac{\text{cells}}{\text{ml}}\right) = \alpha . e^{\beta . OD_{600}} , \quad (4\text{-}6)$$

where, in the case of our experiments, $\alpha = 9{,}202{,}824$ and $\beta = 5.6024$ with and R^2 value of 0.995.

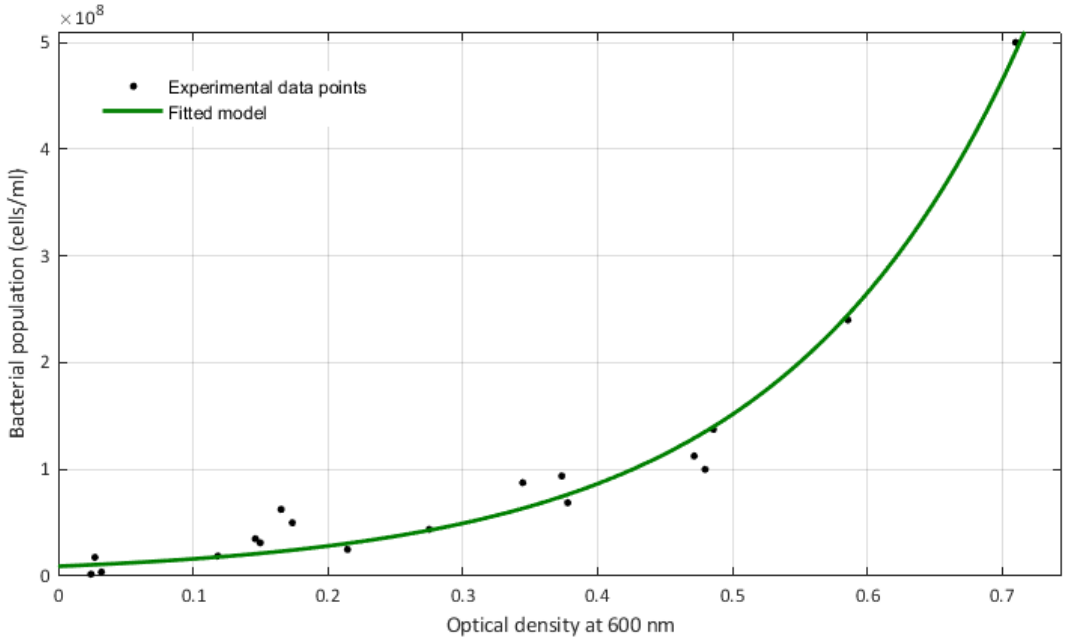

Figure 4-6*. Shows the exponential relationship between the optical density measurements at 600 nm with the direct count of bacteria obtained from hemocytometry. The green line is the developed model describing the relationship.*

The exponential increase in the number of viable cells growing over time is practically due to the smaller mass (volume)/cell ratio that occurs in the samples at higher optical densities. This behavior over the course bacterial proliferation has also been noticed before by Sezonov et al. (Sezonov et al, 2007), where they found that the mass per cell ratio declines at higher optical absorbances. Therefore, as bacterial cells start to reproduce and the number of cells increase, the mass/cell ratio decreases. Hence, the turbidity induced by a certain number of bacterial cells would be lower than expected at the beginning of the proliferation and before maturation of cells in terms of their size.

4.4.5 Biomass estimation, detection threshold, and limit

The biofilm analyzer proved to provide real-time growth monitoring. The logarithmic growth of bacteria occurs in all samples, that have the potential to grow logarithmically. The optical density measurements that were carried out simultaneous to the impedance tracking, allowed us to discover the absorbance of every sample at the point in time when the impedance sensing device

starts to see a rapid spike in capacitance. By populating the data of all the samples, it was possible to find a relationship between the change in capacitance (C´) and population of bacteria (P´) from their starting values (C_0 and P_0) for all the samples. This relationship, that enables us to estimate the increase in bacterial population at any point of time by knowing the change in capacitance, is an exponential curve that is described in Equation 4-7. A lower limit of detection exists due to the inherent limitation of the optical spectrophotometer in finding an absorbance value for samples with lower than 9.2×10^6 cells/ml (Equation 4-6). The estimation of population was achieved by using the optical density measurements and the pre-derived exponential equation of population against optical density (Equation 4-6) as well as the measured capacitance values at 1,000 Hz over time. Through curve fitting, the model that could provide the smallest standard deviation from the experimental data was obtained. This model is an exponential relationship as such:

$$P' \left(\frac{\text{cells}}{\text{ml}}\right) = A.\, e^{B.C'}, \tag{4-7}$$

As was also mentioned in section 2.7, the population increases exponentially against optical density. The values of the coefficients are summarized in Figure 4-7.

Since the absolute capacitance values differ from channel to channel due to physical reasons, the change in capacitance (C´) over the change in population of bacteria (P´) was selected to find correlations between impedance measurements and bacterial concentrations, Figure 4-7. The change in capacitance and the change in population at any point of time (C_t and P_t) from their initial values (C_0 and P_0) were calculated using the equations 4-8 and 4-9, respectively, to remove the bias that exists in the capacitance measurements due to the inherent capacitance magnitude in different channels.

$$C' = C_t - C_0 \tag{4-8}$$

$$P' = P_t - P_0 \tag{4-9}$$

By plotting C´ against P´ for all samples, exponential curves could be fit to data as the population change estimation models with respect to change in capacitance. Figure 4-7 shows the change in population over the change in capacitance for all the samples. Exponential models that were found as the best possible fits are described in the plot in terms of their

exponential coefficients (values A and B in Equation 4-7), and their R^2 as the representative of the fitting goodness.

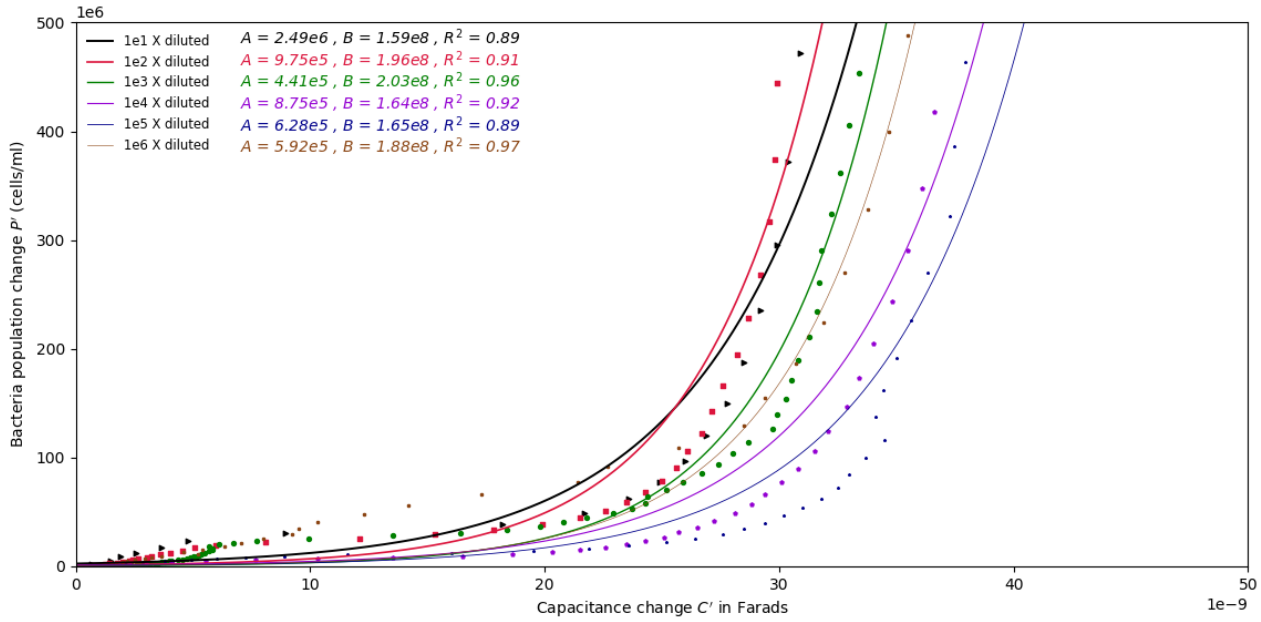

Figure 4-7. *This graph shows the change in population over the change in capacitance for all the samples. Exponential models fit the curves of all samples. The change in population over change in capacitance does not show dependence on the initial concentration of bacteria.*

In order to have a generic relationship between the bacterial concentration and capacitance change regardless of bacterial initial concentration, a single model was developed that is also governed by an exponential relationship such as Equation 4-7. This model, that is developed by calculating the mean of the population estimation curves of all the 6 samples, is capable of estimating bacterial populations of up to 5×10^8 cells/ml. The values of the corresponding coefficients in Equation 4-7 for this curve are summarized in the Figure 4-8(a).

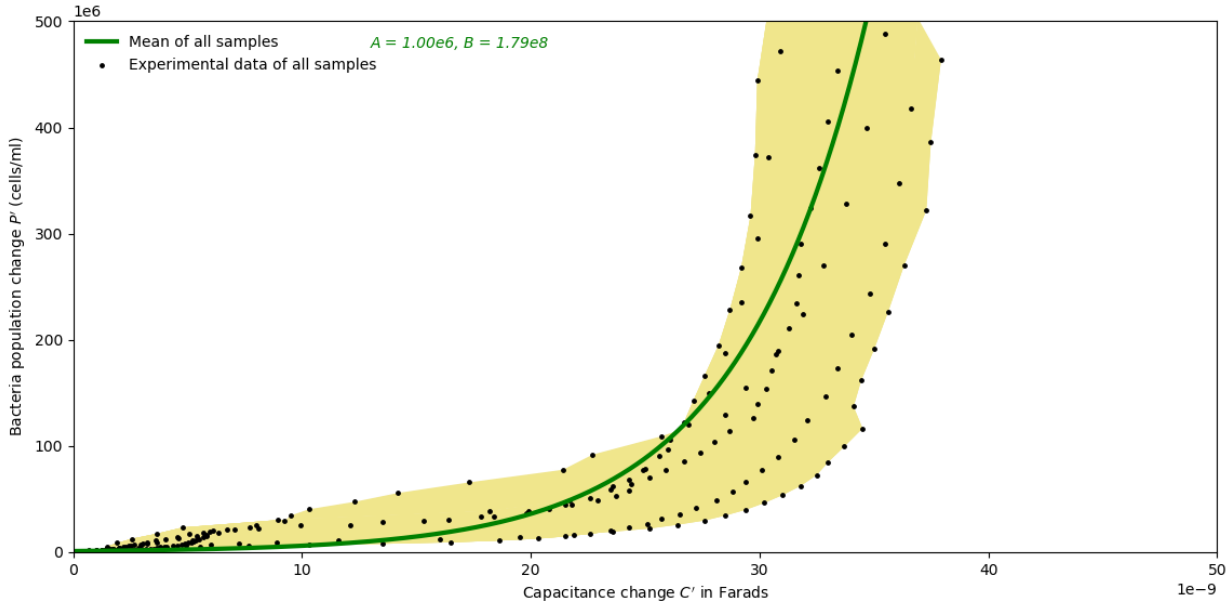

(a)

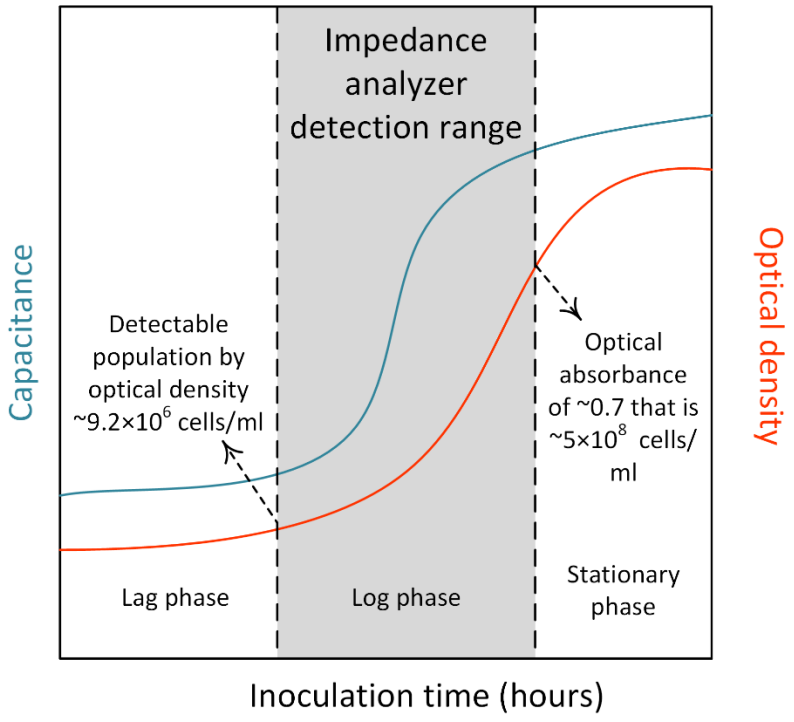

(b)

Figure 4-8. (a) *This plot aims to provide a population change estimation relationship against the change in capacitance. The filled khaki-colored area is the in-between area of all the data points measured from samples that started the experiment with less than 9.2×10^6 cells/ml. Calculating the mean of the exponential population estimation curves from all samples lead to the development of the generic model that is drawn by a green line.* ***(b)*** *A schematic plot of the capacitance and optical density change over time. The logarithmic growth phase occur at the same time as the capacitance increase happens. The*

pre-derived relationship of population against optical density sets a lower detection limit of 9.2×10^6 cells/ml, and the stoppage of the capacitance change sets an upper limit of 5×10^8 cells/ml.

It is regarded as a conclusion that the fact that bacterial growth observed via optical density measurements are simultaneous to the spikes in capacitance values allowed us to develop and estimation curve between the change of capacitance from initial value and the change of bacterial population from the starting amount. However, as schematically shown in Figure 4-8(b), the spike in capacitance occurs a little while earlier than the exponential increase in the optical density measurements. One may surmise that, due to the long-term monitoring of bacterial impedance, some evaporation may occur in the wells that might affect the results. To minimize this effect, during the experiments, lids and caps were used for the samples both in the wells for impedance monitoring and the samples in the cuvettes for optical absorbance monitoring, respectively. That being said, further evaluation of how evaporation can affect the impedimetric changes could be conducted.

4.4.6 Replicate measurements of 90% stepwise diluted samples

A couple of experiments were conducted to further verify the results obtained from the impedimetric monitoring of the 1:10 serially diluted samples. In both of these tests, the steady-state bacterial solution, that was prepared by overnight culturing of bacteria in LB broth, was serially diluted by 1:10 ratio, ranging from 10 times more dilute to 10^7 more dilute bacterial samples.

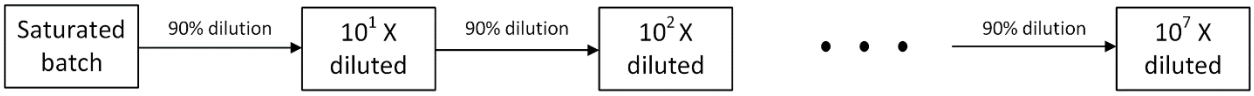

***Figure 4-9**. Depicts the creation procedure of 10-fold serially diluted bacterial samples*

The samples were inoculated inside the 7 wells of the electrode plate. The 8^{th} channel was intentionally left without sample to be connected of a controlled and constant RC value as a baseline to measure any possible external noises in the system.

***Figure 4-10**. Shows the distribution layout of bacterial samples in the 8 wells of the E-plate microelectrode for the impedance testing of samples 50% stepwise dilution.*

Both of these tests are trials for replicating of the same experiment as discussed in section 4.4.1 to gain extra confidence in the claims and conclusions. The only difference is, instead of using the 7^{th} channel for the monitoring of the steady-state bacterial solution, sample that was diluted 10^7 was monitored. That means for these tests, 7 samples serially diluted 1:10 were prepared as opposed to previously discussed test where 6 samples serially diluted 1:10 were prepared and tested together with the non-diluted sample, as the control sample. As well, due to possible initial concentration difference between the biological samples prepared in one test compared to the other, even though similar incubation and dilution procedure was followed for the preparation of the samples, these results are presented in separate graphs and in the following sections.

4.4.6.1 First replication of 90% dilution test results

The results of this experiment do not show any discrepancy with the previous conclusions asserted and reviewed in section 4.4.1. In this experiment, the impedimetric sudden changes occur in the sequence of the concentration of bacterial solutions. Generally, the impedance magnitude displays a sudden decrease and the capacitance shows a spike in their values. Figure 4-11 includes the results of impedimetric monitoring of the serially diluted samples at 1,000 Hz over time. It can be seen in Figure 4-11 (b and c) that the resistance and phase angle have random fluctuations and do not seem to show uninterrupted alterations. As well, the amount of change in the phase angle is quite minimal from the beginning to the end of the experiment, around 3% of variation. Therefore,

capacitance and impedance magnitude could provide a more continual means of monitoring of bacterial growth.

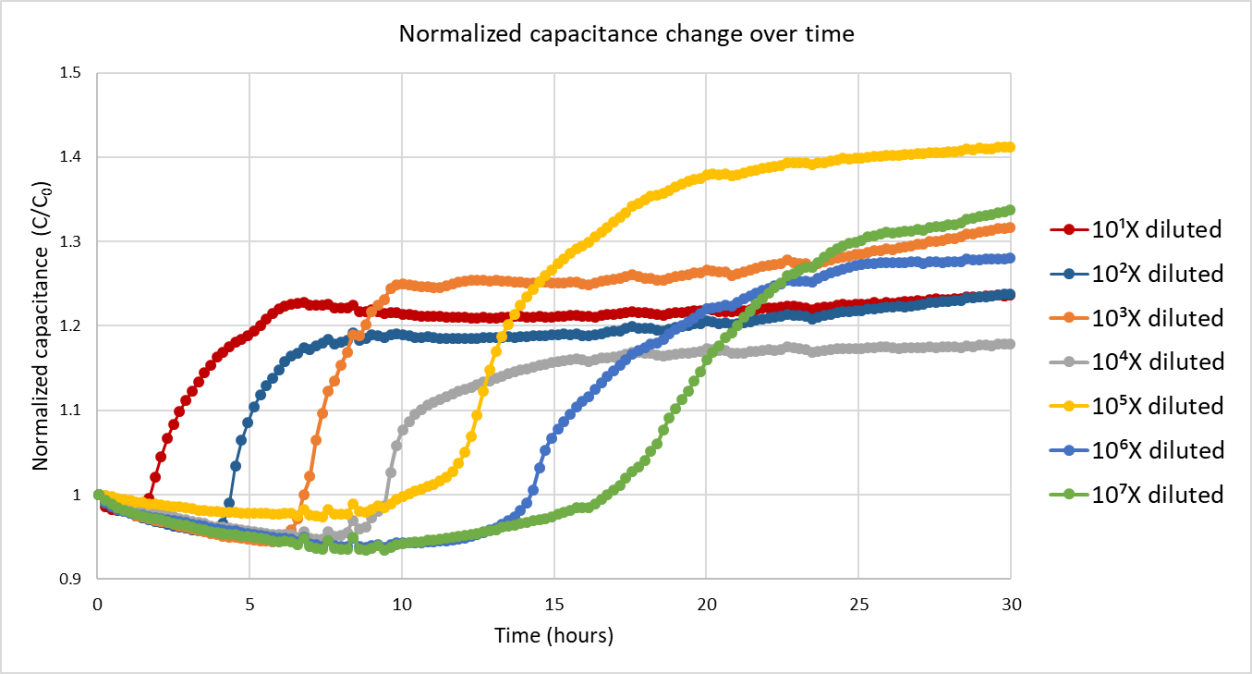

(a)

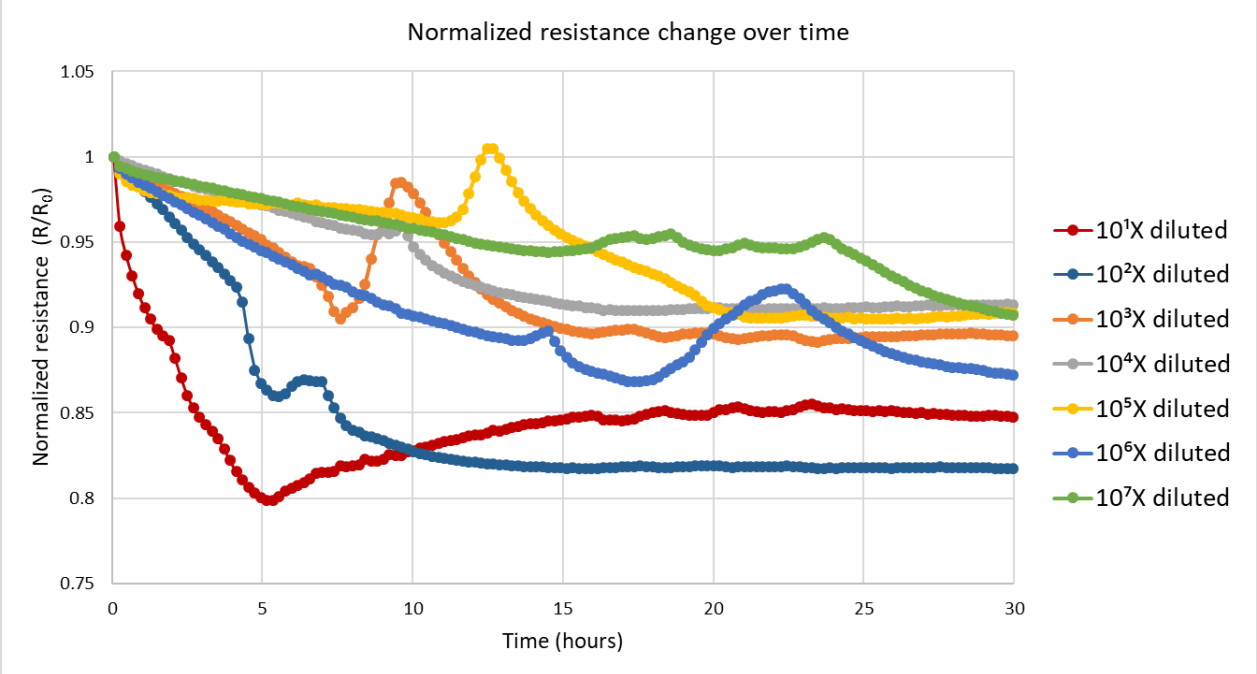

(b)

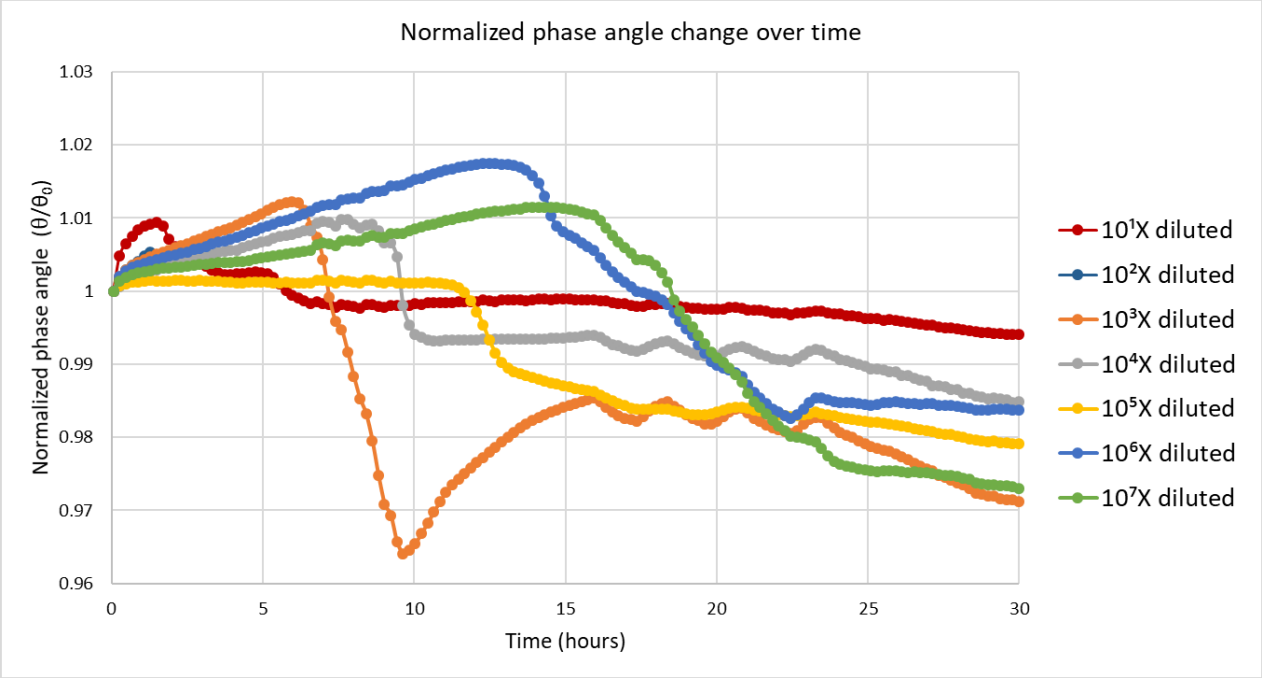

(c)

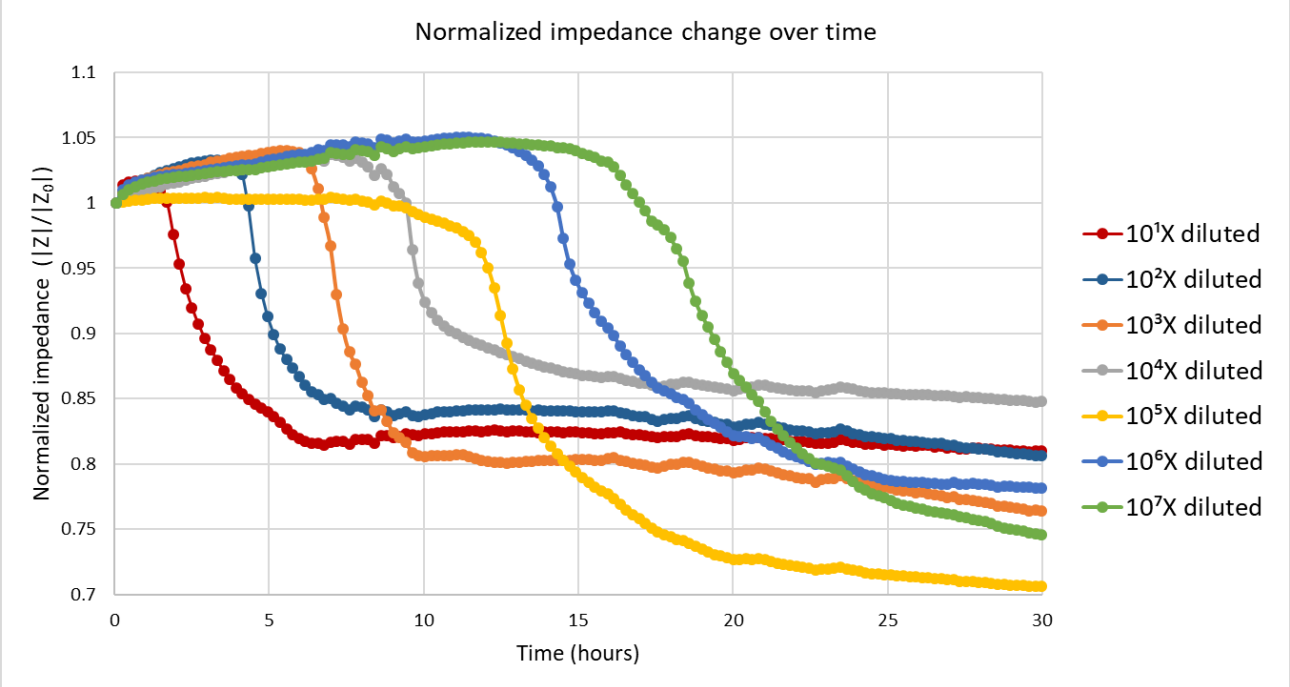

(d)

Figure 4-11. *Monitoring of the impedance values over time for all the 7 samples at 1,000 Hz.* ***(a)*** *Capacitance of the samples start to increase rapidly one after another in the order of their concentration. Data points are obtained approximately every 12.2 minutes.* ***(b)*** *The resistances of the samples do not represent continuously increasing or decreasing trend, even though it has decreased overall for all samples compared to their starting point.* ***(c)*** *Shows the changes in*

normalized phase angle measured from the samples. The variations are insignificant, about 3%. ***(d)*** *The impedance magnitudes of the samples start to plummet one after another in the order of their concentration. The higher initial concentration, the earlier the plunge in the impedance magnitude.*

4.4.6.2 Second replication of 90% dilution test results

This experiment was also carried out as the second replication of impedance measurement of 10-fold serially diluted samples to further evaluate the capabilities and robustness of the system. The normalized impedimetric changes of samples over time at an excitation frequency of 1,000 Hz is provided in the Figure 4-12 (a-d). Attesting the previously presented results, the capacitance and impedance magnitude provide clear rapid increases and decreases in their values, respectively. The resistances of the samples decrease compared to their starting point. The normalized phase angle values show some increase at the beginning but do not stay persistent over the course of the experiment.

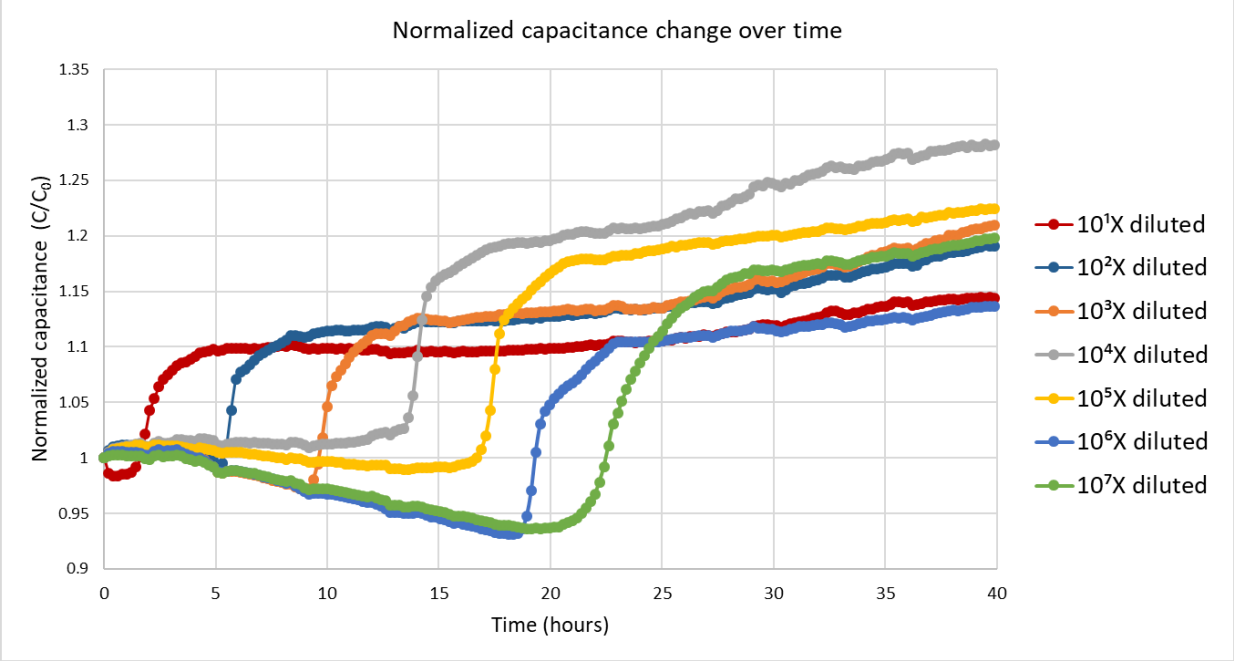

(a)

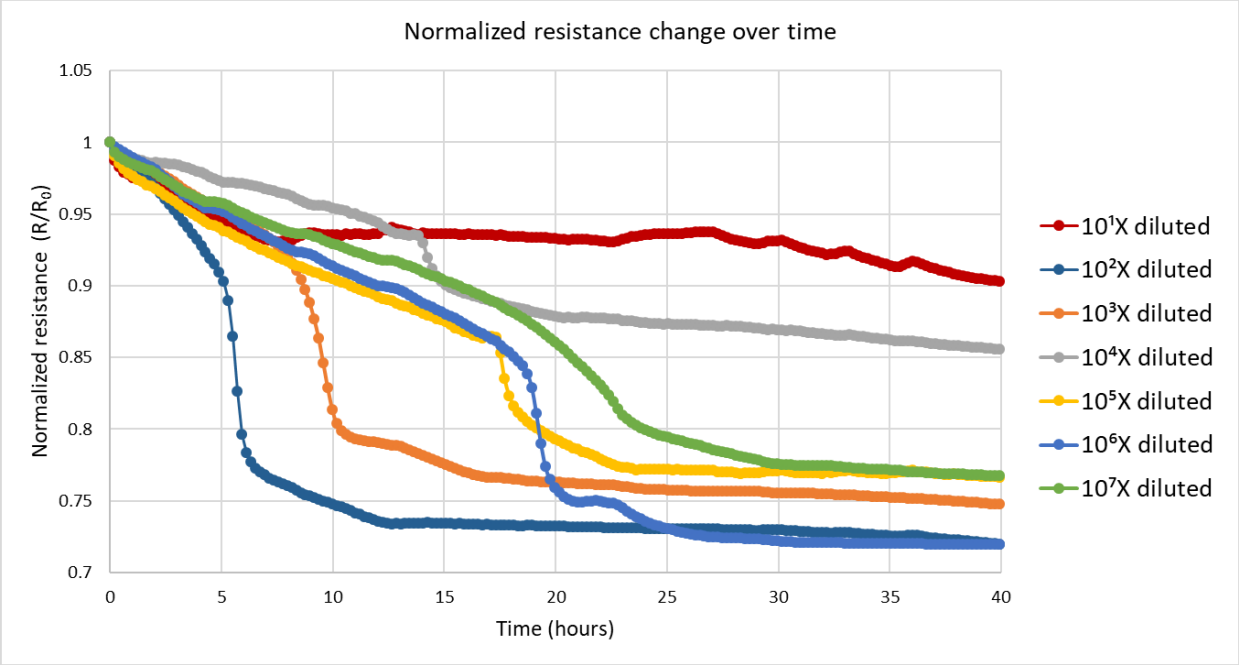
Normalized resistance change over time
Normalized resistance (R/R0)
Time (hours)
10¹X diluted
10²X diluted
10³X diluted
10⁴X diluted
10⁵X diluted
10⁶X diluted
10⁷X diluted

(b)

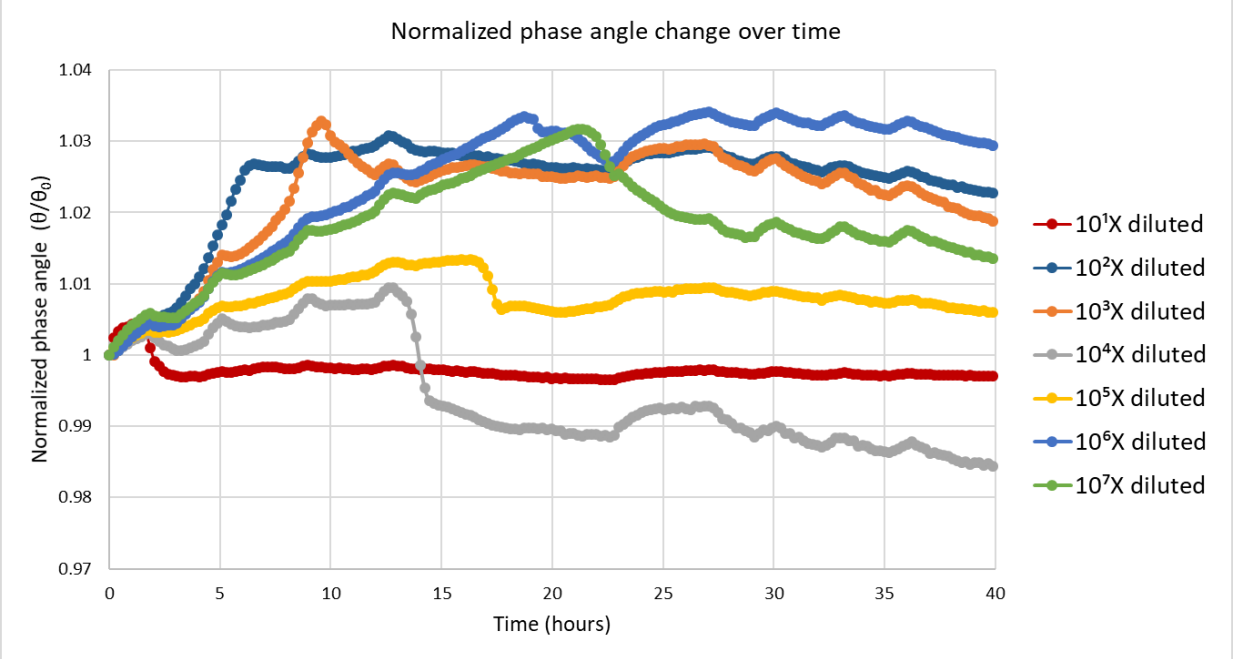
Normalized phase angle change over time
Normalized phase angle (θ/θ0)
Time (hours)
10¹X diluted
10²X diluted
10³X diluted
10⁴X diluted
10⁵X diluted
10⁶X diluted
10⁷X diluted

(c)

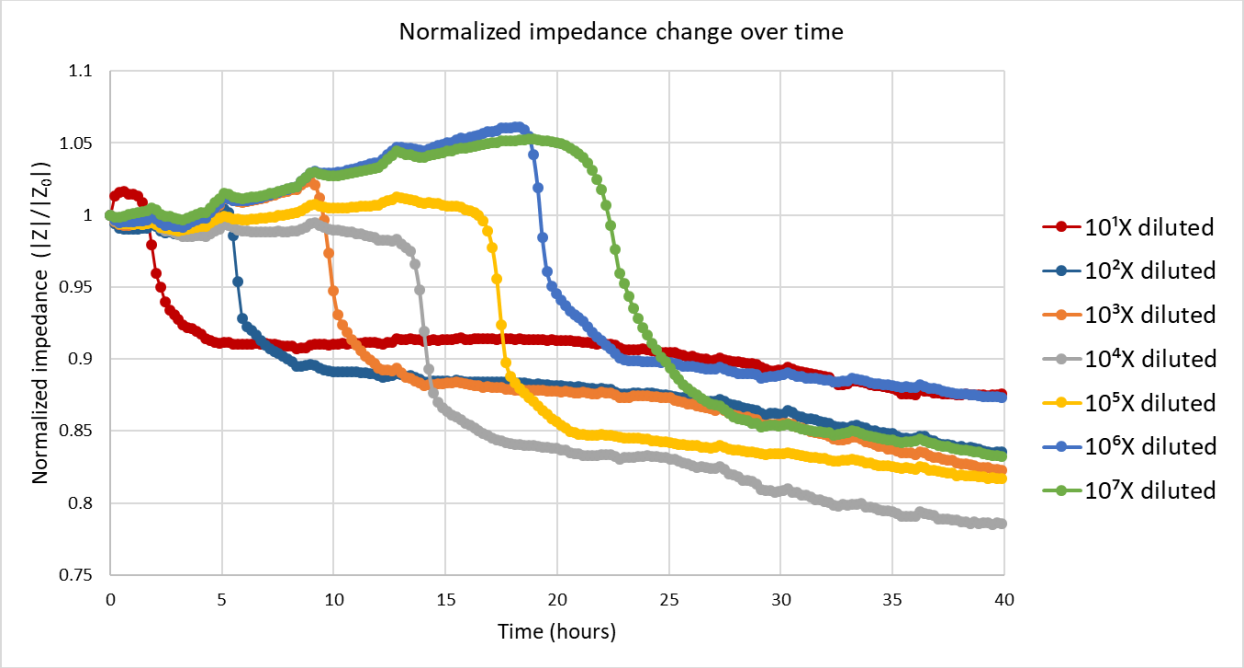

(d)

Figure 4-12*. Monitoring of the impedance values over time for all the 7 samples at 1,000 Hz.* ***(a)*** *Capacitance of the samples start to increase rapidly one after another in the order of their concentration. Data points are obtained approximately every 12.2 minutes.* ***(b)*** *The resistances of the samples do not represent continuously increasing or decreasing trend, even though it has decreased overall for all samples compared to their starting point.* ***(c)*** *Shows the changes in normalized phase angle measured from the samples. The variations are insignificant, about 3%.* ***(d)*** *The impedance magnitudes of the samples start to plummet one after another in the order of their concentration. The higher initial concentration, the earlier the plunge in the impedance magnitude.*

4.5 Conclusions

An affordable bacterial analyzer was manufactured, tested and verified for the purpose of real-time bacterial monitoring that utilizes impedance spectroscopy. The growth of a strain of *Pseudomonas Putida* was evaluated with this setup and the results show that the setup is capable of monitoring the growth of bacteria. Further analysis was executed to correlate impedance results to biomass concentration and availability. Novelties demonstrated in the present work are the automation and affordability of the monitoring system as well as the bacterial growth validation in tandem of the impedance measurements which further confirms the capability of the system. Other bacterial strains could potentially be tested with the same setup. This system can be used in many different applications, such as biomass availability estimation in the wastewater facilities. To date, no tool with similar working principle has been used for such application. Further work

could be conducted to improve the portability of the system, such as using small-sized impedance evaluation circuit boards and power supplies. The detection range of the system may also be improved if an optimization study is conducted on the size of the microelectrodes. As well, the counting of bacteria, biomass availability calibration, and the preventing of evaporation of samples could be improved by utilization other methods.

Chapter 5 CONCLUSIONS & RECOMMENDATIONS

5.1 General conclusions

This research focused on the in-situ monitoring means of bacterial biofilms for the purpose of water quality improvement. There is a vast necessity in the development of monitoring sensors for the improvement of bioremediation facilities efficacy. This thesis provides a big picture of the available and experimented methods of monitoring biological existence in general and elucidates the novel in situ methods that have the potential of utilization in field applications. The strengths and weaknesses of each method were reviewed with respect to the application of interest and the proposed method, impedance microbiology, together with its verification means, optical monitoring and hemocytometry direct counting, were introduced. An impedance sensing system capable of long-term monitoring of the impedance of 8 different samples at adjustable frequencies and voltage magnitudes was crafted. A set of experiments was carried out to obtain useful information about the capability of the system.

5.2 Tool development conclusions

The impedance-based monitoring system achieved automated, real-time, easy-to-use, low cost, long term measurements and promising capability, in that the monitored impedimetric properties showed relatively reasonable sensitivity to bacterial growth. This sensing ability was confirmed by using optical and microscopic methods on samples in tandem with the impedance measurements. Using manual direct counting of samples with known optical densities, relationships between the optical density and the count of cells in bacterial solutions was developed. Once the calibration of spectral absorbance was achieved by the help of direct counting of bacteria, the impedance measurements were interpreted in terms of bacterial concentration and biomass availability. By calibrating the optical spectrophotometry using hemocytometry, the latter method, that is a much more cumbersome, time-consuming, and sophisticated task was replaced by the former, spectrophotometry, that provides rapid measurements and could be used to measure bacterial concentration on samples of similar origin as the ones that are under impedance spectroscopy. Such strategy lead to the development of a relationship between the capacitance changes in the sample and the growth of bacteria in the sample under impedance testing.

Supplementary testing and evaluation could be conducted for the improvement of accuracy and robustness of the developed mathematical relationships.

The development of the setup introduced in this thesis provided an inexpensive means of bacterial monitoring that is less than one tenth of the similar products available on the market. To name a couple, ACEA biosciences Inc. and Applied Biophysics are among the very few manufacturers and developers of bacterial monitoring sensors. Their products are impedance-based sensing setups that start from $30,000 and above, whereas our benchtop setup cost about $8,000 and with further improvements mentioned in the Recommendations section below, the cost could even be less than half this amount.

As part of the tool development throughout this research project, an obsolete Olympus IMT-2 microscope was refurbished and is currently capable of being utilized for brightfield, phase contrast and fluorescence microscopy with the means of digital imaging. The upgrades that were done on the microscope's camera, imaging software, and the fluorescence filter cube guarantees the performance of the microscope. In case of needing to upgrade the microscope, there is no need of purchasing a new camera as the currently installed camera is a high-end digital 20.8 MP camera and can be used towards the new setup.

5.3 Recommendations for future work

The current impedance monitoring setup has the capacity of becoming a portable measurement system. This can be achieved by replacing the current precision benchtop components with small evaluation and integrated circuit boards. For instance, instead of the current benchtop LCR meter, AD5933 made by Analog Devices could be used, that is a high precision impedance converter system capable of conducting impedance spectroscopy tests of up to 100 kHz. This on-board frequency generator is also highly affordable and can save thousands of dollars in the overall cost of the system. Other component that could be considered for replacement by portable devices with equivalent capabilities include the power supply used to power the analog switch. These changes can move the system steps closer for in situ monitoring of biofilm.

Further testing could be done to collect more data and therefore, confidence in the calibration of the system. Using the same optical density protocols there is a need of long-term manual monitoring of samples using spectrophotometer. This requires more than one person

during the testing days (usually two-day time span) to take the optical density measurements at the same time as the impedance testing is running, so that optical absorbance data points during the growth of samples are not missed for long periods. More testing could not only improve the confidence of the system's capability but might also lead to the amelioration of the detection range and limits. Other than optical absorbance other methods could be explored as alternative calibration methods for higher accuracy. More hemocytometry of samples could result in improvements in the biomass estimation curves, especially if hemocytometry is accompanied by using an image processing software, such as ImageJ, for the counting of more populated bacterial samples. Human eye can always be inaccurate. As well, biomass assessment methods can be used to calibrate the impedance measurements beyond 5×10^8 cells/ml.

More advanced testing could include the growth measurement of various bacterial strains to see if other usual biofilm-forming microorganisms could induce impedimetric changes during via their growth. Further investigation could also involve the testing of semi-liquid slimy environments to mimic real field conditions. Another aspect of the future developments can be the formulation of a chemically defined growth media with known resistance and capacitance and capable of providing enough nutrients to microorganisms. Such standard liquid media could help with the monitoring of solid samples, such as soil samples, as it provides enough conductivity for the solid sample to be monitored. This can be helpful when field samples are extracted and an impedimetric baseline is required to be compared with the sample for the estimation of its biomass availability.

For higher precision and maximum noise cancelling, it is best to conduct future testing in temperature-controlled environment. In an enclosed lab with HVAC units, the ambient temperature can be set to a specific setpoint to minimize temperature variances during the daytime and nighttime. As well, a thermo-regulated chamber can be crafted for the purpose of supplying a temperature-controlled environment for the microelectrode wells by keeping their ambient temperature at a constant target level. Such chambers, that technically do a similar job as incubators, can also be integrated in a portable setup.

Nanofabricating e-plates or microelectrodes of customized specifications with respect to the biomass size. The microelectrodes used for the testing of the system showed fascinating sensitivity to microbial metabolism. For future work, it perhaps is a good idea to attempt the

manufacturing of such microelectrodes in house using photolithography. This could help cutting the cost down for future purposes. The E-plates from ACEA Biosciences, however, are high quality products and though labelled as disposable, they can be used at least a couple of times by proper and gentle washing with water and soap. As the data indicated, they are well-engineered microelectrodes seeming to provide enough potential for biofilm monitoring. Other microelectrode manufacturer of multi-well microelectrodes that may be a potential supplier is Micrux Technologies in Spain.

Overall, the crafted prototype of the impedance-based bacterial monitoring system may not be ready for field or wide-scale use, but it has provided a powerful first and preliminary steps in reaching the ultimate objective.

REFERENCES

Ahmad, I., Khan, M. S., Altaf, M. M., Qais, F. A., Ansari, F. A. & Rumbaugh, K. P. (2017) Biofilms: an overview of their significance in plant and soil health. *Biofilms in plant and soil health. Wiley, Hoboken*, 1-26.

Alfred B. Cunningham, J. E. L., and Rockford J. Ross (2008) *Biofilms: The hypertextbook*.

Ansari, F. A., Jafri, H., Ahmad, I. & Abulreesh, H. H. (2017) Factors Affecting Biofilm Formation in in vitro and in the Rhizosphere. *Biofilms in plant and soil health*, 275.

Ashworth, T. (2017) LCR Meter vs Impedance Analyzer. 10/10/2019. Available online: https://www.zhinst.com/blogs/tim/2017/08/11/lcr-meter-vs-impedance-analyzer/ [Accessed.

Azeredo, J., Azevedo, N. F., Briandet, R., Cerca, N., Coenye, T., Costa, A. R., Desvaux, M., Di Bonaventura, G., Hébraud, M. & Jaglic, Z. (2017) Critical review on biofilm methods. *Critical reviews in microbiology*, 43(3), 313-351.

Baum, M. M., Kainović, A., O'Keeffe, T., Pandita, R., McDonald, K., Wu, S. & Webster, P. (2009) Characterization of structures in biofilms formed by a Pseudomonas fluorescens isolated from soil. *BMC microbiology*, 9(1), 103.

Belimov, A., Kunakova, A., Safronova, V., Stepanok, V., Yudkin, L. Y., Alekseev, Y. V. & Kozhemyakov, A. (2004) Employment of rhizobacteria for the inoculation of barley plants cultivated in soil contaminated with lead and cadmium. *Microbiology*, 73(1), 99-106.

Bergmans, L., Moisiadis, P., Van Meerbeek, B., Quirynen, M. & Lambrechts, P. (2005) Microscopic observation of bacteria: review highlighting the use of environmental SEM. *International endodontic journal*, 38(11), 775-788.

Brian C. Matlock, R. W. B., David L. Ash, Michael W. Allen, and Andrew F. Page Analyzing Differences in Bacterial Optical Density Measurements between Spectrophotometers.

Brosel-Oliu, S., Uria, N., Abramova, N. & Bratov, A. (2015) Impedimetric Sensors for Bacteria Detection, in Rinken, T. (ed), *Biosensors Micro and Nanoscale Applications*.

Cabala, J. & Teper, L. (2007) Metalliferous constituents of rhizosphere soils contaminated by Zn–Pb mining in southern Poland. *Water, Air, and Soil Pollution*, 178(1-4), 351-362.

Carpentier, B. & Cerf, O. (1993) Biofilms and their consequences, with particular reference to hygiene in the food industry. *Journal of applied bacteriology*, 75(6), 499-511.

Chroma Systems Solutions, I. (2019) *2019: Series & Parallel Impedance Parameters and Equivalent Circuits.*

Colquhoun, K., Timms, S. & Fricker, C. (1995) Detection of Escherichia coli in potable water using direct impedance technology. *Journal of applied bacteriology*, 79(6), 635-639.

Cristiani, P., Franzetti, A. & Bestetti, G. (2008) Monitoring of electro-active biofilm in soil. *Electrochimica acta*, 54(1), 41-46.

Daniels, J. S. & Pourmand, N. (2007) Label-free impedance biosensors: Opportunities and challenges. *Electroanalysis: An International Journal Devoted to Fundamental and Practical Aspects of Electroanalysis*, 19(12), 1239-1257.

Davis, C. A., Atekwana, E., Atekwana, E., Slater, L. D., Rossbach, S. & Mormile, M. R. (2006) Microbial growth and biofilm formation in geologic media is detected with complex conductivity measurements. *Geophysical Research Letters*, 33(18).

Davis, C. A., Pyrak-Nolte, L. J., Atekwana, E. A., Werkema Jr, D. D. & Haugen, M. E. (2010) Acoustic and electrical property changes due to microbial growth and biofilm formation in porous media. *Journal of Geophysical Research: Biogeosciences*, 115(G3).

de Carvalho, C. C. & da Fonseca, M. M. R. (2007) Assessment of three-dimensional biofilm structure using an optical microscope. *BioTechniques*, 42(5), 616-620.

Decho, A. W. & Gutierrez, T. (2017) Microbial extracellular polymeric substances (EPSs) in ocean systems. *Frontiers in microbiology*, 8, 922.

Del Pozo, J. & Patel, R. (2007) The challenge of treating biofilm-associated bacterial infections. *Clinical Pharmacology & Therapeutics*, 82(2), 204-209.

Delatolla, R., Tufenkji, N., Comeau, Y., Lamarre, D., Gadbois, A. & Berk, D. (2009) In situ characterization of nitrifying biofilm: Minimizing biomass loss and preserving perspective. *Water research*, 43(6), 1775-1787.

Dellis, J. & Carpentier, J. (1993) Nelder and Mead algorithm in impedance spectra fitting. *Solid state ionics*, 62(1-2), 119-123.

Devendra H. Dusane , V. L., Travis Jones , Casey W. Peters , Devin Sindeldecker , Amitava Das , Sashwati Roy , Chandan K. Sen , Vish V. Subramaniam , Daniel J. Wozniak , Shaurya Prakash & Paul Stoodley (2019) Electroceutical Treatment of *Pseudomonas aeruginosa* Biofilms. *Scientific Reports*.

Dheilly, A., Linossier, I., Darchen, A., Hadjiev, D., Corbel, C. & Alonso, V. (2008) Monitoring of microbial adhesion and biofilm growth using electrochemical impedancemetry. *Applied microbiology and biotechnology*, 79(1), 157-164.

Donlan, R. M. (2002) Biofilms: microbial life on surfaces. *Emerging infectious diseases*, 8(9), 881.

Donlan, R. M. & Costerton, J. W. (2002) Biofilms: survival mechanisms of clinically relevant microorganisms. *Clinical microbiology reviews*, 15(2), 167-193.

Dunne, W. M. (2002) Bacterial adhesion: seen any good biofilms lately? *Clinical microbiology reviews*, 15(2), 155-166.

Ehosioke, S., Garré, S., Kremer, T., Kemna, A., Huisman, J. A., Zimmermann, E., Javaux, M. & Nguyen, F. (2018) A new method for characterizing the complex electrical properties of root segments.

Electronics-Tutorials (2014) *AC Capacitance and Capacitive Reactance*, 2014. Available online: https://www.electronics-tutorials.ws/accircuits/ac-capacitance.html [Accessed.

Ertürk, G. & Mattiasson, B. (2017) Capacitive biosensors and molecularly imprinted electrodes. *Sensors*, 17(2), 390.

Firstenberg-Eden, R. & Klein, C. S. (1983) Evaluation of a rapid impedimetric procedure for the quantitative estimation of coliforms. *Journal of food science*, 48(4), 1307-1311.

Fischer, M., Triggs, G. & Krauss, T. F. (2016) Optical sensing of microbial life on surfaces. *Appl. Environ. Microbiol.*, 82(5), 1362-1371.

Fischer, M., Wahl, M. & Friedrichs, G. (2012) Design and field application of a UV-LED based optical fiber biofilm sensor. *Biosensors and Bioelectronics*, 33(1), 172-178.

Flemming, H.-C., Schaule, G., McDonogh, R. & Ridgway, H. F. (1994) Effects and extent of biofilm accumulation in membrane systems. *Biofouling and biocorrosion in industrial water systems*, 63-89.

Flemming, H.-C., Tamachkiarowa, A., Klahre, J. & Schmitt, J. (1998) Monitoring of fouling and biofouling in technical systems. *Water science and technology*, 38(8-9), 291-298.

Fujishige, N. A., Kapadia, N. N. & Hirsch, A. M. (2006) A feeling for the micro-organism: structure on a small scale. Biofilms on plant roots. *Botanical journal of the Linnean Society*, 150(1), 79-88.

Garbarini, D. R. & Lion, L. W. (1986) Influence of the nature of soil organics on the sorption of toluene and trichloroethylene. *Environmental science & technology*, 20(12), 1263-1269.

Gnan, S. & Luedecke, L. O. (1982) Impedance measurements in raw milk as an alternative to the standard plate count. *Journal of food protection*, 45(1), 4-7.

Grohmann, E. & Vaishampayan, A. (2017) Techniques in Studying Biofilms and Their Characterization: Microscopy to Advanced Imaging System in vitro and in situ. *Biofilms in Plant and Soil Health*, 215.

Grossi, M., Lanzoni, M., Pompei, A., Lazzarini, R., Matteuzzi, D. & Riccò, B. (2010) An embedded portable biosensor system for bacterial concentration detection. *Biosensors and Bioelectronics*, 26(3), 983-990.

Hannig, C., Follo, M., Hellwig, E. & Al-Ahmad, A. (2010) Visualization of adherent micro-organisms using different techniques. *Journal of Medical Microbiology*, 59(1), 1-7.

Hannig, C., Hannig, M., Rehmer, O., Braun, G., Hellwig, E. & Al-Ahmad, A. (2007) Fluorescence microscopic visualization and quantification of initial bacterial colonization on enamel in situ. *Archives of oral biology*, 52(11), 1048-1056.

Hardy, D., Kraeger, S., Dufour, S. & Cady, P. (1977) Rapid detection of microbial contamination in frozen vegetables by automated impedance measurements. *Appl. Environ. Microbiol.*, 34(1), 14-17.

Hsieh, C.-h. & Davis, A. P. (2005) Evaluation and optimization of bioretention media for treatment of urban storm water runoff. *Journal of Environmental Engineering*, 131(11), 1521-1531.

Inc., A. D. (2019) *ADG708/ADG709 Data sheet* Available online: https://www.analog.com/media/en/technical-documentation/data-sheets/ADG708_709.pdf [Accessed.

Janknecht, P. & Melo, L. F. (2003) Online biofilm monitoring. *Reviews in Environmental Science and Biotechnology*, 2(2-4), 269-283.

Jr., J. P. (1996) Bacterial Metabolism, in Baron S, e. (ed), *Medical Microbiology*, 4th edition edition. Galveston (TX): University of Texas Medical Branch at Galveston.

Kalam, S., Basu, A. & Ankati, S. (2017) Plant Root–Associated Biofilms in Bioremediation. *Biofilms in Plant and Soil Health*, 337.

Khan, U. T. (December, 2010) *Bioretention cell efficacy in cold climates*. MASTER OF SCIENCE The University of Calgary.

Kim, S., Yu, G., Kim, T., Shin, K. & Yoon, J. (2012) Rapid bacterial detection with an interdigitated array electrode by electrochemical impedance spectroscopy. *Electrochimica Acta*, 82, 126-131.

Kim, T., Kang, J., Lee, J.-H. & Yoon, J. (2011) Influence of attached bacteria and biofilm on double-layer capacitance during biofilm monitoring by electrochemical impedance spectroscopy. *Water research*, 45(15), 4615-4622.

Lawrence, J., Korber, D., Hoyle, B., Costerton, J. W. & Caldwell, D. (1991) Optical sectioning of microbial biofilms. *Journal of bacteriology*, 173(20), 6558-6567.

LeFevre, G. H. (2012) Fate and degradation of petroleum hydrocarbons in stormwater bioretention cells.

LeFevre, G. H., Paus, K. H., Natarajan, P., Gulliver, J. S., Novak, P. J. & Hozalski, R. M. (2014) Review of dissolved pollutants in urban storm water and their removal and fate in bioretention cells. *Journal of Environmental Engineering*, 141(1), 04014050.

Lei, Y., Chen, W. & Mulchandani, A. (2006) Microbial biosensors. *Analytica chimica acta*, 568(1-2), 200-210.

Lewandowski, Z. & Beyenal, H. (2003) Biofilm monitoring: a perfect solution in search of a problem. *Water Science and Technology*, 47(5), 9-18.

Liu, L., Xu, Y., Cui, F., Xia, Y., Chen, L., Mou, X. & Lv, J. (2018) Monitoring of bacteria biofilms forming process by in-situ impedimetric biosensor chip. *Biosensors and Bioelectronics*, 112, 86-92.

Lone, M. I., He, Z.-l., Stoffella, P. J. & Yang, X.-e. (2008) Phytoremediation of heavy metal polluted soils and water: progresses and perspectives. *Journal of Zhejiang University Science B*, 9(3), 210-220.

Luster, J., Göttlein, A., Nowack, B. & Sarret, G. (2009) Sampling, defining, characterising and modeling the rhizosphere—the soil science tool box. *Plant and Soil*, 321(1-2), 457-482.

MacKay, S., Abdelrasoul, G., Tamura, M., Lin, D., Yan, Z. & Chen, J. (2017) Using Impedance Measurements to Characterize Surface Modified with Gold Nanoparticles. *Sensors*, 17(9), 2141.

Mallén-Alberdi, M., Vigués, N., Mas, J., Fernández-Sánchez, C. & Baldi, A. (2016) Impedance spectral fingerprint of E. coli cells on interdigitated electrodes: A new approach for label free and selective detection. *Sensing and bio-sensing research*, 7, 100-106.

Mendoza Gonzalez, I. M. & Kloc, J. J. (2012) The study of biological wastewater treatment through biofilm development on synthetic material vs. membranes.

Mihelcic, J. R., Zimmerman, J. B. & Auer, M. T. (2010) *Environmental engineering : fundamentals, sustainability, design*. Hoboken, NJ Chichester: Wiley ; John Wiley [distributor].

Min, J. & Baeumner, A. J. (2004) Characterization and optimization of interdigitated ultramicroelectrode arrays as electrochemical biosensor transducers. *Electroanalysis: An International Journal Devoted to Fundamental and Practical Aspects of Electroanalysis*, 16(9), 724-729.

Ming, Y., Gessei, T., Miyajima, K., Munkhjargal, M., Arakawa, T. & Mitsubayashi, K. (2013) Fluorometric gas-phase biosensor (bio-sniffer) with UV-LED emission light for formaldehyde vapor, *2013 International Conference on Optical MEMS and Nanophotonics (OMN)*. IEEE.

Monroe, D. (2007) Looking for chinks in the armor of bacterial biofilms. *PLoS biology*, 5(11), e307.

Morgan, R., Kohn, S., Hwang, S.-H., Hassett, D. J. & Sauer, K. (2006) BdlA, a chemotaxis regulator essential for biofilm dispersion in Pseudomonas aeruginosa. *Journal of bacteriology*, 188(21), 7335-7343.

Neu, T. R., Manz, B., Volke, F., Dynes, J. J., Hitchcock, A. P. & Lawrence, J. R. (2010) Advanced imaging techniques for assessment of structure, composition and function in biofilm systems. *FEMS microbiology ecology*, 72(1), 1-21.

Nivens, D. E., Chambers, J. Q., Anderson, T. R. & White, D. C. (1993) Long-term, on-line monitoring of microbial biofilms using a quartz crystal microbalance. *Analytical Chemistry*, 65(1), 65-69.

Ntarlagiannis, D., Williams, K. H., Slater, L. & Hubbard, S. (2005a) Low-frequency electrical response to microbial induced sulfide precipitation. *Journal of Geophysical Research: Biogeosciences*, 110(G2).

Ntarlagiannis, D., Yee, N. & Slater, L. (2005b) On the low-frequency electrical polarization of bacterial cells in sands. *Geophysical Research Letters*, 32(24).

O'Toole, G. A. & Ghannoum, M. A. (2004) Introduction to biofilms: conceptual themes, *Microbial Biofilms*American Society of Microbiology, 1-3.

Ominami, Y. (2018) Environmental SEM (Atmospheric SEM), *Compendium of Surface and Interface Analysis*Springer, 165-169.

Pal, N., Sharma, S. & Gupta, S. (2016) Sensitive and rapid detection of pathogenic bacteria in small volumes using impedance spectroscopy technique. *Biosensors and Bioelectronics*, 77, 270-276.

Pamp, S. J., Sternberg, C. & Tolker-Nielsen, T. (2009) Insight into the microbial multicellular lifestyle via flow-cell technology and confocal microscopy. *Cytometry Part A: The Journal of the International Society for Analytical Cytology*, 75(2), 90-103.

Pamp, S. J. & Tolker-Nielsen, T. (2007) Multiple Roles of Biosurfactants in Structural Biofilm Development by Pseudomonas aeruginosa. *Journal of Bacteriology*, 189(6), 2531-2539.

Paredes, J., Becerro, S. & Arana, S. (2014a) Comparison of real time impedance monitoring of bacterial biofilm cultures in different experimental setups mimicking real field environments. *Sensors and Actuators B: Chemical*, 195, 667-676.

Paredes, J., Becerro, S. & Arana, S. (2014b) Label-free interdigitated microelectrode based biosensors for bacterial biofilm growth monitoring using Petri dishes. *Journal of microbiological methods*, 100, 77-83.

Paredes, J., Becerro, S., Arizti, F., Aguinaga, A., Del Pozo, J. & Arana, S. (2012) Real time monitoring of the impedance characteristics of Staphylococcal bacterial biofilm cultures with a modified CDC reactor system. *Biosensors and Bioelectronics*, 38(1), 226-232.

Paredes, J., Becerro, S., Arizti, F., Aguinaga, A., Del Pozo, J. & Arana, S. (2013) Interdigitated microelectrode biosensor for bacterial biofilm growth monitoring by impedance spectroscopy technique in 96-well microtiter plates. *Sensors and Actuators B: Chemical*, 178, 663-670.

Pompei, A., Grossi, M., Lanzoni, M., Perretti, G., Lazzarini, R., Riccò, B. & Matteuzzi, D. (2012) Feasibility of lactobacilli concentration detection in beer by automated impedance technique. *MBAA Technical Quarterly*, 49(1), 11-18.

Radhakrishnan, R., Suni, I. I., Bever, C. S. & Hammock, B. D. (2014) Impedance biosensors: Applications to sustainability and remaining technical challenges. *ACS sustainable chemistry & engineering*, 2(7), 1649-1655.

Radke, S. M. & Alocilja, E. C. (2004) Design and fabrication of a microimpedance biosensor for bacterial detection. *IEEE sensors journal*, 4(4), 434-440.

Rajeb, A. B., Kallali, H., Aissa, N. B., Bouzaiene, O., Jellali, S., Jedidi, N. & Hassen, A. (2009) Soil microbial growth and biofilm expansion assessment under wastewater infiltration percolation treatment process: column experiments. *Desalination*, 246(1-3), 514-525.

Revil, A., Coperey, A., Shao, Z., Florsch, N., Fabricius, I. L., Deng, Y., Delsman, J., Pauw, P., Karaoulis, M. & de Louw, P. (2017) Complex conductivity of soils. *Water Resources Research*, 53(8), 7121-7147.

Reyes-Romero, D., Behrmann, O., Dame, G. & Urban, G. (2014) Dynamic thermal sensor for biofilm monitoring. *Sensors and Actuators A: Physical*, 213, 43-51.

Rodriguez-Mozaz, S., de Alda, M. J. L. & Barcelo, D. (2006) Biosensors as useful tools for environmental analysis and monitoring. *Analytical and bioanalytical chemistry*, 386(4), 1025-1041.

Sammer, M., Laarhoven, B., Mejias, E., Yntema, D., Fuchs, E. C., Holler, G., Brasseur, G. & Lankmayr, E. (2019) Biomass measurement of living Lumbriculus variegatus with impedance spectroscopy. *Journal of Electrical Bioimpedance*, 5(1), 92-98.

Schad, P. A. Preparation and Restriction Digestion of Escherichia coli Chromosomal DNA in garose Plugs for Use in PFGE.

Schaule, G., Griebe, T. & Flemming, H.-C. (2000) Steps in biofilm sampling and characterization in biofouling cases. *Biofilms. Technomic, Lancaster*, 1-21.

Seneviratne, G., Wijepala, P. & Chandrasiri, K. (2017) Developed Biofilm-Based Microbial Ameliorators for Remediating Degraded Agroecosystems and the Environment. *Biofilms in Plant and Soil Health*, 327.

Sezonov, G., Joseleau-Petit, D. & D'Ari, R. (2007) Escherichia coli Physiology in Luria-Bertani Broth. *Journal of Bacteriology*, 189(23), 8746-8749.

Singh, R., Paul, D. & Jain, R. K. (2006) Biofilms: implications in bioremediation. *Trends in microbiology*, 14(9), 389-397.

Sorrells, K. M. (1981) Rapid Detection of Bacterial Content in Cereal Grain Products by Automated Impedance Measurements. *Journal of Food Protection*, 44(11), 832-834.

Strauss, W., Malaney, G. & Tanner, R. (1984) The impedance method for monitoring total coliforms in wastewaters. *Folia microbiologica*, 29(2), 162-169.

Su, L., Jia, W., Hou, C. & Lei, Y. (2011) Microbial biosensors: a review. *Biosensors and bioelectronics*, 26(5), 1788-1799.

Tamachkiarow, A. & Flemming, H.-C. (2003) On-line monitoring of biofilm formation in a brewery water pipeline system with a fibre optical device. *Water Science and Technology*, 47(5), 19-24.

Torres, C. I., Kato Marcus, A. & Rittmann, B. E. (2008) Proton transport inside the biofilm limits electrical current generation by anode-respiring bacteria. *Biotechnology and Bioengineering*, 100(5), 872-881.

Tubía, I., Paredes, J., Pérez-Lorenzo, E. & Arana, S. (2018) Antibody biosensors for spoilage yeast detection based on impedance spectroscopy. *Biosensors and Bioelectronics*, 102, 432-438.

Turolla, A., Di Mauro, M., Mezzera, L., Antonelli, M. & Carminati, M. (2019) Development of a miniaturized and selective impedance sensor for real-time slime monitoring in pipes and tanks. *Sensors and Actuators B: Chemical*, 281, 288-295.

Van Gerwen, P., Laureyn, W., Laureys, W., Huyberechts, G., De Beeck, M. O., Baert, K., Suls, J., Sansen, W., Jacobs, P. & Hermans, L. (1998) Nanoscaled interdigitated electrode arrays for biochemical sensors. *Sensors and Actuators B: Chemical*, 49(1-2), 73-80.

Vanhala, H. & Soininen, H. (1995) Laboratory technique for measurement of spectral induced polarization response of soil sampies 1. *Geophysical prospecting*, 43(5), 655-676.

Varshney, M. & Li, Y. (2008) Double interdigitated array microelectrode-based impedance biosensor for detection of viable Escherichia coli O157: H7 in growth medium. *Talanta*, 74(4), 518-525.

Varshney, M. & Li, Y. (2009) Interdigitated array microelectrodes based impedance biosensors for detection of bacterial cells. *Biosensors and bioelectronics*, 24(10), 2951-2960.

Vasiljevic, D., Kojic, S., Radovanovic, M., Pivas, B., Tadic, A., Mirkovic, S. & Medic, D. COST-EFFECTIVE INTERDIGITATED CAPACITIVE SENSORS FOR EFFICIENT BACTERIA DETECTION.

Vlamakis, H., Chai, Y., Beauregard, P., Losick, R. & Kolter, R. (2013) Sticking together: building a biofilm the Bacillus subtilis way. *Nature Reviews Microbiology*, 11(3), 157.

Wang, R., Lum, J., Callaway, Z., Lin, J., Bottje, W. & Li, Y. (2015) A label-free impedance immunosensor using screen-printed interdigitated electrodes and magnetic nanobeads for the detection of E. coli O157: H7. *Biosensors*, 5(4), 791-803.

Winston, R. J., Dorsey, J. D. & Hunt, W. F. (2016) Quantifying volume reduction and peak flow mitigation for three bioretention cells in clay soils in northeast Ohio. *Science of the Total Environment*, 553, 83-95.

Xu, Y., Dhaouadi, Y., Stoodley, P. & Ren, D. (2020) Sensing the unreachable: challenges and opportunities in biofilm detection. *Current opinion in biotechnology*, 64, 79-84.

Xu, Y., Xie, X., Duan, Y., Wang, L., Cheng, Z. & Cheng, J. (2016) A review of impedance measurements of whole cells. *Biosensors and Bioelectronics*, 77, 824-836.

Yang, L. (2008) Electrical impedance spectroscopy for detection of bacterial cells in suspensions using interdigitated microelectrodes. *Talanta*, 74(5), 1621-1629.

Yang, L., Li, Y. & Erf, G. F. (2004) Interdigitated array microelectrode-based electrochemical impedance immunosensor for detection of Escherichia c oli O157: H7. *Analytical chemistry*, 76(4), 1107-1113.

Yates, M., Strycharz-Glaven, S., Golden, J., Roy, J., Tsoi, S., Erickson, J., El-Naggar, M., Barton, S. C. & Tender, L. (2018) Characterizing electron transport through living biofilms. *JoVE (Journal of Visualized Experiments)*(136), e54671.

Yu, T. (2015) *Modelling biofilm activity in bioretention cells*.

Ziarati, P. & Alaedini, S. (2014) The phytoremediation technique for cleaning up contaminated soil by Amaranthus sp. *J Environ Anal Toxicol*, 4(208), 2161-0525.1000208.

Zibaii, M. I., Kazemi, A., Latifi, H., Azar, M. K., Hosseini, S. M. & Ghezelaiagh, M. H. (2010) Measuring bacterial growth by refractive index tapered fiber optic biosensor. *Journal of Photochemistry and Photobiology B: Biology*, 101(3), 313-320.

APPENDIX A SUPPLEMENTARY DATA

Other than the test results presented in Chapter 4, the results of a set of other testing is presented in this chapter that were carried out as part of the experimental plan for the monitoring system. As the sensing system was first launched and debugged and became ready for testing, the effort was to evaluate its capability and performance. At the beginning, there existed no sense of the system's capability in monitoring bacterial growth. Despite the hypotheses of possible monitoring through impedance measurements learned from literature review, experimentation was required to obtain confidence regarding the system's performance. In this respect, our knowledge of the capability of this system was broadened as each test results were acquired. This means that the experiments were designed based on the lessons learnt from the prior or initial experiments. In this research, a few different goal-oriented tests were conducted. After verifying the device's precision in measuring the impedance of known RC circuits, the first biological test was conducted to understand its capability of showing sensitivity to bacterial growth. All the biological samples of this work were prepared from *Pseudomonas putida* strain. The first few tests were carried using the samples of bacterial cells of unknown concentrations in growth media (LB broth) to compare with results from deionized water. Due to the inconsistencies in sample preparation such initial experiments, next tests were, that are going to be discussed in the next sections, conducted on samples prepared by using specific procedures.

A.1 Monitoring samples centrifuged at different speeds

In this test, a unified set of exercise was applied to the preparation of all the samples. A steady-state batch of bacterial sample was divided into smaller tubes and each tube was centrifuged at a different speed. Using 1,000 g, 3,500 g, and 15,000 g for 2 minutes, the steady-state bacterial samples were centrifuged, and the supernatant was decanted onto the wells of the E-plate for testing, as depicted in Figure A-1.

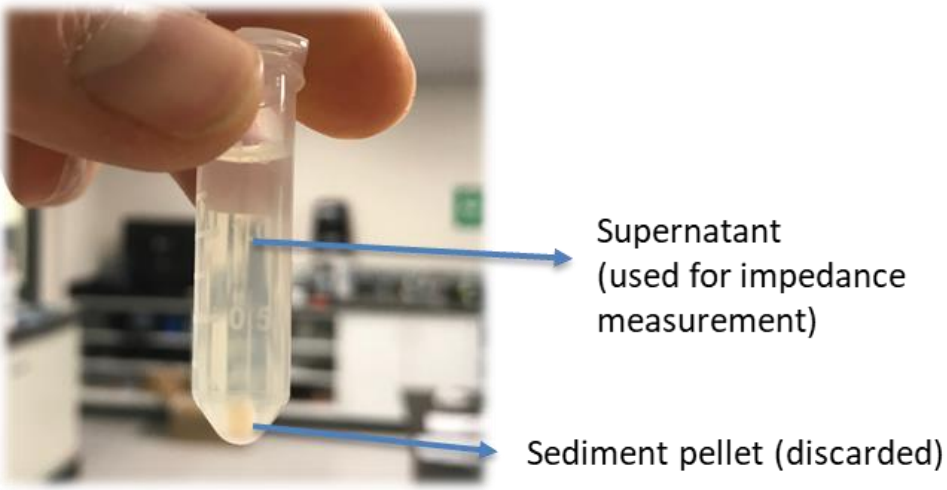

Figure A-1. *The separation of bacterial cells from the solution using centrifugation. The higher the centrifugation speed, the more sedimented bacterial cells and the clearer the supernatant*

The higher the centrifugation speed, the higher sedimentation of bacterial cells, and therefore, the less concentrated the supernatant obtained for the testing. Therefore, varying centrifugation speeds would confidently provide a wide range of concentrations in the bacteria samples. Two duplicates of each samples were used to fill two different wells of the E-plate for further confidence in the results. As depicted in the Figure A-2, channels 1 and 5, were filled with supernatant of 1,000 g centrifugation. The samples centrifuged at 3,500 g were placed in the 2nd and 6th channels, and the sample centrifuged at 15,000 g were situated in channel 3 and 7. Channels 4 and 8 were filled with the uncentrifuged sample, that was basically the steady-state bacterial solution.

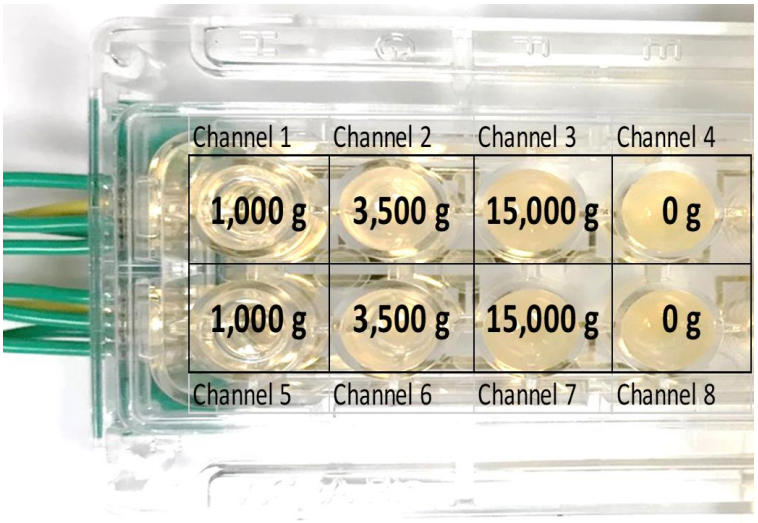

***Figure A-2**. Shows the distribution layout of bacterial samples in the 8 wells of the E-plate microelectrode for the testing of supernatants prepared via centrifugation at different speeds.*

The impedimetric changes of the samples at a fixed frequency of 1,000 Hz are shown in Figure A-2 (a-d). Same as the impedance variation figures presented in Chapter 4, all the impedimetric values presented in this chapter are also normalized by their initial value at time zero of the testing to eliminate the inherent bias of the system.

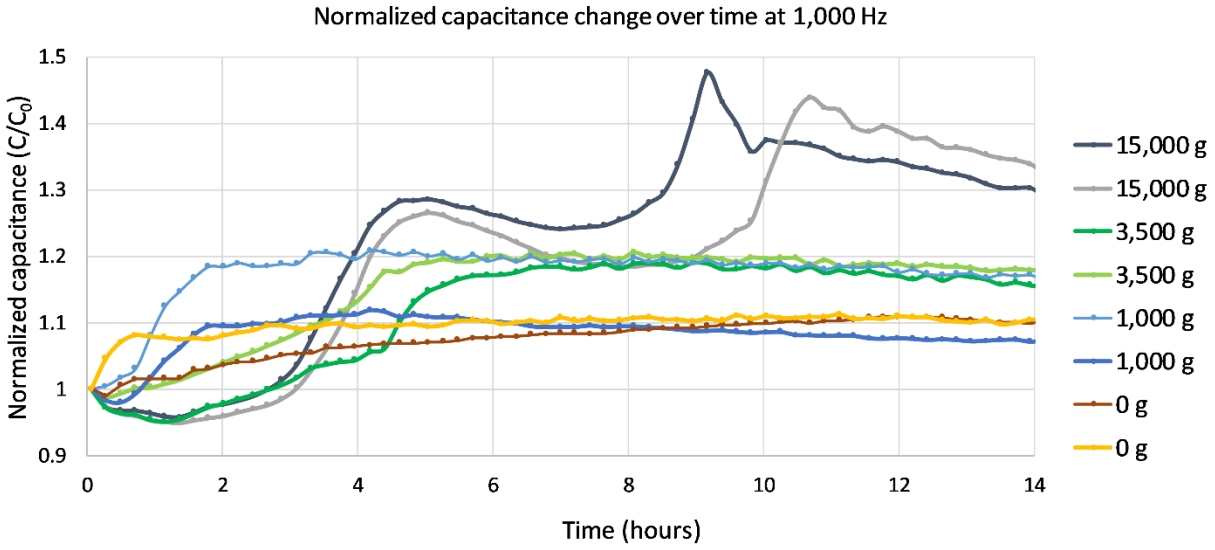

(a)

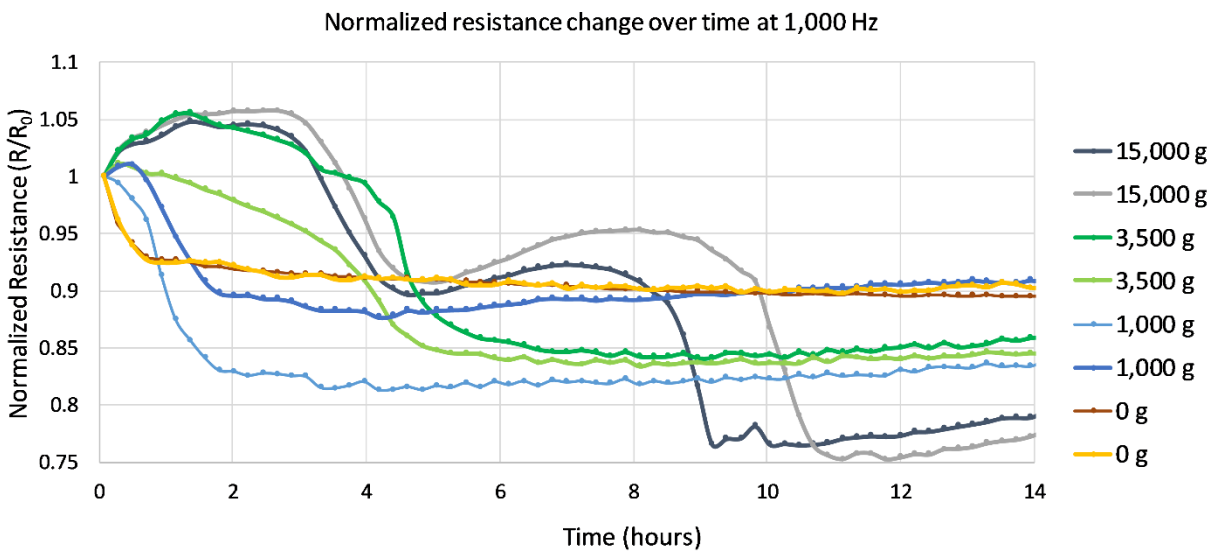
Normalized resistance change over time at 1,000 Hz
Normalized Resistance (R/R0)
1.1
1.05
1
0.95
0.9
0.85
0.8
0.75
0
2
4
6
8
10
12
14
Time (hours)
15,000 g
15,000 g
3,500 g
3,500 g
1,000 g
1,000 g
0 g
0 g

(b)

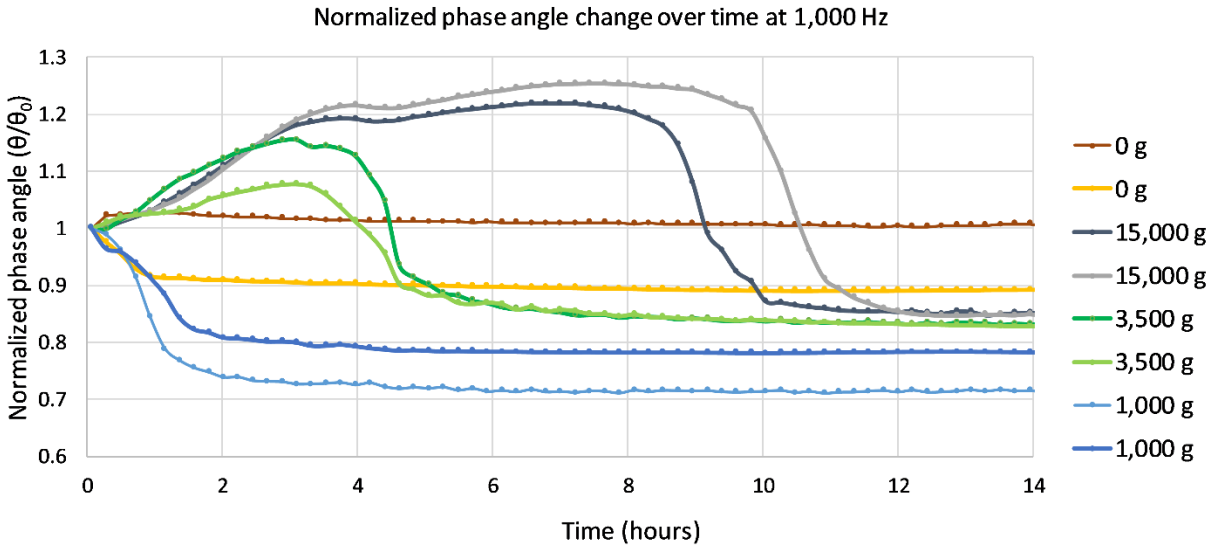
Normalized phase angle change over time at 1,000 Hz
Normalized phase angle (θ/θ0)
1.3
1.2
1.1
1
0.9
0.8
0.7
0.6
0
2
4
6
8
10
12
14
Time (hours)
0 g
0 g
15,000 g
15,000 g
3,500 g
3,500 g
1,000 g
1,000 g

(c)

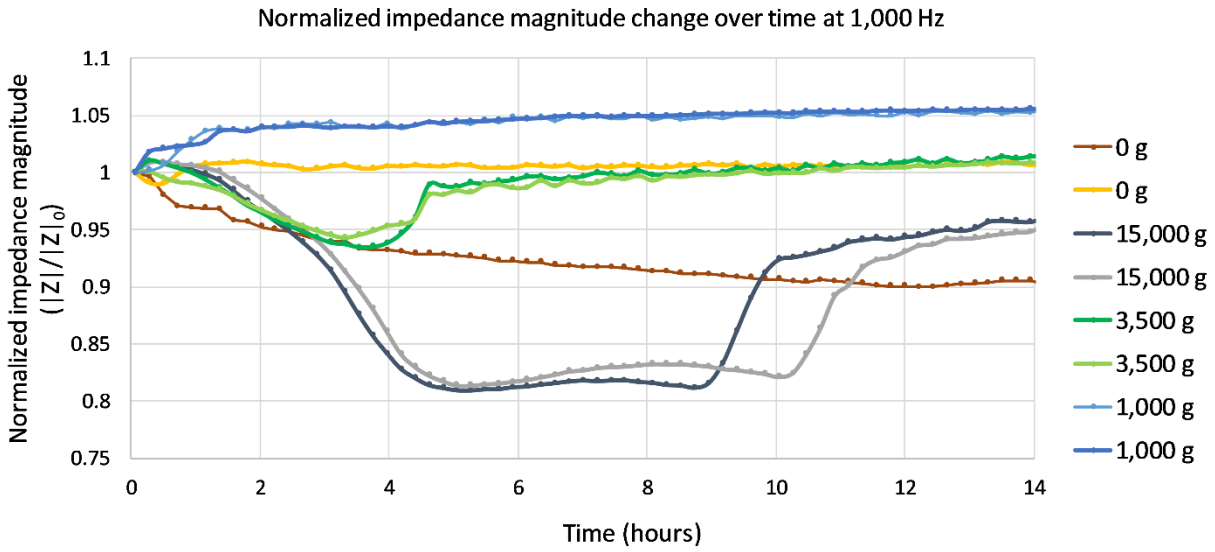

(d)

Figure A-3. *Monitoring of the impedance values over time for all the 6 samples at 1,000 Hz.* ***(a)*** *Capacitance of the samples start to increase rapidly one after another in the order of their dilution. Data points are obtained approximately every 12.2 minutes.* ***(b)*** *The resistances of the samples represent a decrease in their values as the time progresses. These changes are simultaneous to the changes in capacitance.* ***(c)*** *Shows the changes in phase angle of the samples. There exists a solid increase in the phase angle of the samples in the order of their initial concentrations.* ***(d)*** *The impedance magnitudes of the samples start to vary at the same time as other parameters.*

As can be noticed in the Figures A-3 (a-d), the two samples that were centrifuged at higher speed displayed impedimetric changes the latest. Subsequently, samples centrifuged at 1,000 g and 35,00 g showed changes in their impedimetric properties the first and second, respectively. The bacterial samples that were not centrifuged (0 g) stayed mostly constant in terms of the impedimetric features throughout the experiments. The capacitance of the samples demonstrates a more persistent change (increase) over time compared to other parameters. Impedance magnitudes as well as phase angle, for instance, display rises and falls throughout the test. Overall, the observed results comply with the expectations because of three main conclusions. First, the uncentrifuged samples did not show any changes because they had already reached their stationary phase in terms of bacterial growth before the experiment was started, and no more growth or proliferation would exist to cause any impedance alterations. Secondly, the order of changes of impedance in the centrifuged samples implies that these changes are probably due to bacterial proliferation as the more concentrated samples were expected to start their reproduction earlier than the less

concentrated ones. Lastly, the pairs of samples that were different from other pairs only in terms of their centrifugation speed, showed similar impedimetric behavior and at the same time. This means that the impedance variances are not due to random glitches or mismeasurements, Rather, they are due to an inherent parameter that is changing in the samples under the test. As discussed in Chapter 4, it was later confirmed that impedimetric alterations are simultaneous to the optical density escalations, and therefore bacterial reproduction. However, this test lacks information about relative bacterial concentration of the samples. Due to this reason, a set of tests were carried out on samples that were diluted serially.

A.2 Measurement of 50% stepwise diluted samples

A set of samples were prepared via serially diluting a steady-state batch of bacterial solution in LB broth media a 1:2 ratio. Eight samples of different dilution factors, 2^0, 2^1, 2^2, 2^3, 2^4, 2^5, 2^6, 2^7 times diluted, were created for the testing, the 2^0 times diluted sample being the steady-state batch. Optical density and periodical hemocytometry of the different samples were taken to obtain direct measurements of the samples that are under the impedance spectroscopy tests.

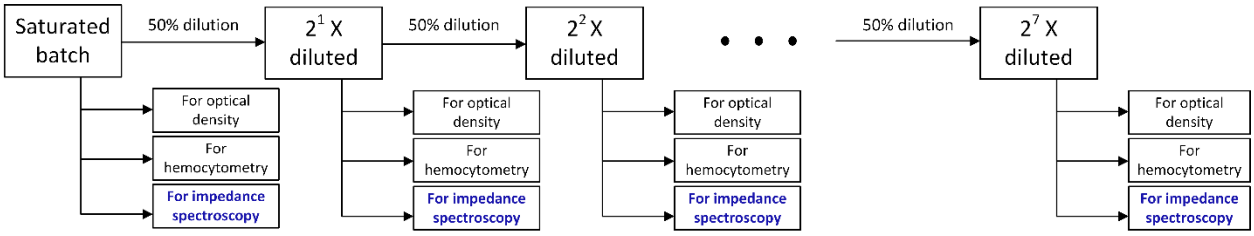

Figure A-4. *This diagram shows the preparation steps taken for the serially diluting samples for the impedance, optical absorbance and hemocytometry measurements.*

Initial optical absorbance values were measured for all samples to find a relationship between the optical density and concentration factor. This was conducted just to make sure about the effectiveness of the serial dilution procedure in providing relative concentrations. As well, this was done at the beginning of the test to eliminate the effect of cell size enhancement that may be influential to the absorbance values. The optical absorbance values of each sample at the start of the test are summarized in Table A-1. The optical transmittance magnitudes are also reported, but absorbance could provide higher number of decimals and therefore higher resolution. In this table and the Figure A-5, the concentration factor (CF) is defined as a value equal to the reverse of the dilution factor for each sample. For example, a sample that is diluted 2^2 from the steady-state batch has a concentration factor of 2^{-2} or $\frac{1}{4}$.

***Table A-1**. The optical absorbance and transmittance values of different samples measured just after the dilution of the samples and before they could have a chance to grow in size or in number.*

Concentration factor	Initial optical absorbance	Initial optical transmittance
1	1.0789	8.3%
2^{-1}	0.6392	23.0%
2^{-2}	0.3571	43.9%
2^{-3}	0.1826	65.7%
2^{-4}	0.0921	80.9%
2^{-5}	0.0458	90.0%
2^{-6}	0.0244	94.5%
2^{-7}	0.0110	97.5%

The relationship obtained from this experiment show that the concentration factor (CF) has a linear relationship with the optical density absorbance, in that:

$$\mathrm{CF} = \gamma . \mathrm{OD}_{600} \quad , \qquad \text{(A-1)}$$

where $\gamma = 0.8702$ in this study and the R^2 for this model is 0.99.

This linear model is depicted in Figure A-5, by plotting the concentration factors and the optical density of the samples.

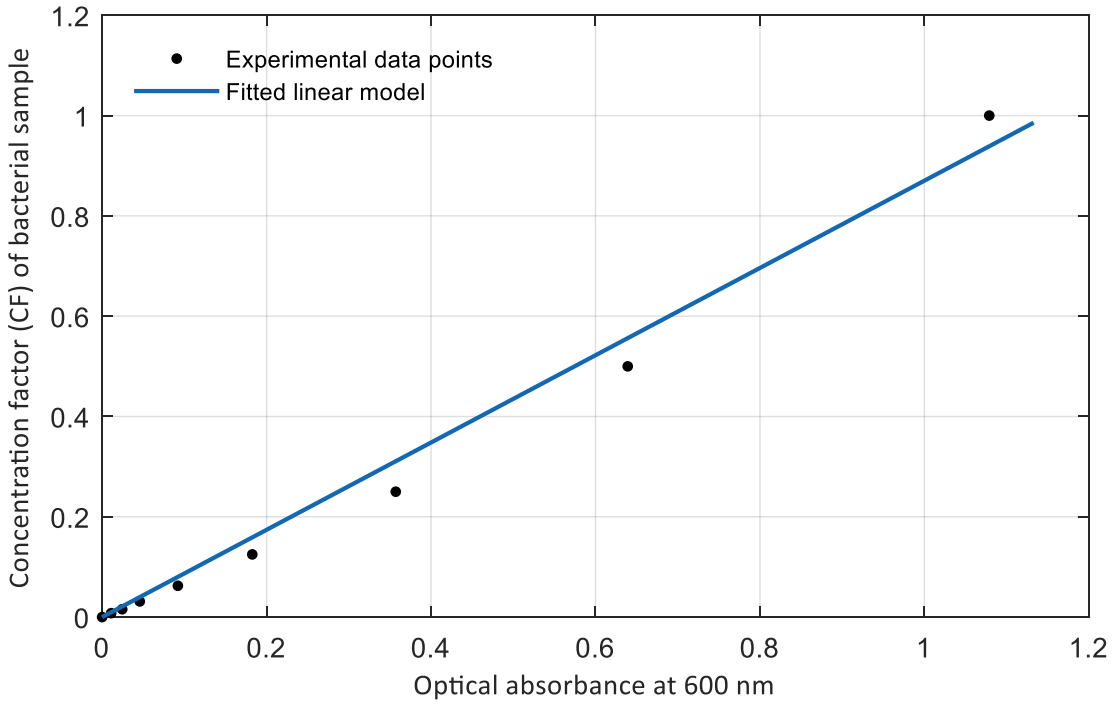

Figure A-5. *Plot includes the linear relationship of the optical density with the concentration factor or the proportionate bacterial density.*

The linearity of the relationship between the dilution factor and optical density is because bacterial cells at different dilutions were not given the chance to grow in size or in number. In essence, the turbidity induced by each cell is technically the same in all samples resulting in a linear relationship between the dilution factor and optical density.

For the impedance measurements, 275 µl of each of the serially diluted samples were decanted onto the eight wells of the E-plate electrode as depicted in the Figure A-6.

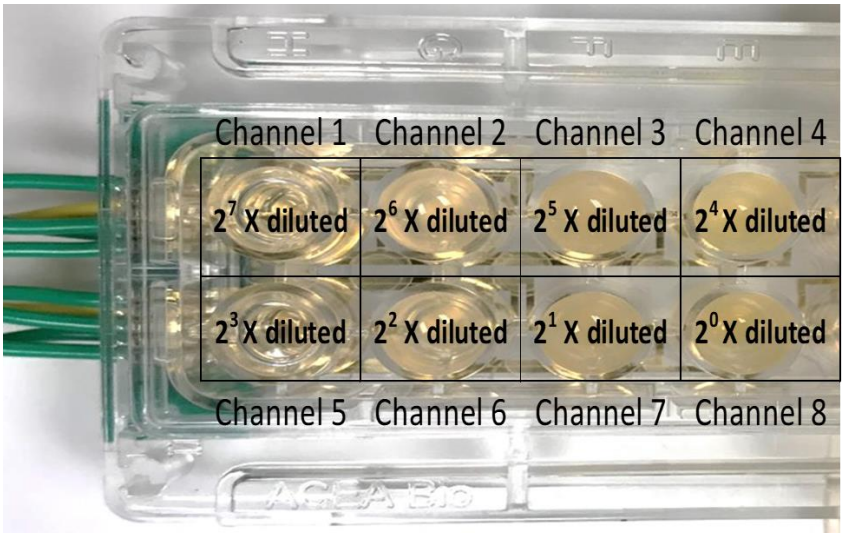

Figure A-6. *Shows the distribution layout of bacterial samples in the 8 wells of the E-plate microelectrode for the impedance testing of samples 50% stepwise dilution.*

The impedance measurements of the samples were obtained from the samples and the results of the changes in the impedimetric properties monitoring over time are summarized in the Figure A-7.

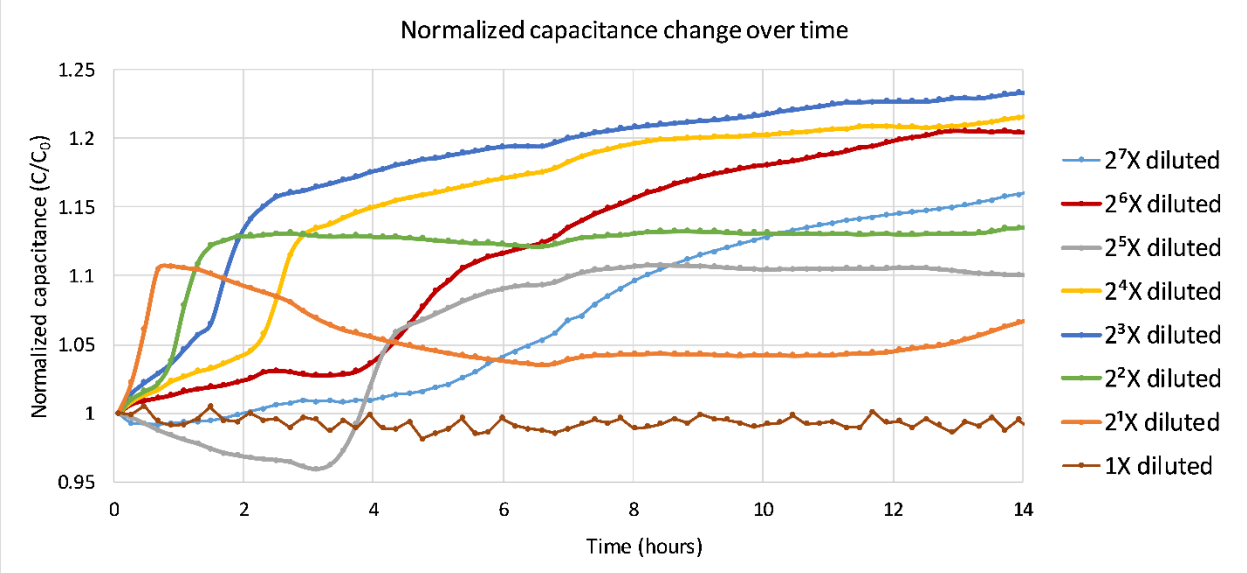

(a)

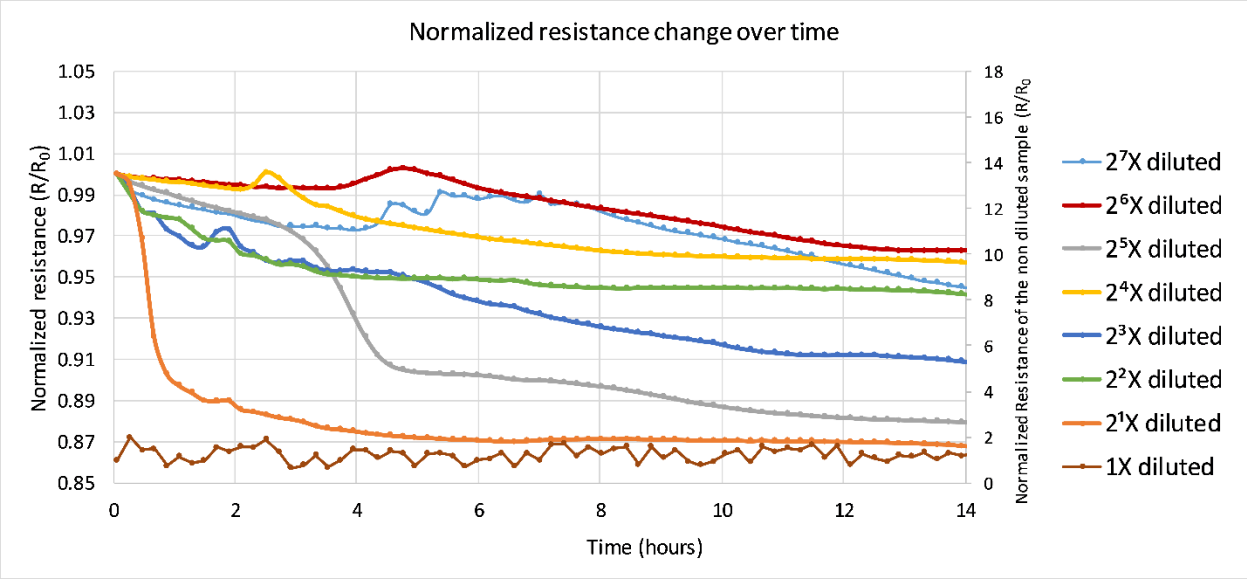
Normalized resistance change over time
Normalized resistance (R/R0)
Normalized Resistance of the non diluted sample (R/R0)
Time (hours)
2^7X diluted
2^6X diluted
2^5X diluted
2^4X diluted
2^3X diluted
2^2X diluted
2^1X diluted
1X diluted

(b)

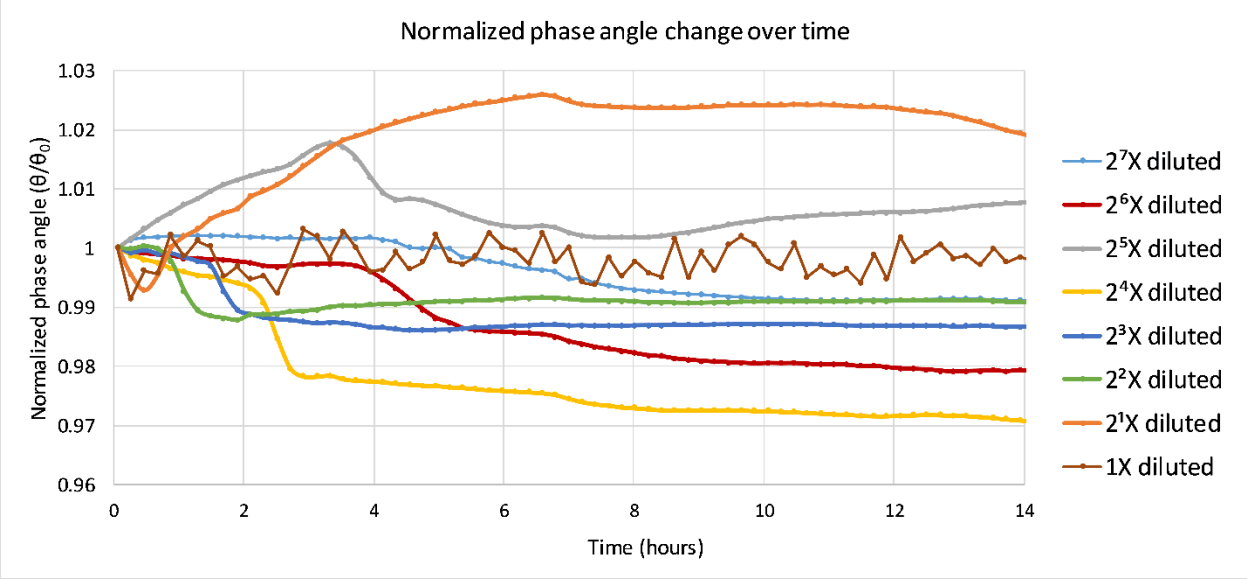
Normalized phase angle change over time
Normalized phase angle (θ/θ0)
Time (hours)
2^7X diluted
2^6X diluted
2^5X diluted
2^4X diluted
2^3X diluted
2^2X diluted
2^1X diluted
1X diluted

(c)

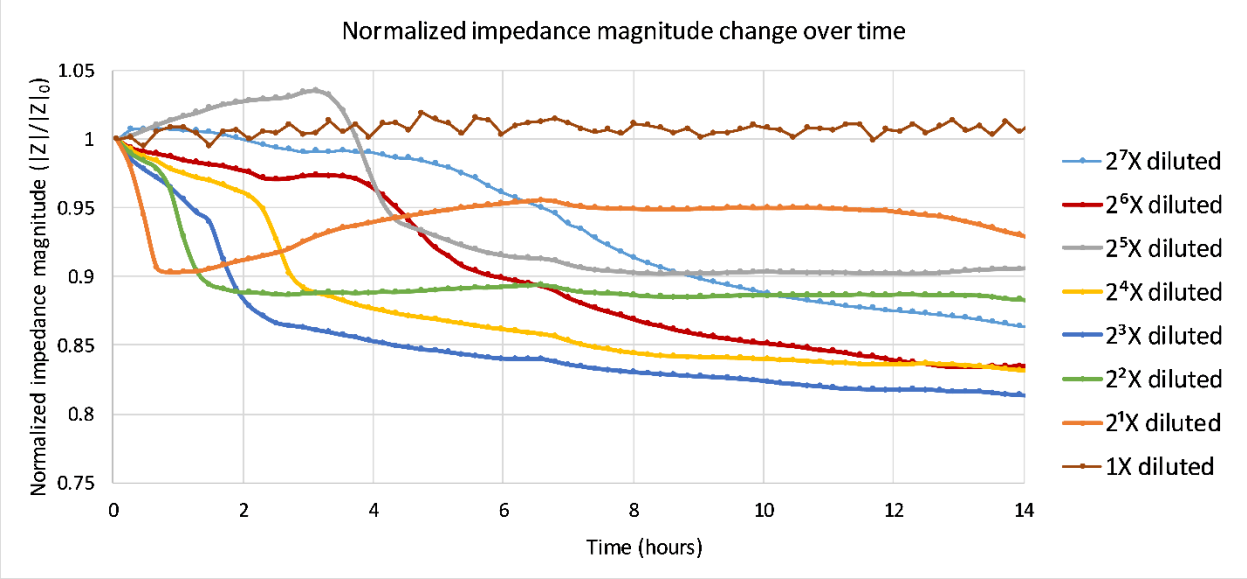

(d)

Figure A-7. *Monitoring of the impedimetric features over time for all the 7 samples at 1,000 Hz. Data points are obtained approximately every 12.2 minutes.* ***(a)*** *Capacitance of the samples start to increase rapidly one after another in the order reverse of their dilution factors.* ***(b)*** *The resistances of the samples do not represent persistent trends, even though there is some decrease observed simultaneous to the capacitance changes in some of the samples.* ***(c)*** *Shows the magnitudes of normalized phase angles. This parameter shows unexpected increases in a couple of the samples.* ***(d)*** *The impedance magnitudes of the samples start to plunge one after another in the order of their dilution.*

Starting from the capacitance of samples over time, as is depicted in Figure A-7(a), the changes sudden occur just after the start of the test within the first 10 hours. The sudden increases in capacitances also occur in the chronological order relative to their starting concentration factor, indicating that the higher the concentration factor, the earlier the occurrence of sudden alterations. In addition, the impedimetric values of the non-diluted (1X diluted – the brown data series) sample, also known as the steady-state sample, remained relatively constant over the course of the experiment, suggesting that the impedimetric changes in other samples are probably due to the reproduction or proliferation of bacterial cells. Resistance, phase angle, and impedance magnitude values were also measured and presented in the Figures A-7 (b-d), respectively. However, as can be seen in the figures, other than expected changes, there exists variances in these parameters that do not seem to have known reasons. This further vindicates the superiority of capacitance in providing consistent and robust measure of bacterial growth over other impedimetric values, as partly discussed in Chapter 4. Other impedimetric properties can be useful in terms of verifying the expected changes. External noises on the system may be also monitored and filtered out from

the system. In later testing, further actions such as using an RC element of known value was implemented for the monitoring and eliminating any possible noise, as was also explained in Chapter 4.

The optical density results that were carried out simultaneous to the impedance measurements on the samples that were put aside for spectroscopy measurements. It is worth noting that these samples were set aside from the same batches of samples as were prepared for the impedance testing. The optical density measurements, that is a measure of the turbidity induced in the growth media due to bacterial activity is depicted in Figure A-8 below.

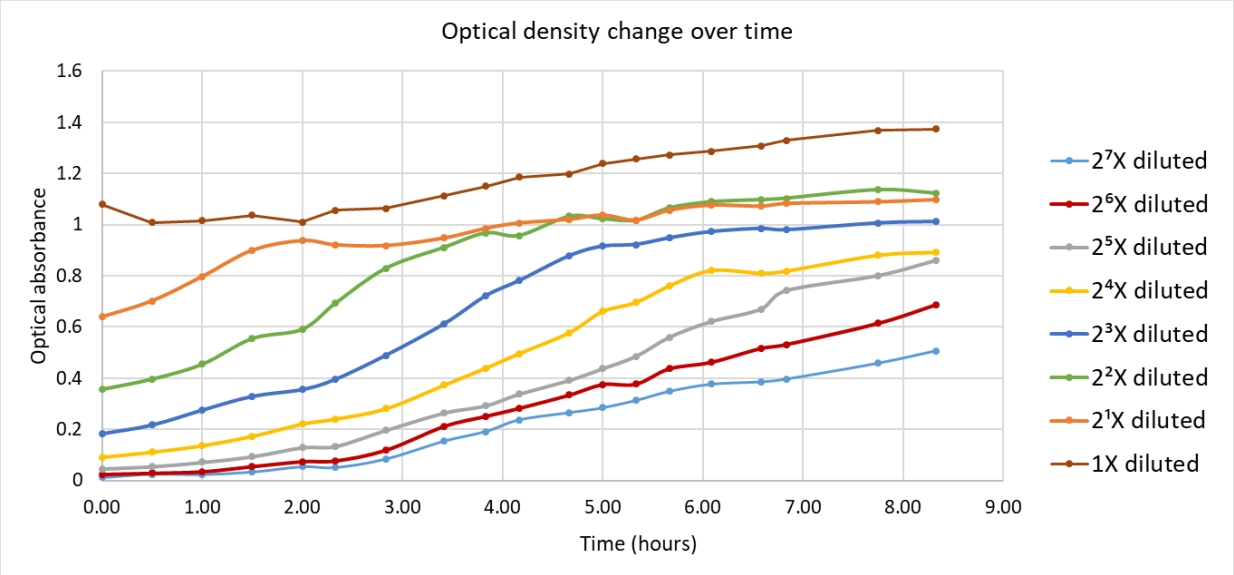

Figure AA-8*. Optical density measurements of all samples showing the ascending trend of the absorbance of samples over time, indicating the occurrence of growth in samples.*

The change of optical absorbance in all samples indicates an ascending trend of growth after the starting time of the test. The non-diluted sample stays near to constant throughout the experiment proving that there was not exponential growth in this sample to cause sudden impedimetric changes.

Periodical hemocytometry measurements of the different samples that could provide the most useful information about the growth trends using direct counting were conducted at the same time as the impedance measurements were running. In Figure A-9, hemocytometry of the sample with lowest initial concentration (2^7 times diluted) is pictured at 40 minutes, 4 hours, 6 hours and 8 hours after the starting time of the test.

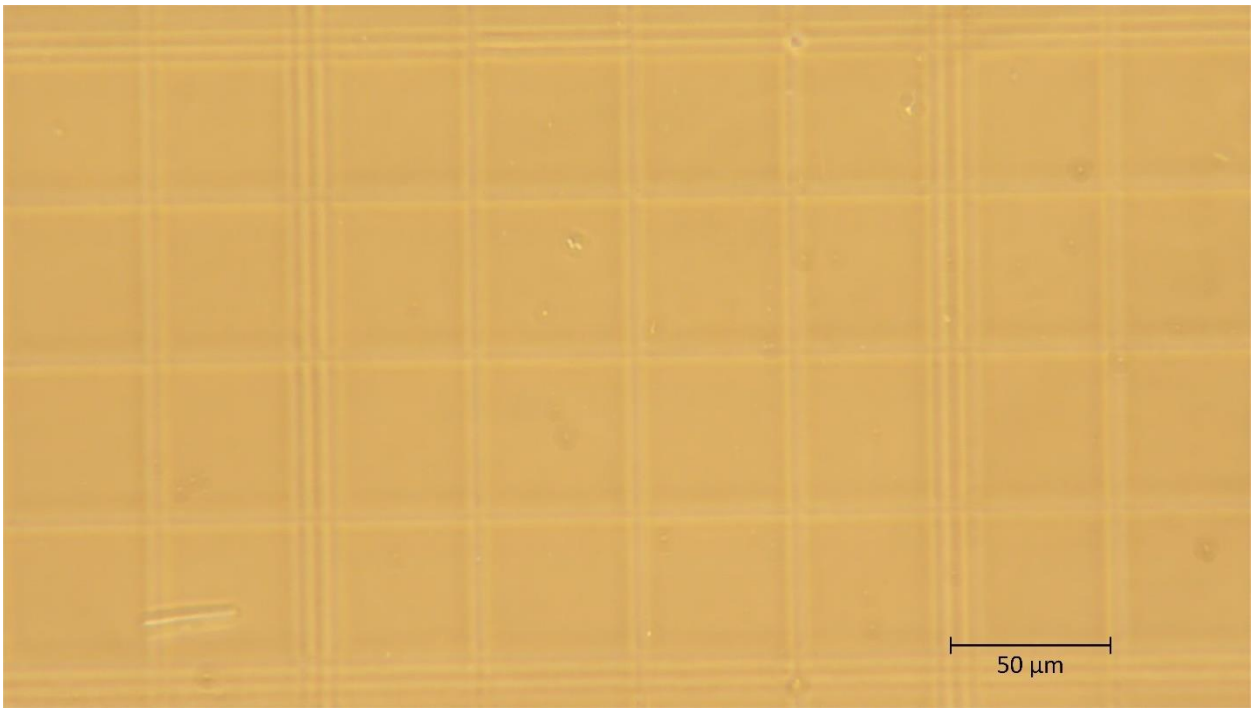

(a)

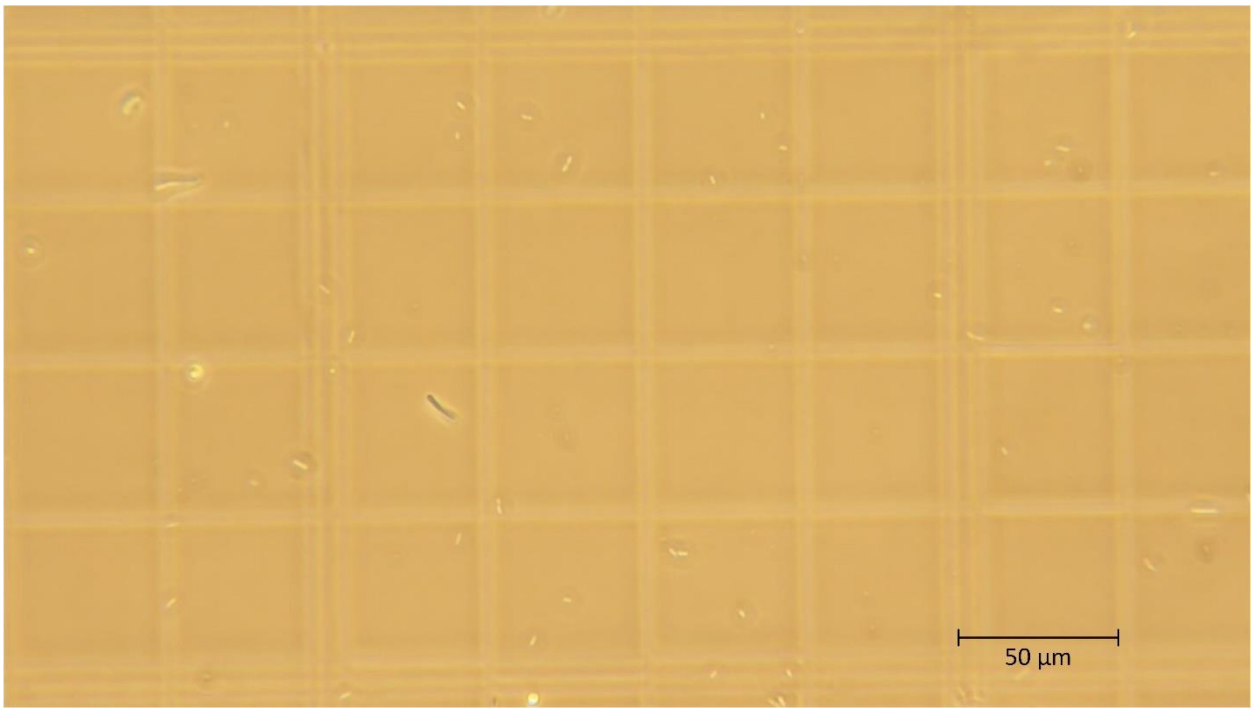

(b)

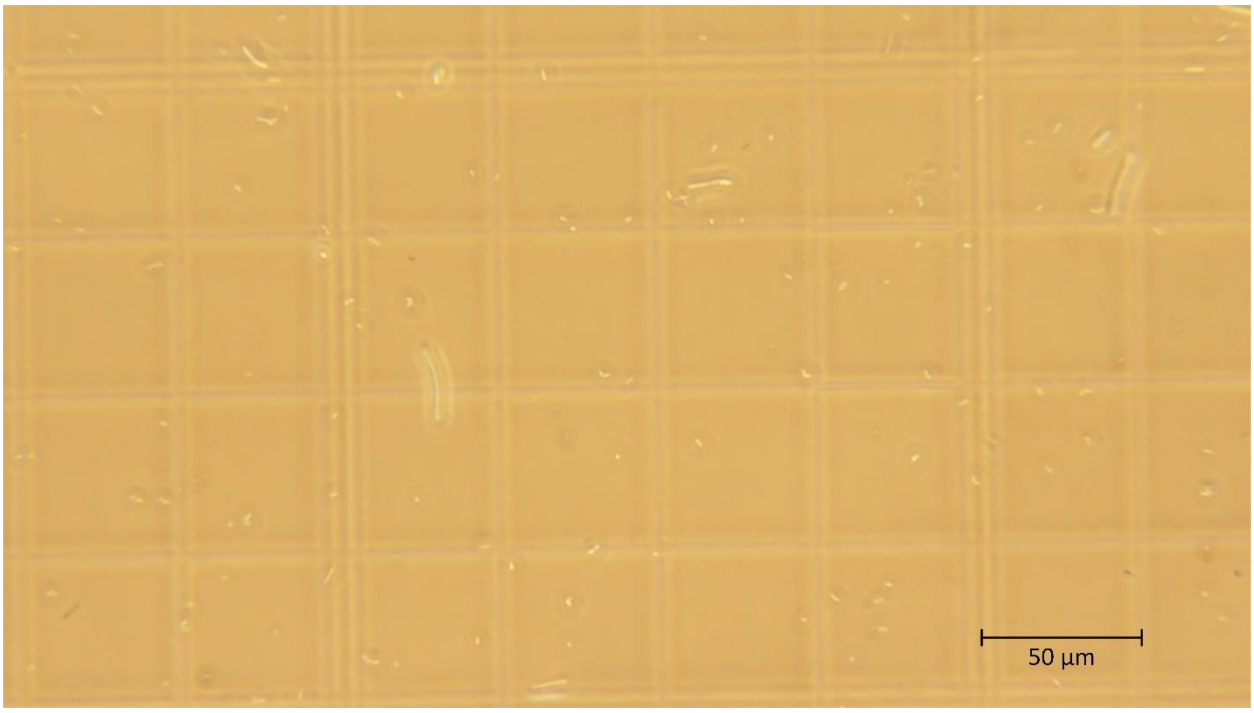

(c)

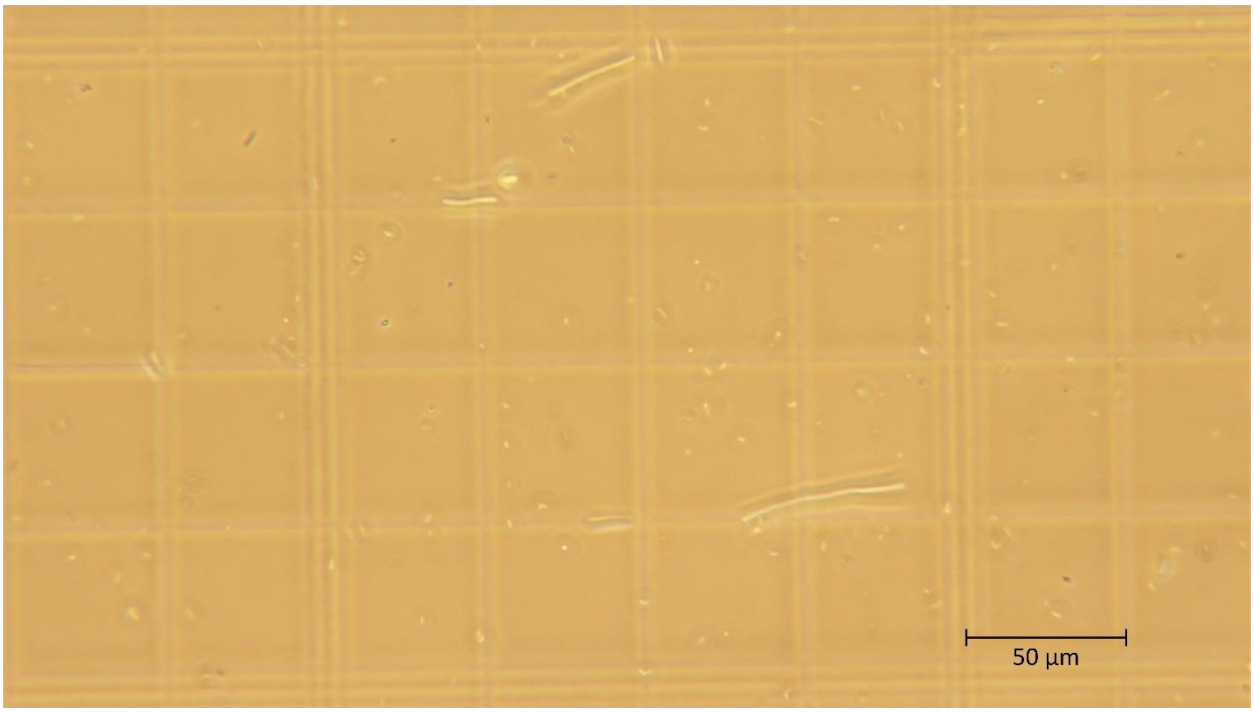

(d)

Figure AA-9. *Hemocytometry images of the 2^7 times diluted sample at* ***(a)*** *40 minutes,* ***(b)*** *4 hours,* ***(c)*** *6 hours, and* ***(d)*** *8 hours after the start of inoculation. The glowing microorganisms are cells existing in the solution*

The enhancement of bacterial population as the time progresses can be observed in the Figures A-9 (a-d). All the images were obtained in a phase contrast microscopy setting.

Hemocytometry was also conducted at 1, 3.5, 4.5, and 5.3 hours after starting time of test on the sample diluted 2^6 times from the steady-state batch. The results are shown in Figures A-10 (a-d).

(a)

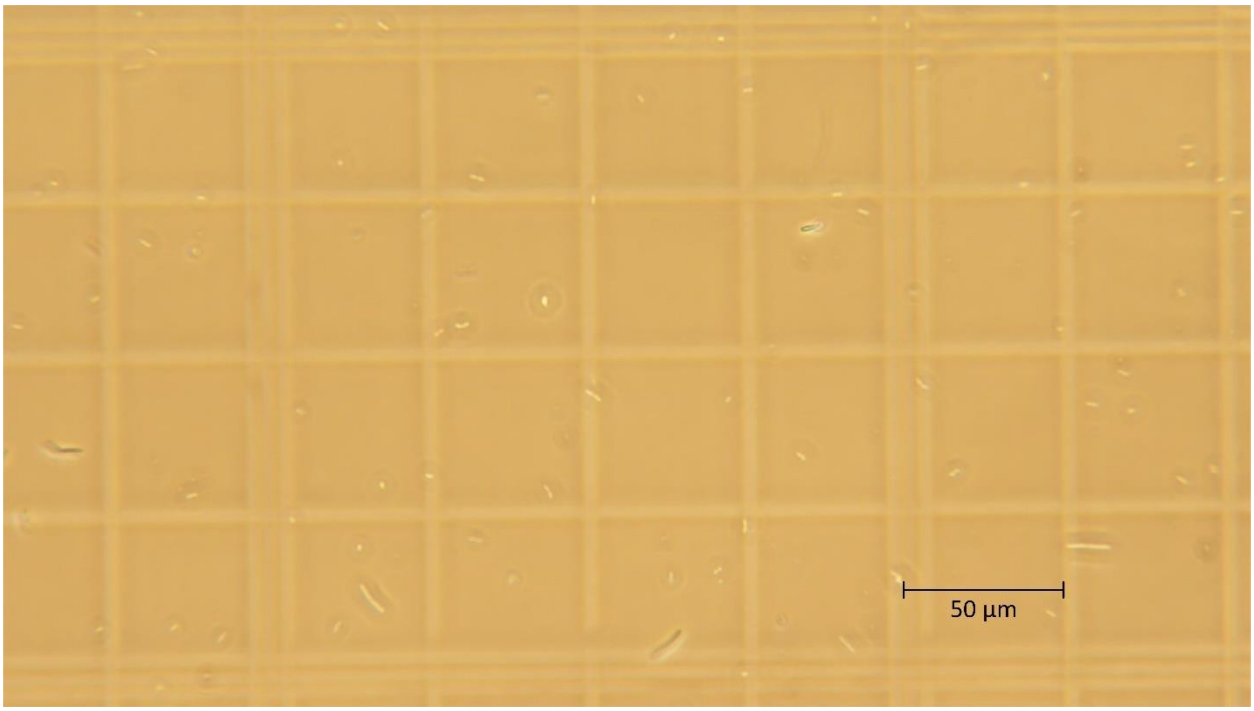

(b)

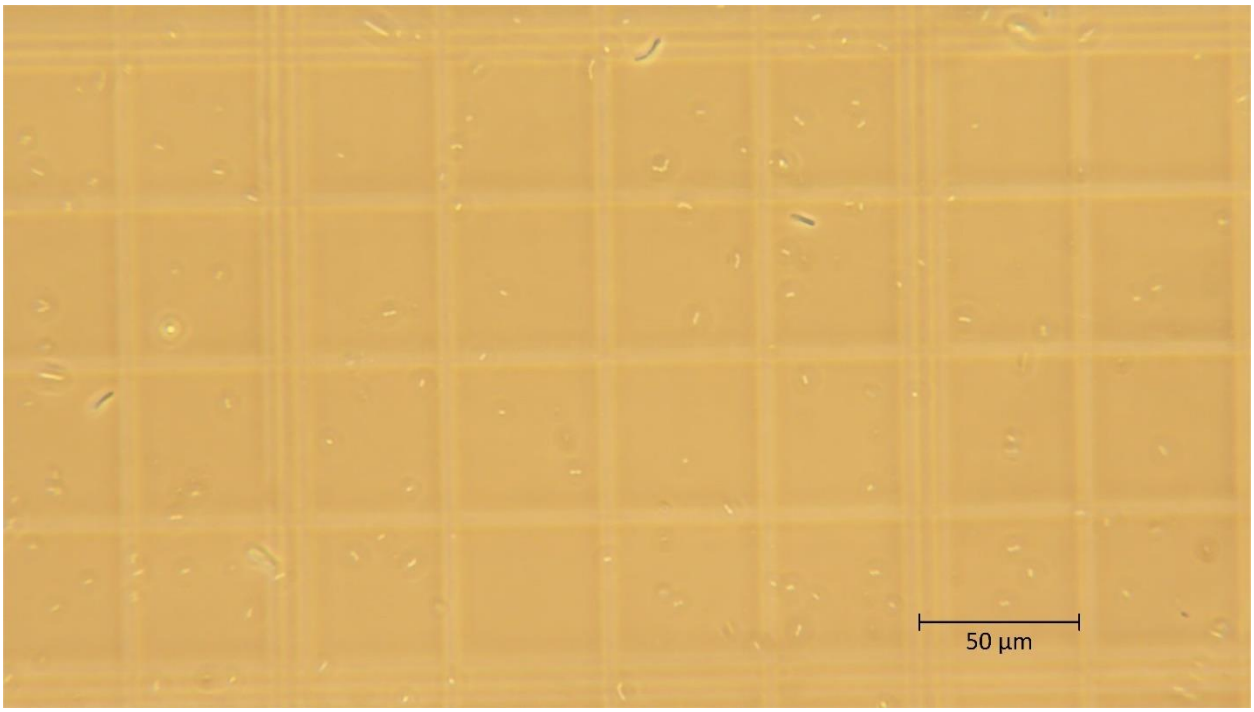

(c)

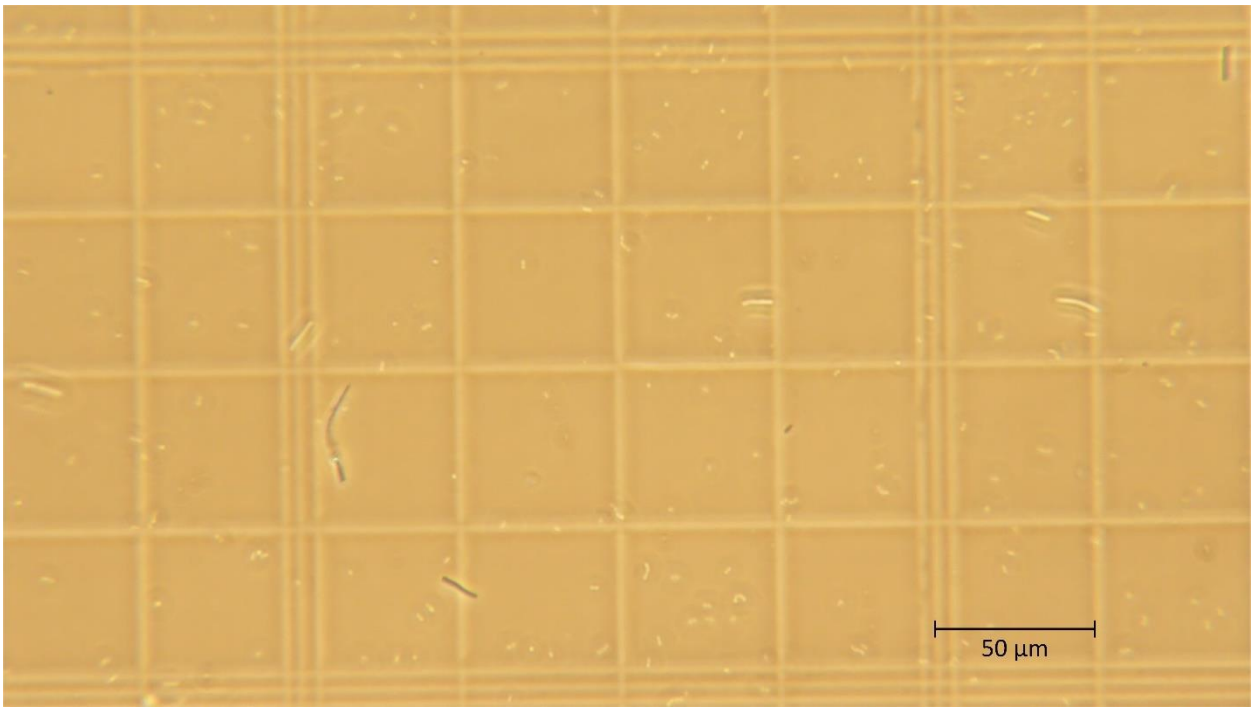

(d)

Figure A-10. *Hemocytometry images of the 2^6 times diluted sample at **(a)** 1 hour, **(b)** 3.5 hours, **(c)** 4.5 hours, and **(d)** 5.3 hours after the start of inoculation. The glowing microorganisms are cells existing in the solution.*

It is noticeable that the population has increased over time in this sample as well.

Sample diluted 2^5 times was also monitored by hemocytometry at 3, 5, and 5.75 hours after the start of the testing. Figure A-11 (a-c) contains the progress of bacterial growth over time in this sample.

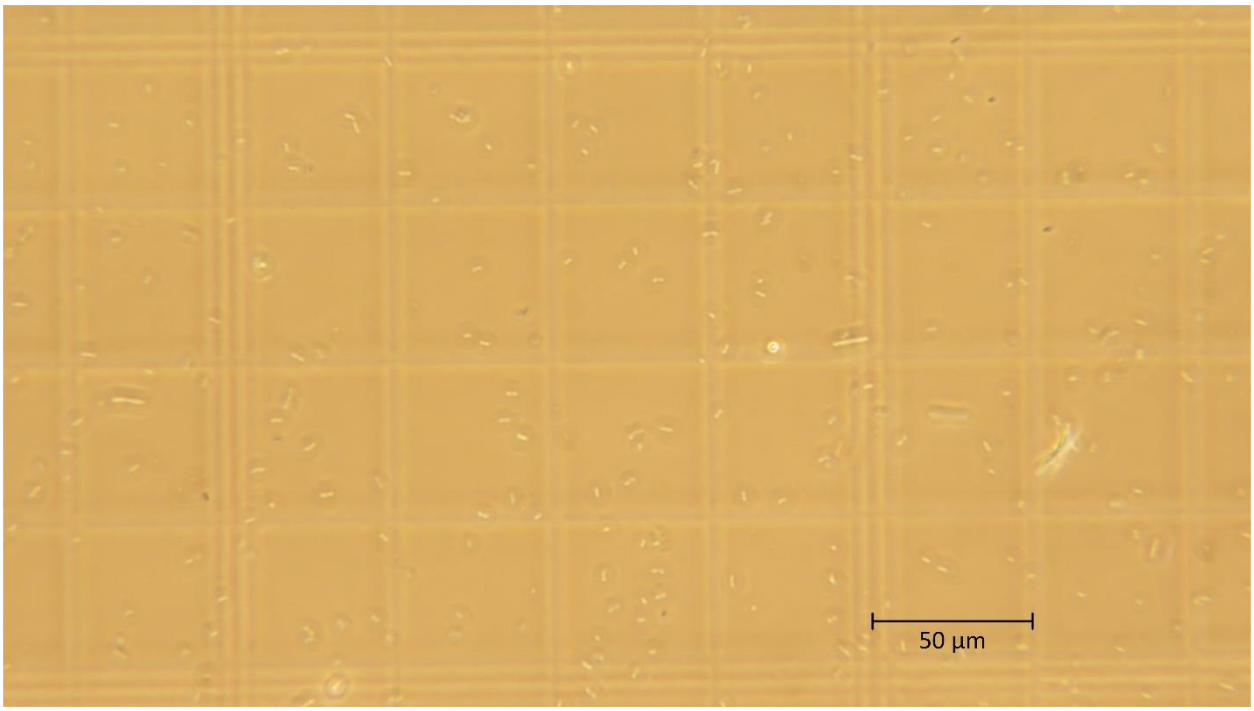

(a)

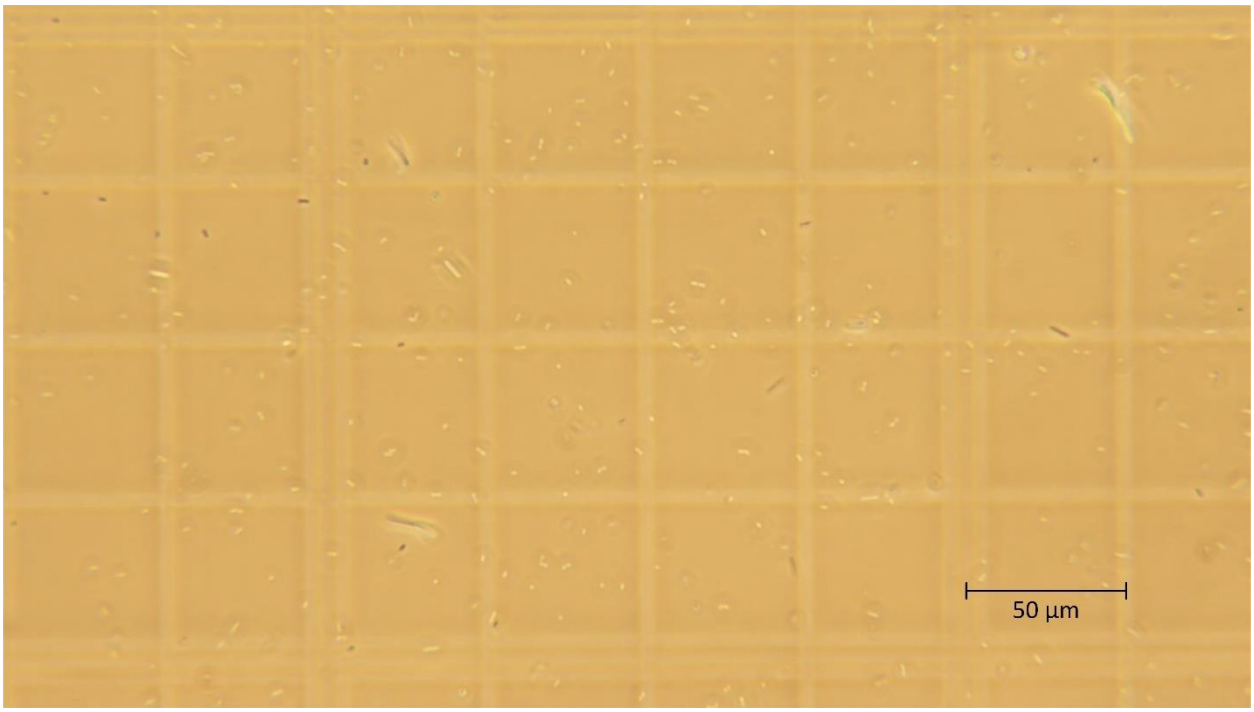

(b)

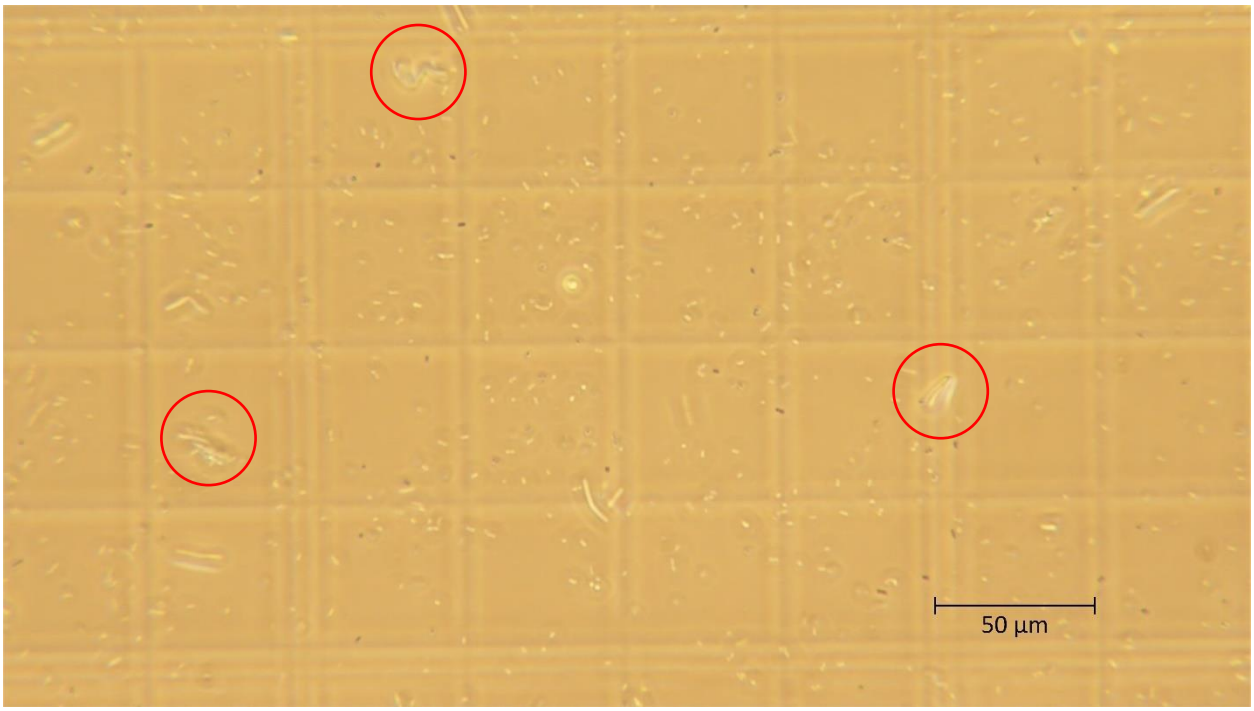

(c)

Figure AA-11. *Hemocytometry images of the 2^5 times diluted sample at **(a)** 3 hour, **(b)** 5 hours, and **(c)** 5.75 hours, after the start of inoculation. In the last image, the small-scale attachments of bacterial cells are highlighted by the depicted red circles. The glowing microorganisms are cells existing in the solution.*

In Figure A-11(c), the bacteria that are starting to form small colonies by attaching to each other can be observed. This can be the beginning of biofilm formation.

In order to obtain an idea of the growth behavior of more concentrated samples, hemocytometry was conducted on the sample that was diluted only 2^1 times. These measurements were conducted at 2.3 and 6.5 hours after the starting time of inoculation. Figures A-12 (c and d) are the hemocytometry images of the same sample 6.5 hours after inoculation at 100X, and 600X magnifications, respectively. These images were taken to further put the biofilm formations under focus.

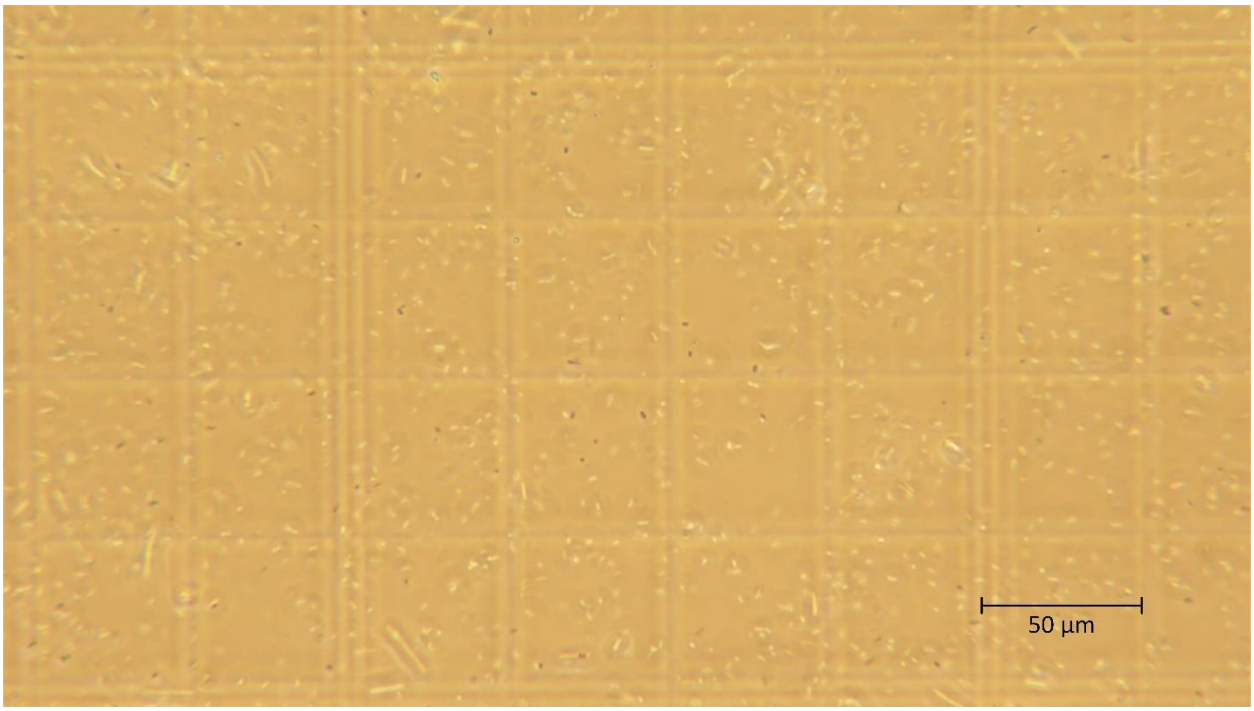

(a)

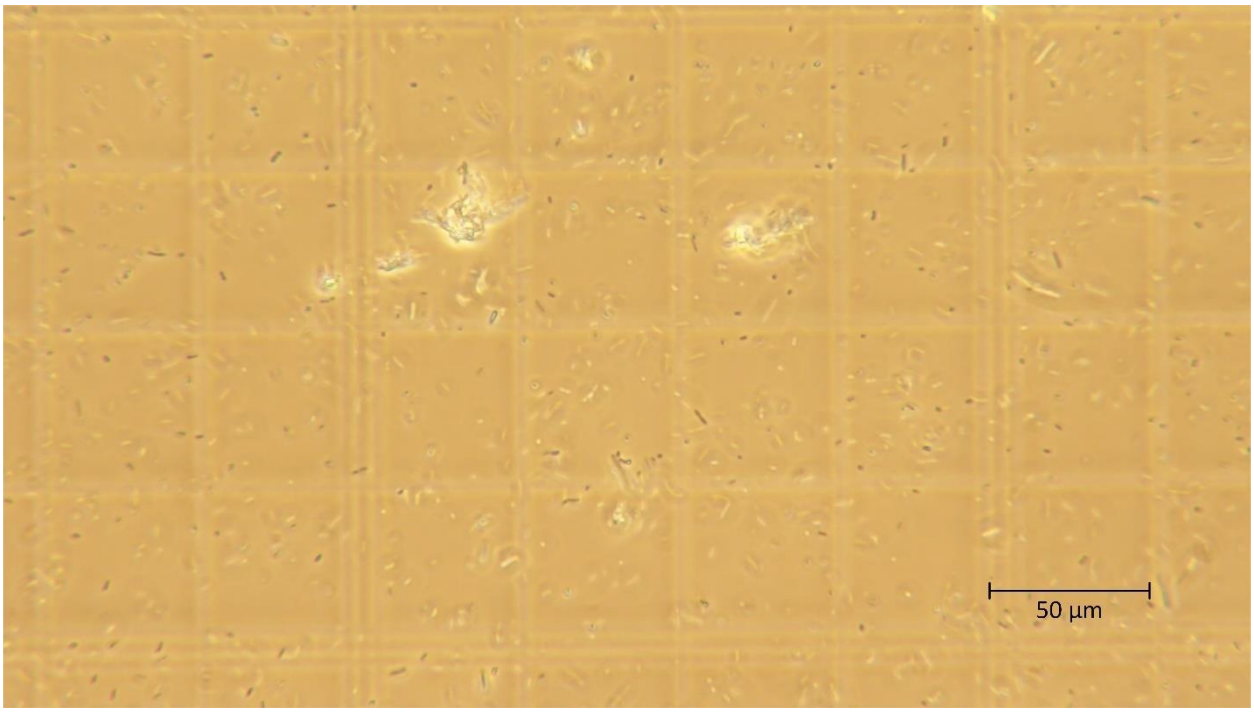

(b)

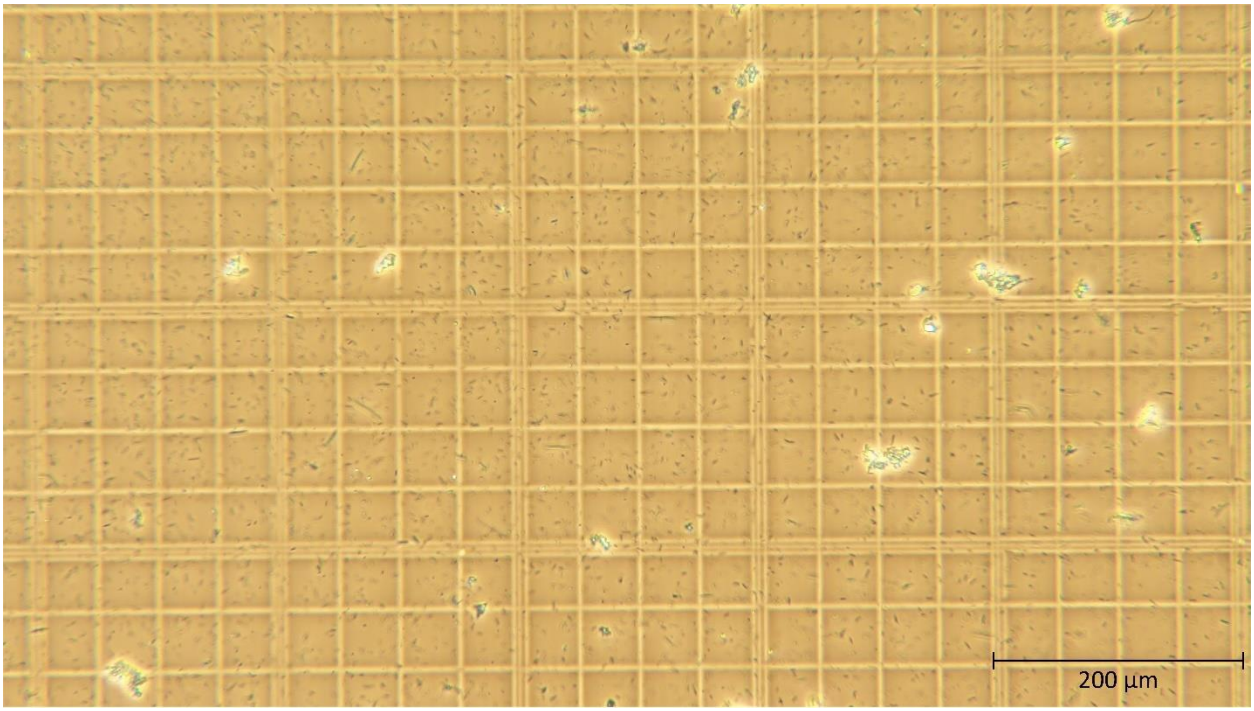

(c)

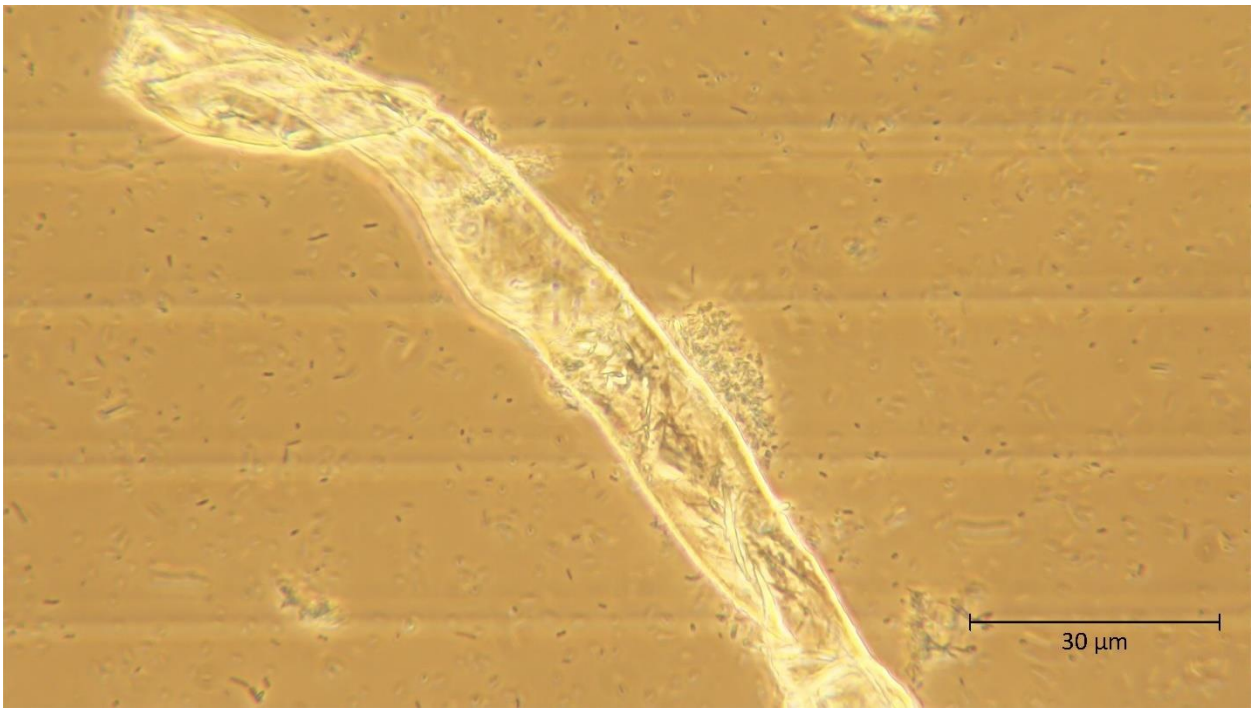

(d)

Figure A-12. *Hemocytometry images of the 2^1 times diluted sample at* ***(a)*** *2.3 hour,* ***(b), (c)*** *6.5 hours after the start of inoculation. The glowing microorganisms are cells existing in the solution. (d) This is a magnified image of an established biofilm, showing the complex matrix together with the surrounding and loosely bound adjacent bacterial cells. At this point the counting of cells becomes almost impossible.*

The formation of biofilm community and its surrounding adherent cells are magnified in Figure A-12 (d). The size of this cluster of biofilm matrix is comparably much bigger than the single planktonic cells available in the area around the biofilm.

Overall, the 50% dilution test met the objectives, but the main drawback of this test is the chronological proximity of the impedance changes in different samples. For more distinct impedimetric variances, the samples must be diluted at a greater level to provide enough concentration difference. Higher level of dilution would also allow us to gain if there is a time range or limit that the impedance monitoring could be effective for bacterial growth assessment. Future tests were designed in a way that it could find the answers to the abovementioned goals.

A.3 Measurement of samples in chemically defined medium

After the attempts in finding the correlation between bacteria growth and the impedance measurements, a new set of testing was designed to address the bacterial growth in medium other than *chemically undefined* biological media (LB broth). This was conducted to answer the hypothesis of whether part of the impedance changes observed in previous tests are due to changes in the nature or composition of the growth media, not just due to bacterial growth. Therefore, the objective of the testing was to monitor of impedance properties of bacterial cells in *chemically defined* growth media. Unlike LB broth that was used as growth medium for previous tests, a chemically defined media only contains chemicals with defined formula and known amount of chemicals that are necessary for bacterial growth. Therefore, bacterial cells in the form of centrifuged bacterial pellets were extracted were inoculated in the chemically defined medium. The key chemical source of food for bacteria, that is supposedly carbon, was provided in the media in form of glucose molecules at three different concentrations. The base solution of the defined media was made by dissolving 6.78 g of Disodium Phosphate (Na_2HPO_4), 3 g of Monopotassium Phosphate (KH_2PO_4), 1 g of Ammonium Chloride (NH_4Cl), and 0.5 g of Sodium Chloride (NaCl) in 1,000 ml of distilled water. Using this base solution and different amount of glucose additions, three different chemically defined media were prepared known as Minimal Salts Media (i) without glucose, (ii) poor in glucose, and (iii) glucose enriched. Hence, all three media were made using the same chemicals except that the poor glucose and glucose enriched media had 1 g and 10 g of glucose was added to them, respectively. All media were sterilized at 121°C for 15 minutes. 4 ml

of steady-state bacterial solution grown overnight in LB broth was collected for the extraction of the cells. This would provide enough bacterial population for the acquisition of growth data. The bacterial cells were extracted from LB broth media using centrifugation at high speed (17,000 g); re-suspended in Phosphate-buffered Solution (to remove the trapped particles of the undefined between in the cells), re-centrifuged, inoculated and re-suspended in the desired medium as part of the preparation method for this testing. The resuspension steps were taken by using vigorous shaking on the vortex mixer. After preparation of the samples, they were placed in the wells of the E-plate for electrical testing. The impedance measurement results at 1,000 Hz are depicted in Figure A-13.

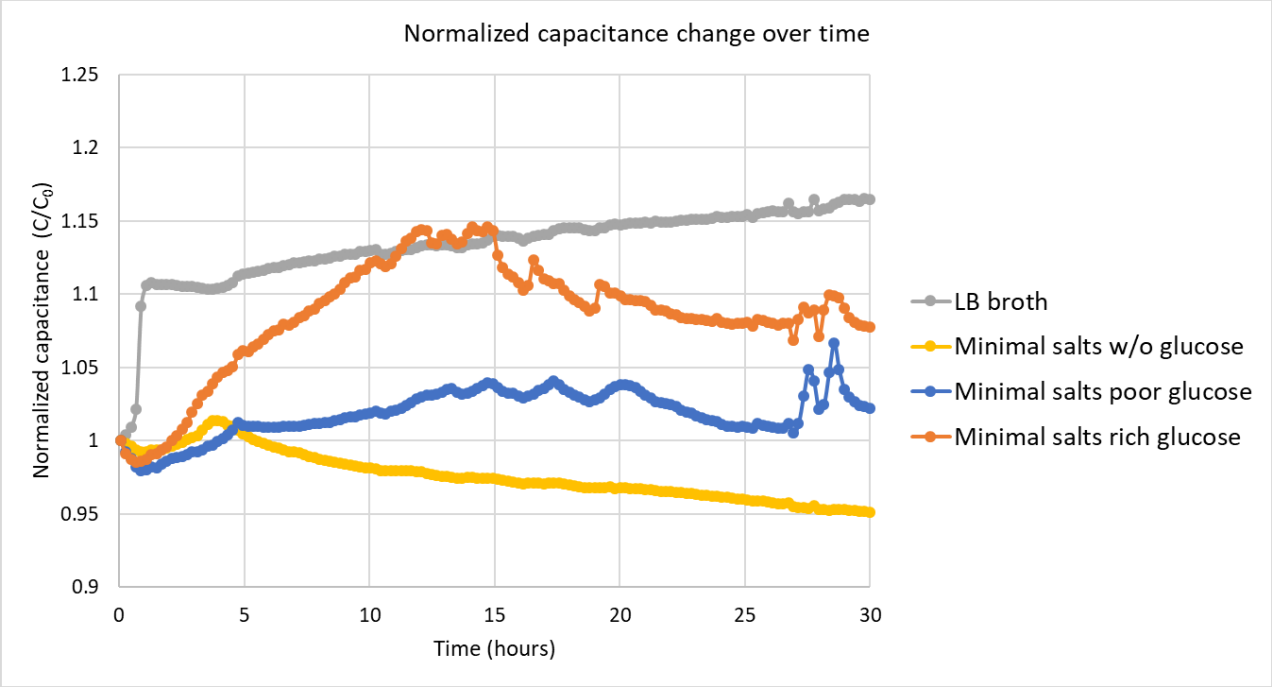

(a)

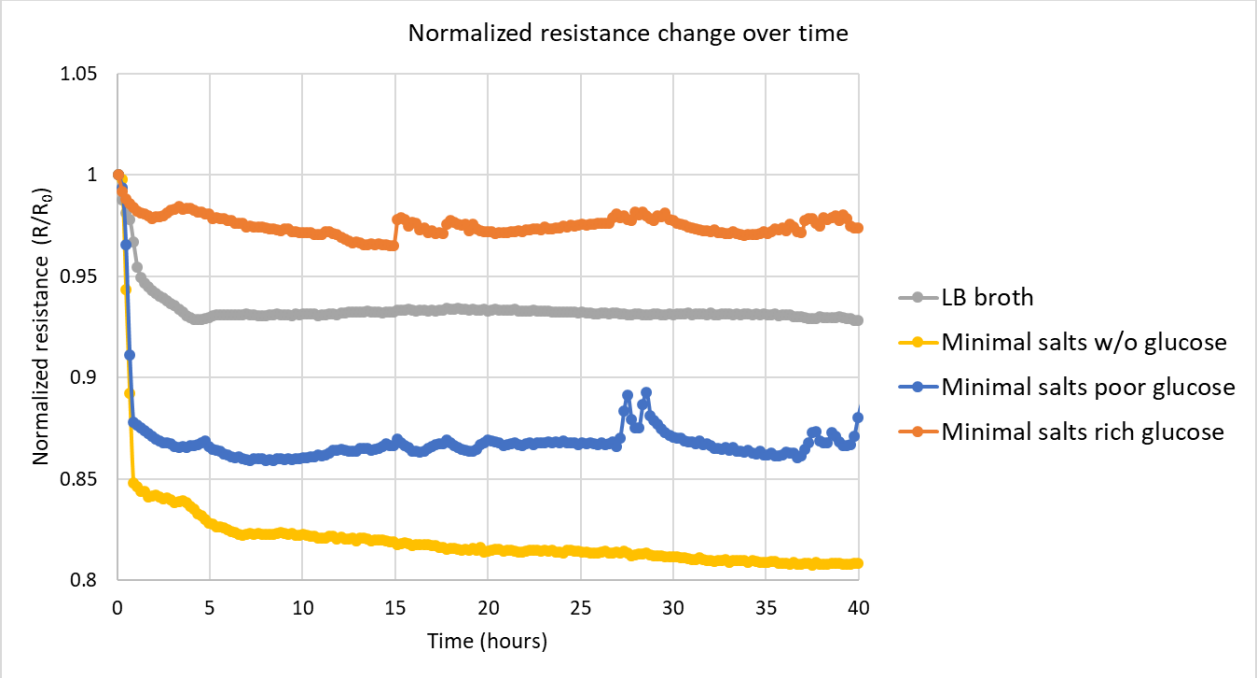
Normalized resistance change over time
Normalized resistance (R/R0)
Time (hours)
LB broth
Minimal salts w/o glucose
Minimal salts poor glucose
Minimal salts rich glucose

(b)

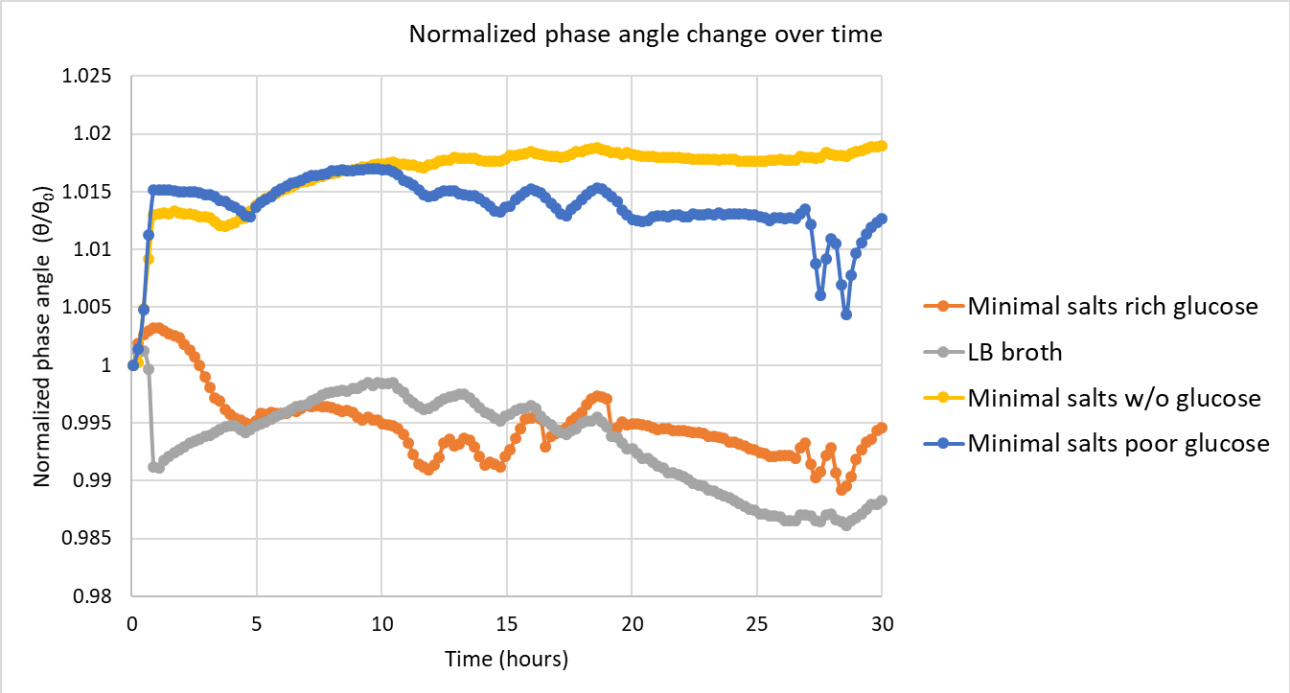
Normalized phase angle change over time
Normalized phase angle (θ/θ0)
Time (hours)
Minimal salts rich glucose
LB broth
Minimal salts w/o glucose
Minimal salts poor glucose

(c)

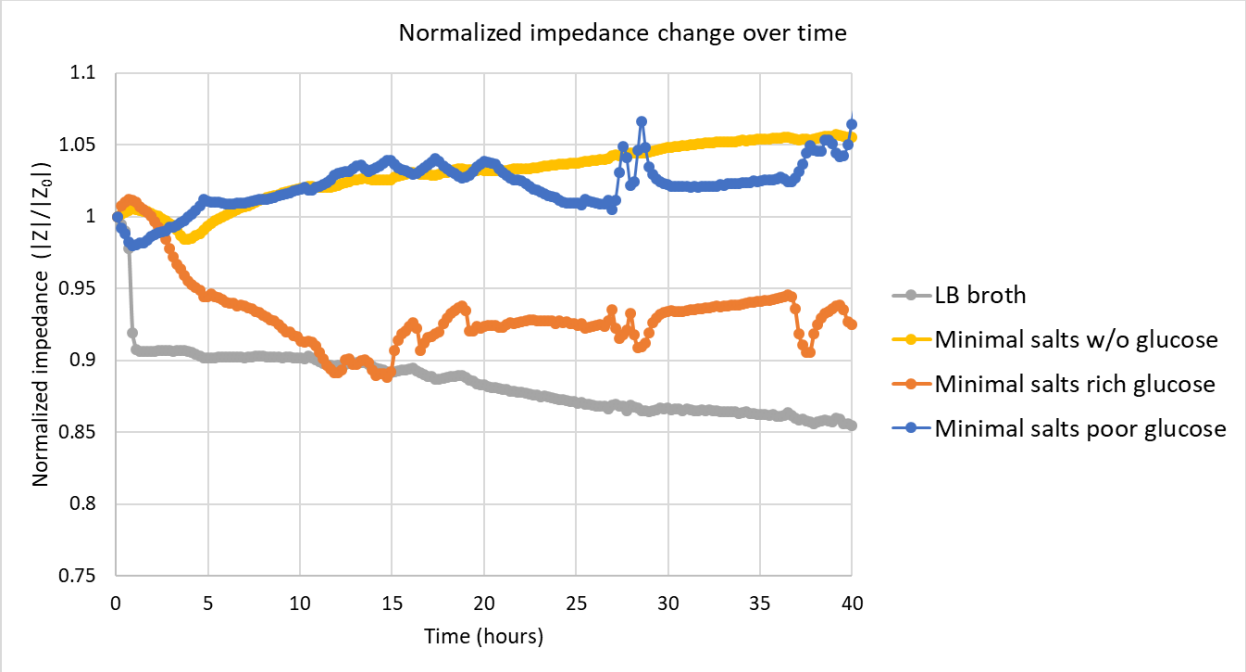

(d)

Figure A-13. *Impedimetric monitoring of bacterial samples in LB broth and the three chemically defined growth media with variant glucose content. (a) Normalized capacitance changes over time. (b) Normalized resistance changes over time. (c) Normalized phase angle changes over time, and (d) normalized impedance magnitude changes over time.*

As can be seen in Figure A-13 (a-d), the cells inoculated in LB broth show a sudden alteration just after the start of test. For the bacterial cells in the minimal salts media, the capacitance shows slight increases in the magnitude for the samples with low and high glucose amounts. The slope of this increase is smaller than the rapid rise observed in the LB broth sample. The bacterial cells in minimal salts media without glucose barely changes throughout the experiment in terms of capacitance magnitude. Other impedimetric features such as resistance and impedance magnitude show some variances for the two samples that contained glucose, but the changes are not persistent enough to be compared.

The optical density measurements were also obtained from the samples at the same time as impedance measurements to provide an insight to the growth of bacteria in the chemically defined media as well as a comparison with the bacteria inoculated in LB broth. Figure A-14 demonstrates how the optical density of the different samples progresses over time. The bacterial cells in LB broth increased up to higher levels of optical absorbance, as expected. The bacterial cells in

chemically defined media showed generally small increase in the turbidity and as a result bacterial concentration.

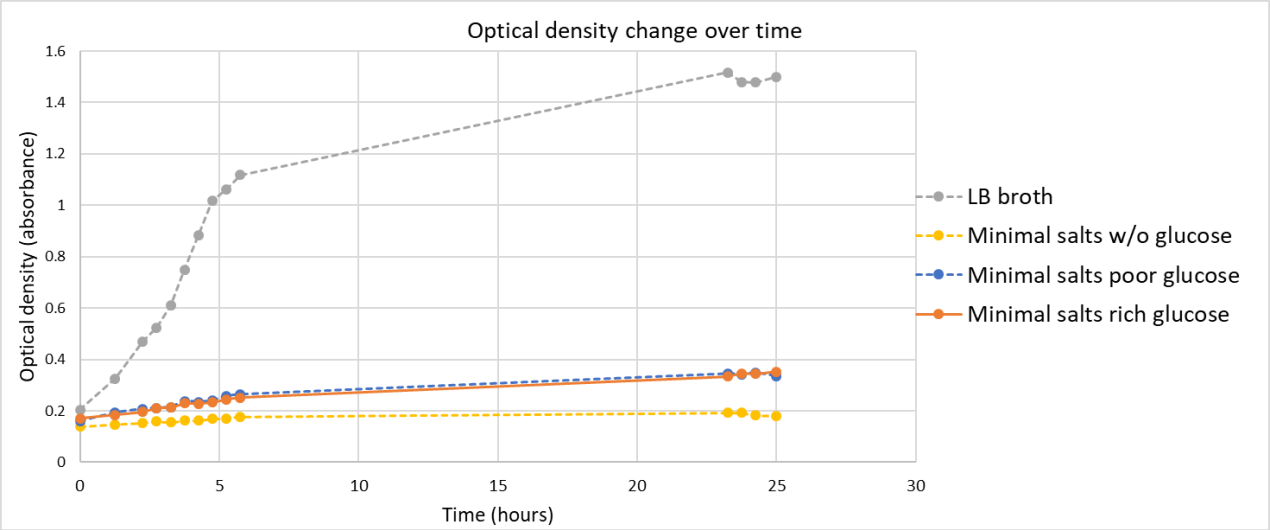

Figure A-14. *Shows the optical density trends of all 4 samples. This was done simultaneous to the impedance measurements for the purpose confirming the increase or possible unchanging of bacterial concentrations.*

Overall, the capacitance results of this test, especially the one that of glucose enriched and poor glucose content media, suggest that changes in capacitance are not due to the composition degradation of growth media, and it can very well be just because of the microbial metabolism escalation. This further indicates that the changes seen in the other tests, during which LB broth was used as the growth media, are due to the growth of bacterial population and metabolism, not due to the change in the composition of the growth media. As well, impedance magnitudes, resistances, and phase angle did not demonstrate reliable capabilities of monitoring the growth of bacteria in the growth media. Therefore, capacitance monitoring is suggested as the most reliable and indicative parameter for monitoring the growth of bacteria.

A.4 Microscopic observation of legume roots

A.4.1 Phase contrast and brightfield imaging

An example of trying to capture microscopic images from lentil seed roots are provided in Figure A-15. Figure A-15 (a) is a brightfield image of the plant roots at 7.6X magnification. As can be noticed, the hair-like features of the roots are captured while still attached to the body of the root. Smaller particles and perhaps microbiota can be observed around the roots. However, this image does not clarify whether the dotted areas contain bacteria or they are just debris and solid

particles. This is known as the main downside of brightfield microscopy when it comes to environmental biofilm observation. Figure A-15 (b) is a phase contrast image of the exact same sample as Figure A-15 (a). Using this technique, live cells can be displayed as glowing components. However, in this case, this causes the plant roots to glow as much as the bacterial cells that may exist around the roots. Hence, this technique, although very useful in applications such as hemocytometry, is not quite applicable to this purpose. Therefore, other methods, such as fluorescence microscopy could be more suitable.

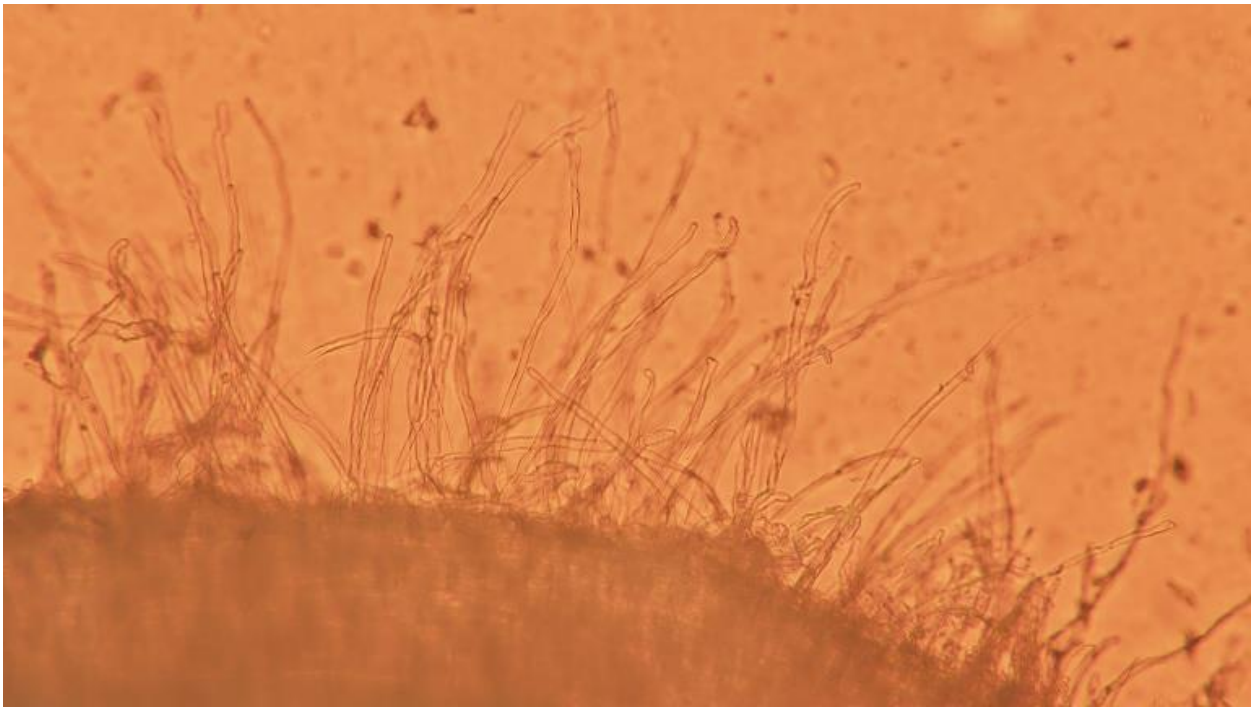

(a)

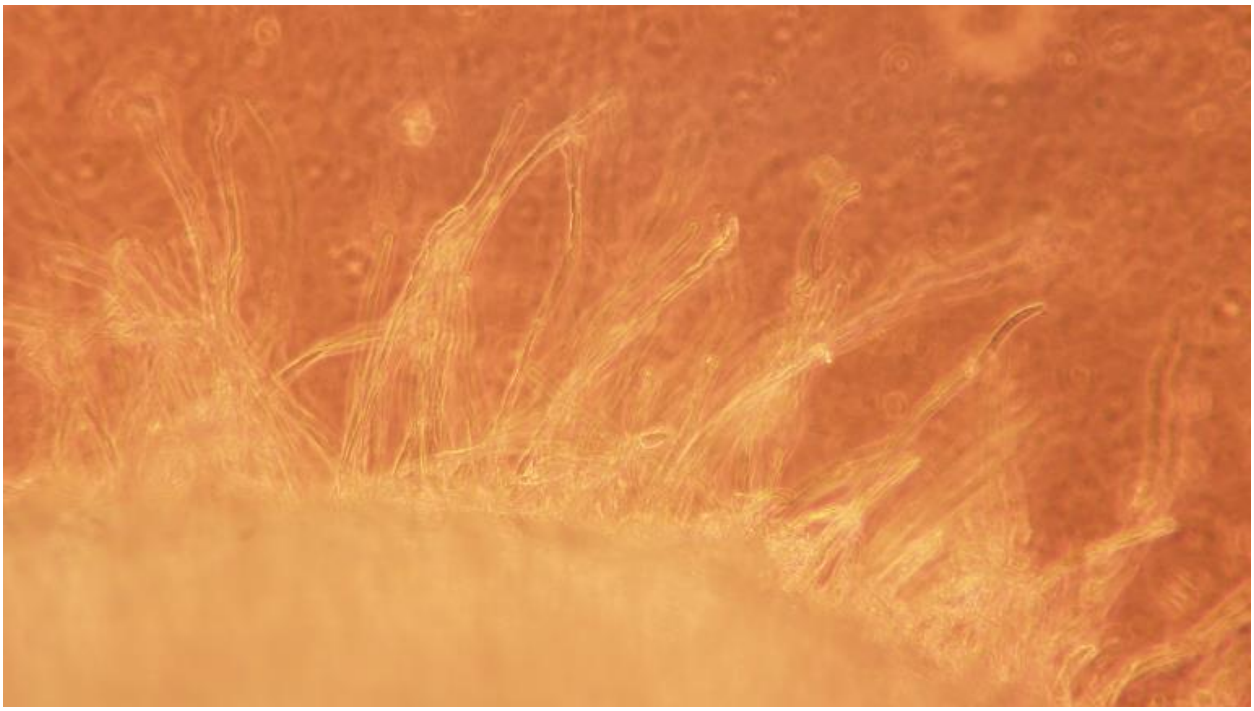

(b)

Figure A-15*. (a) Brightfield image of lentil plant root. (b) Phase contrast image of lentil plant root.*

A.4.2 Fluorescence imaging

Other than the impedance monitoring sensor, a significant improvement of the available equipment was made including the upgrades performed on the microscope available in the laboratory, E-Hut 118. Thanks to these upgrades, fluorescence microscopy of the roots of lentil seeds were possible to be performed. In the following pages, microscopic images of lentil seed roots are provided. The process of growing lentil seedlings together with their root exploitation procedure are provided in Appendix A and B. Figures A-16 (a-s) are acquired by applying FilmTracer Sypro Ruby Biofilm Matrix Stain dye and the excitation of samples using FITC filter cube. This method showed solid success in illuminating the microbial life adjacent to the root surface. The glowing red areas around the yellow areas depicted in the figures below are the existent microbial life around the roots.

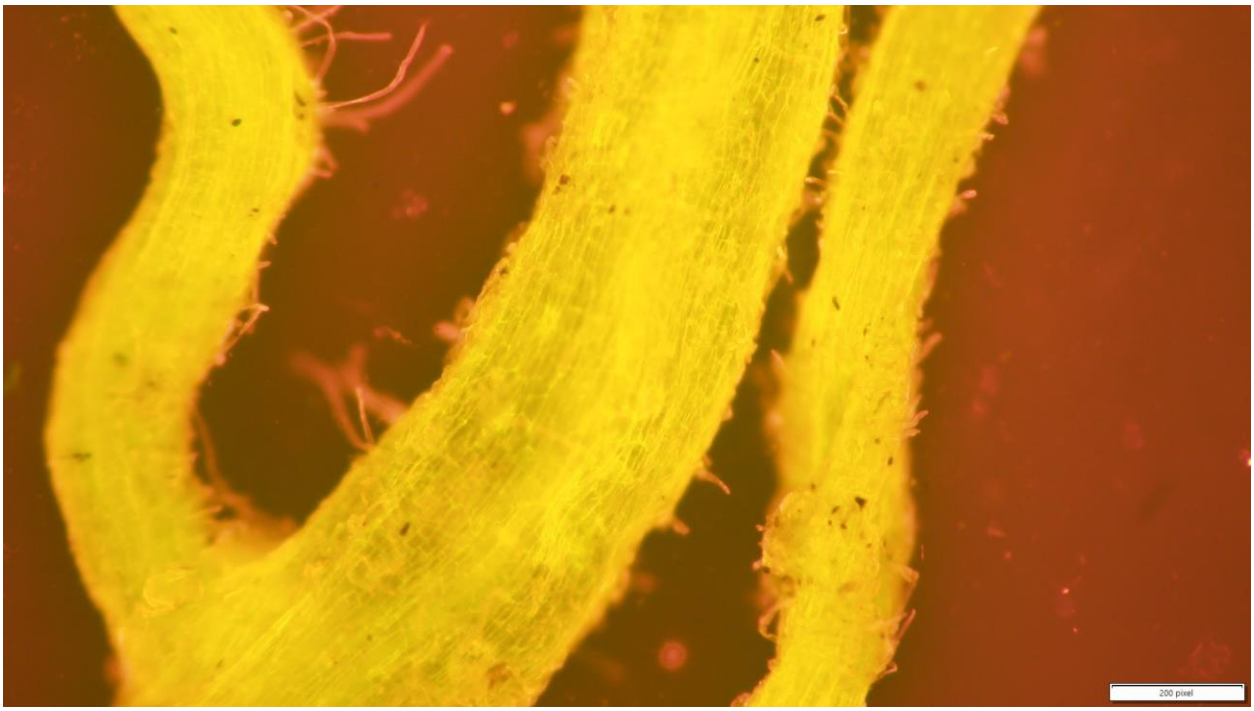

(a)

(b)

(c)

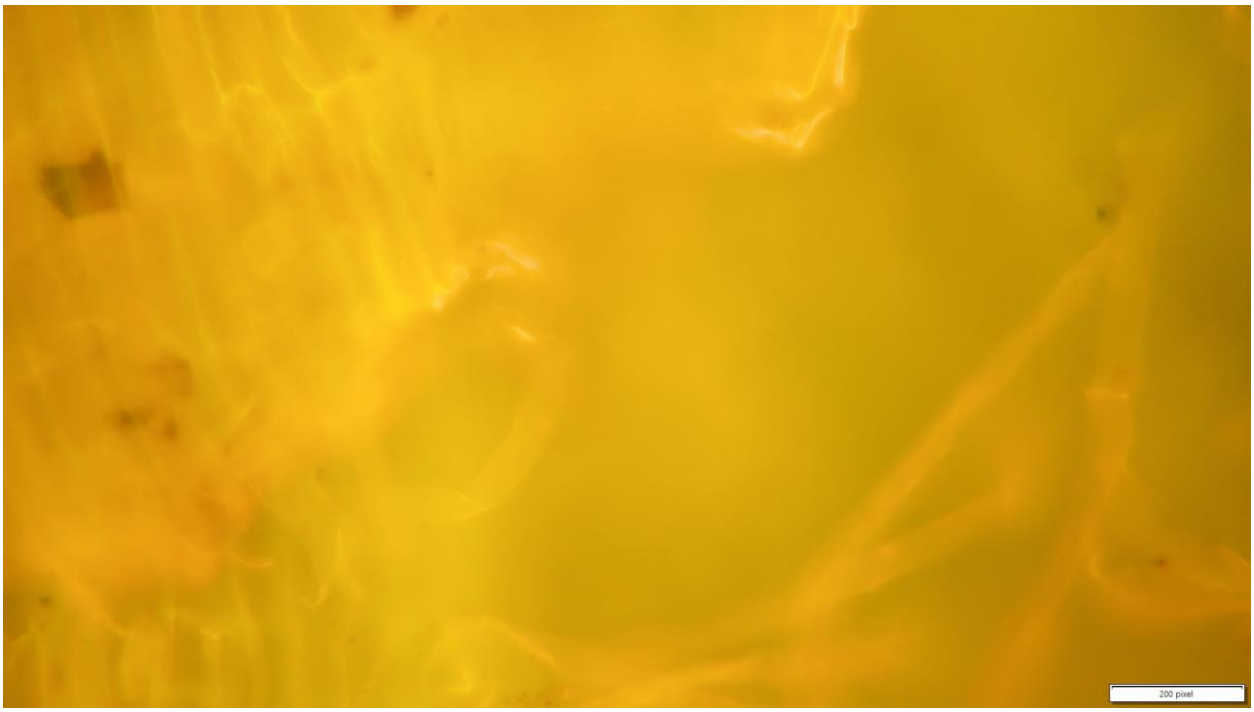

(d)

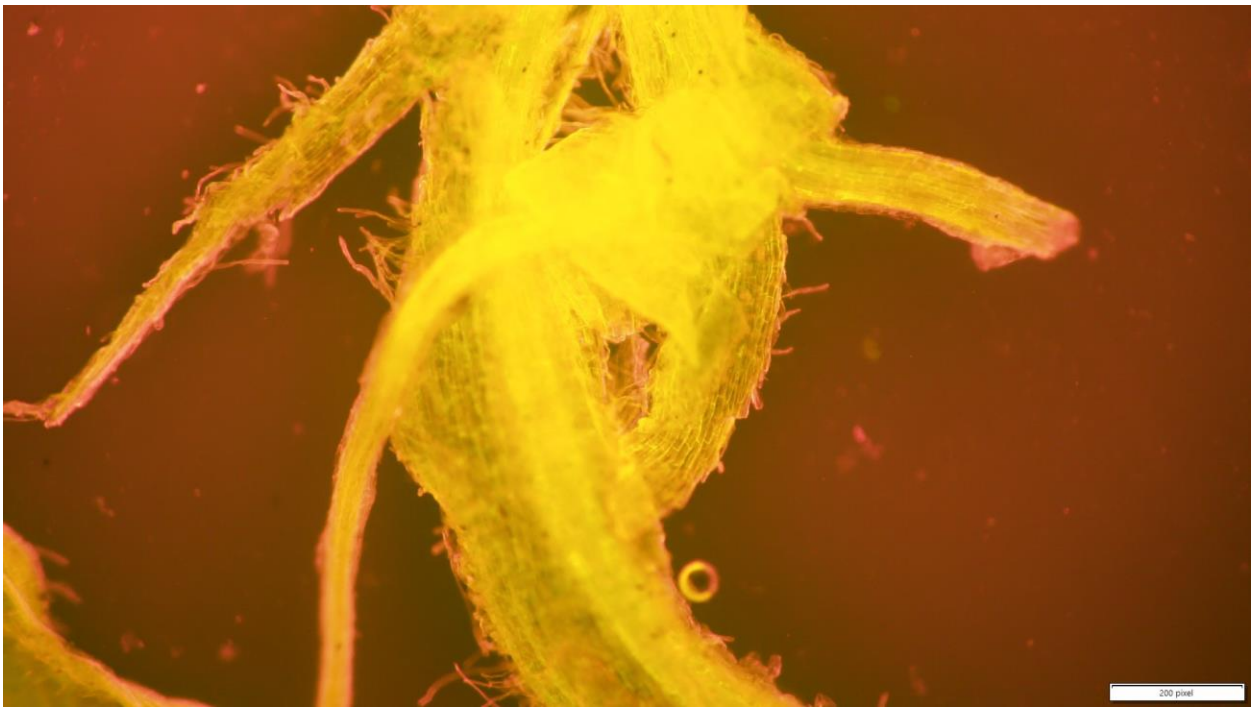

(e)

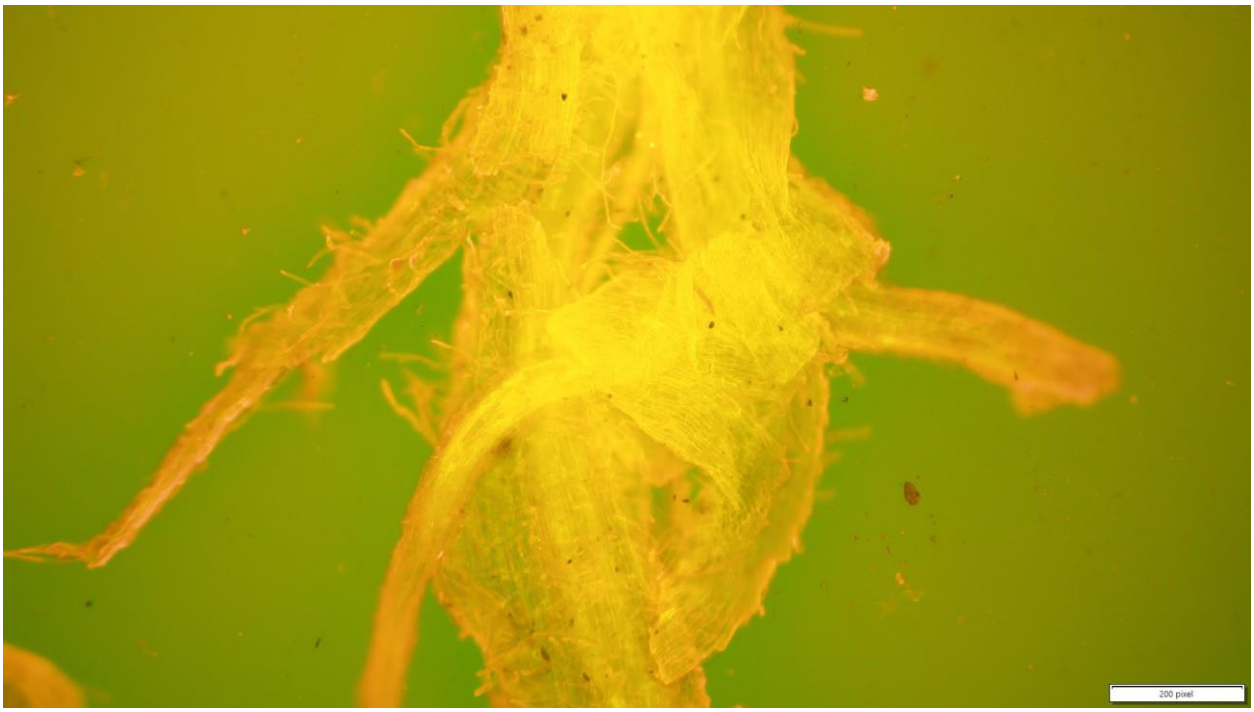

(f)

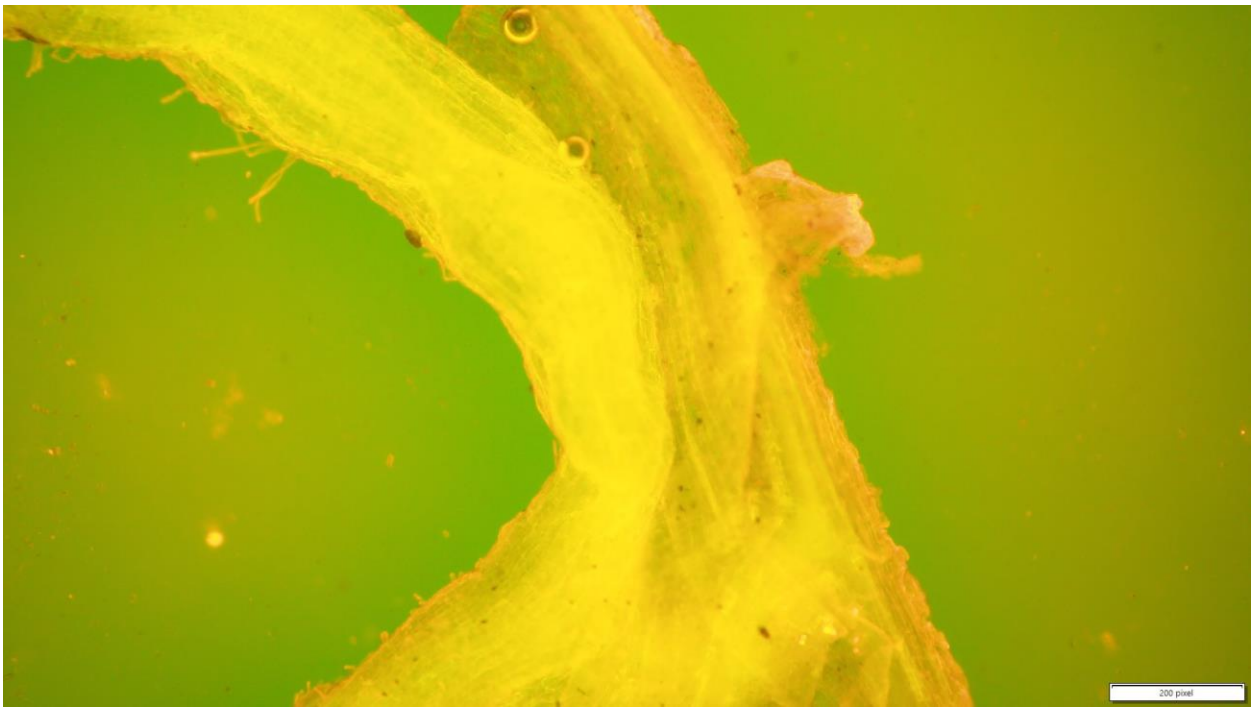

(g)

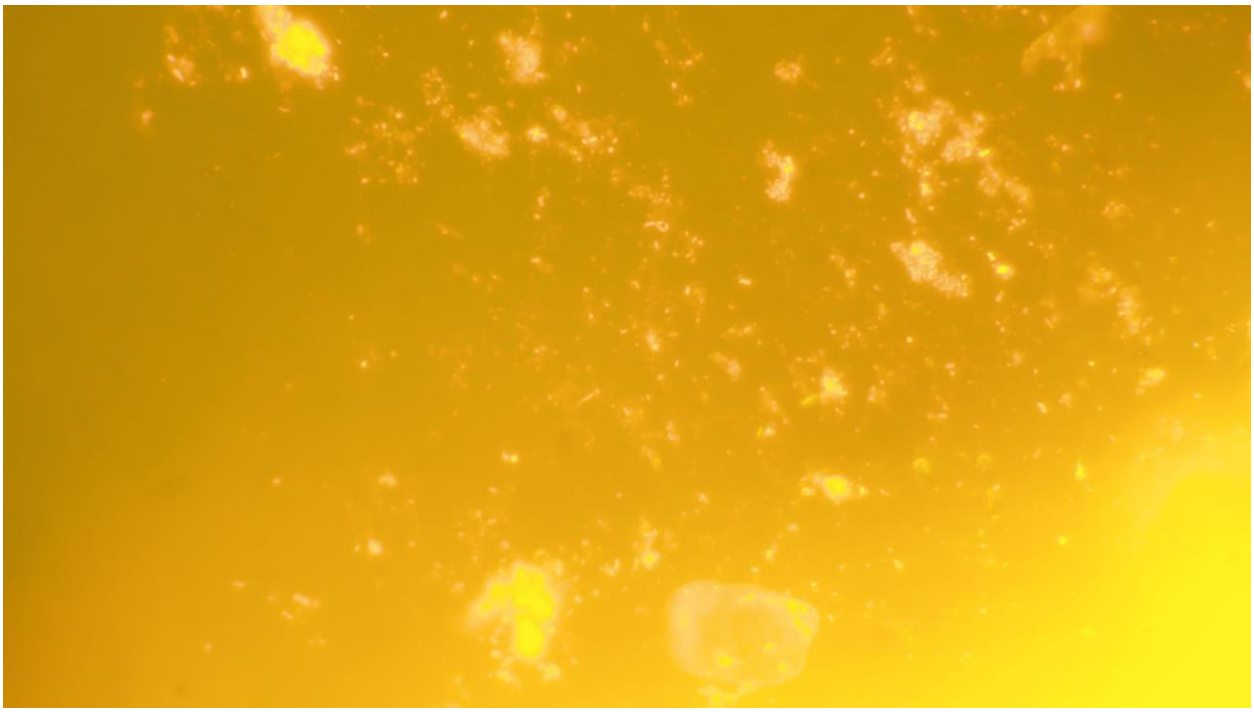

(h)

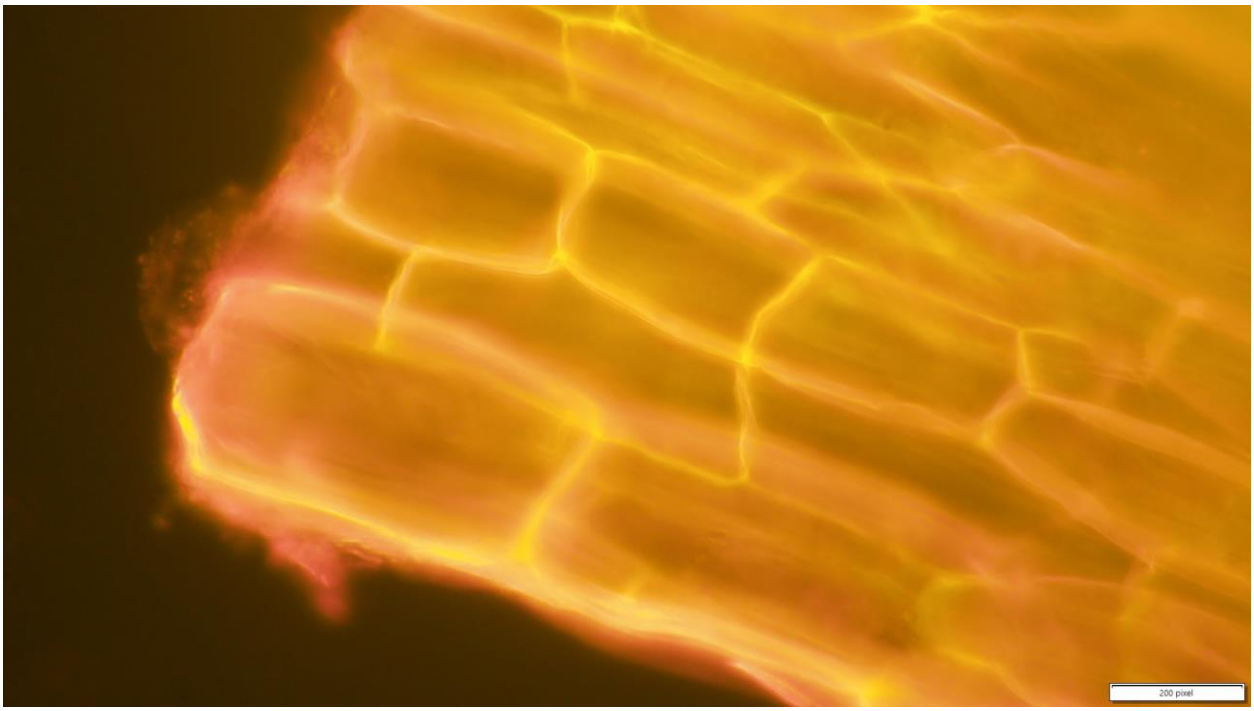

(i)

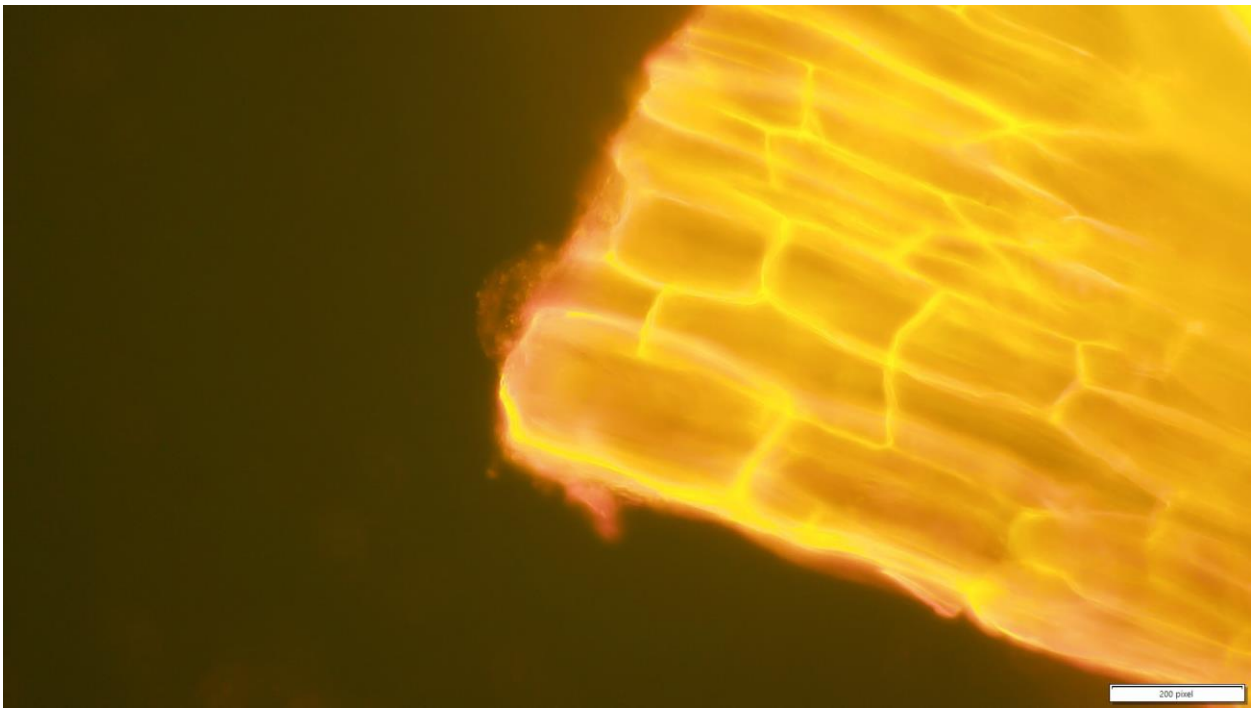

(j)

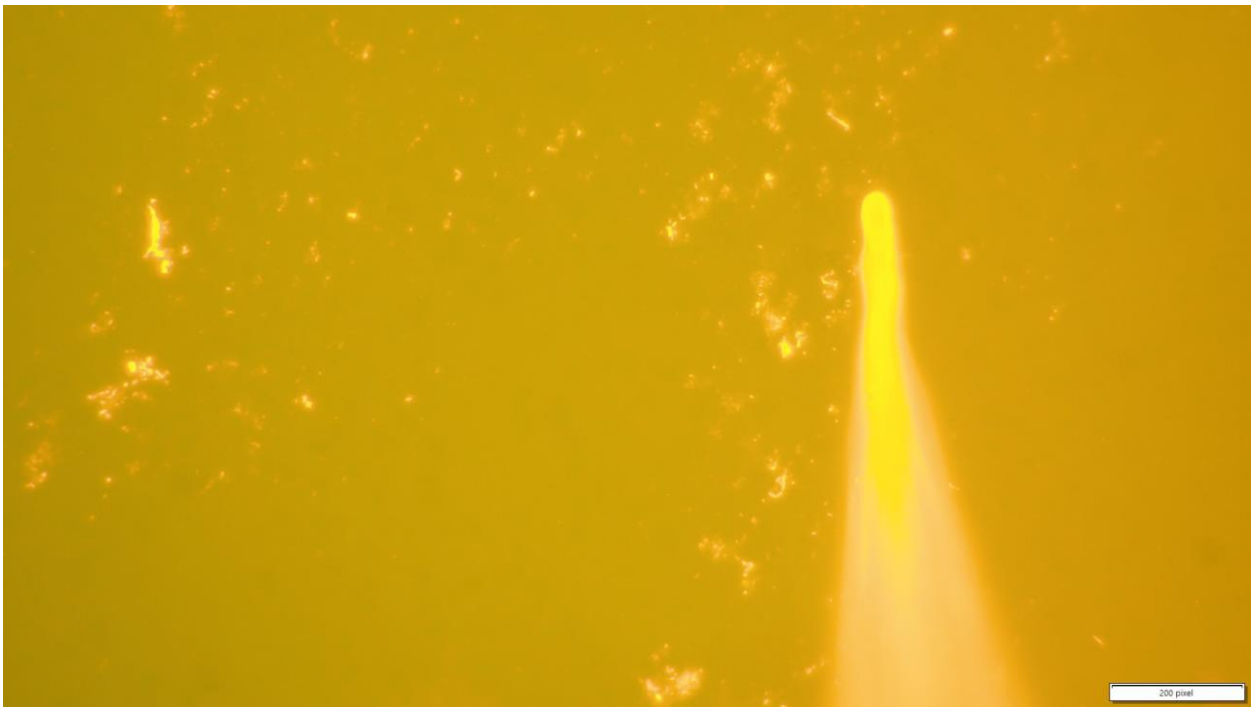

(k)

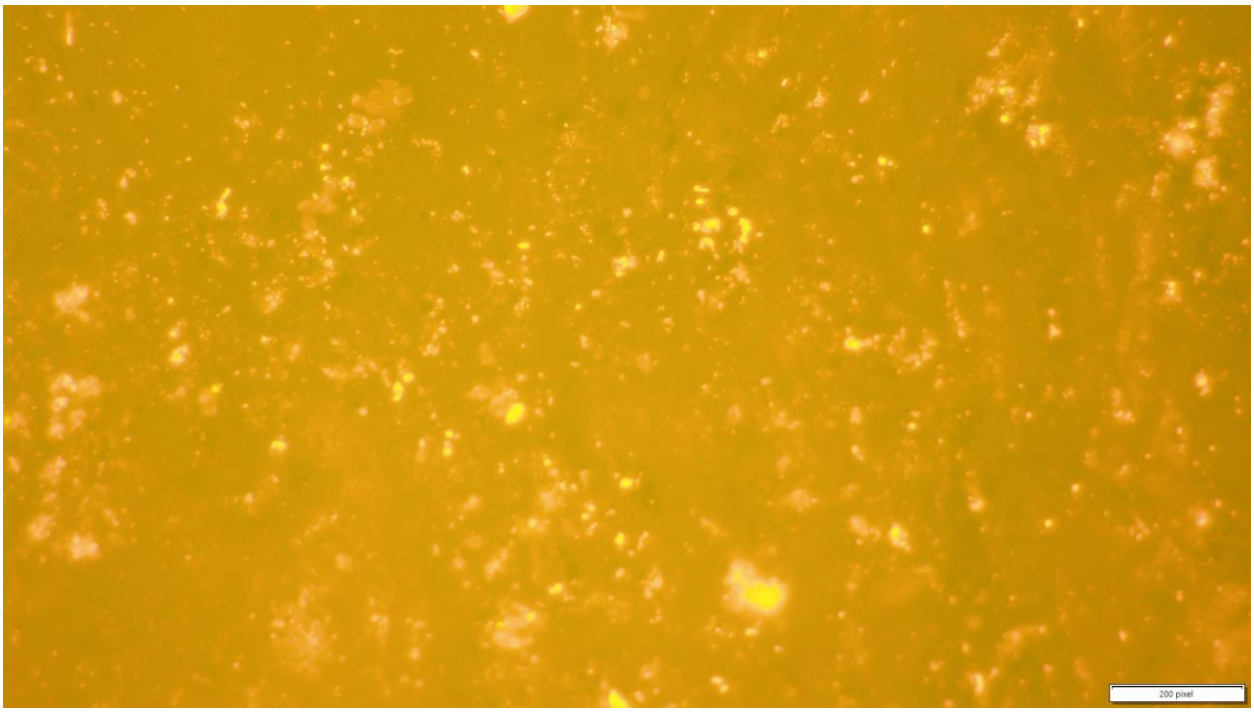

(l)

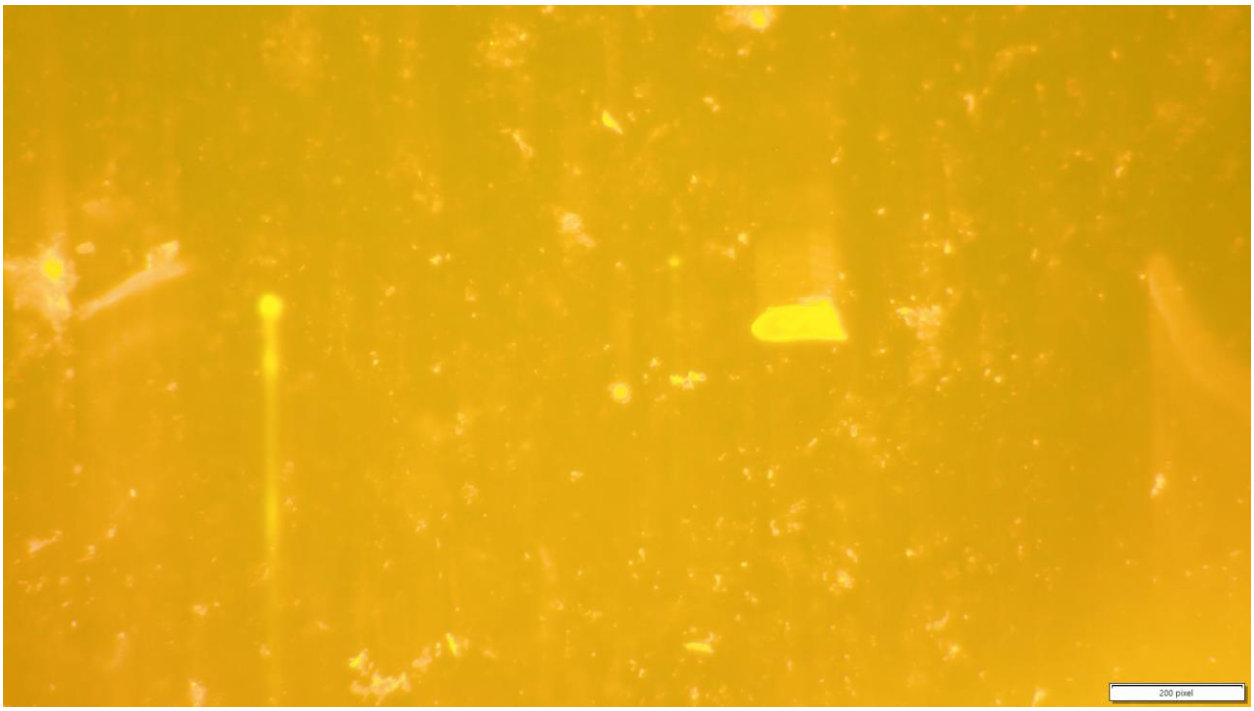

(m)

(o)

(p)

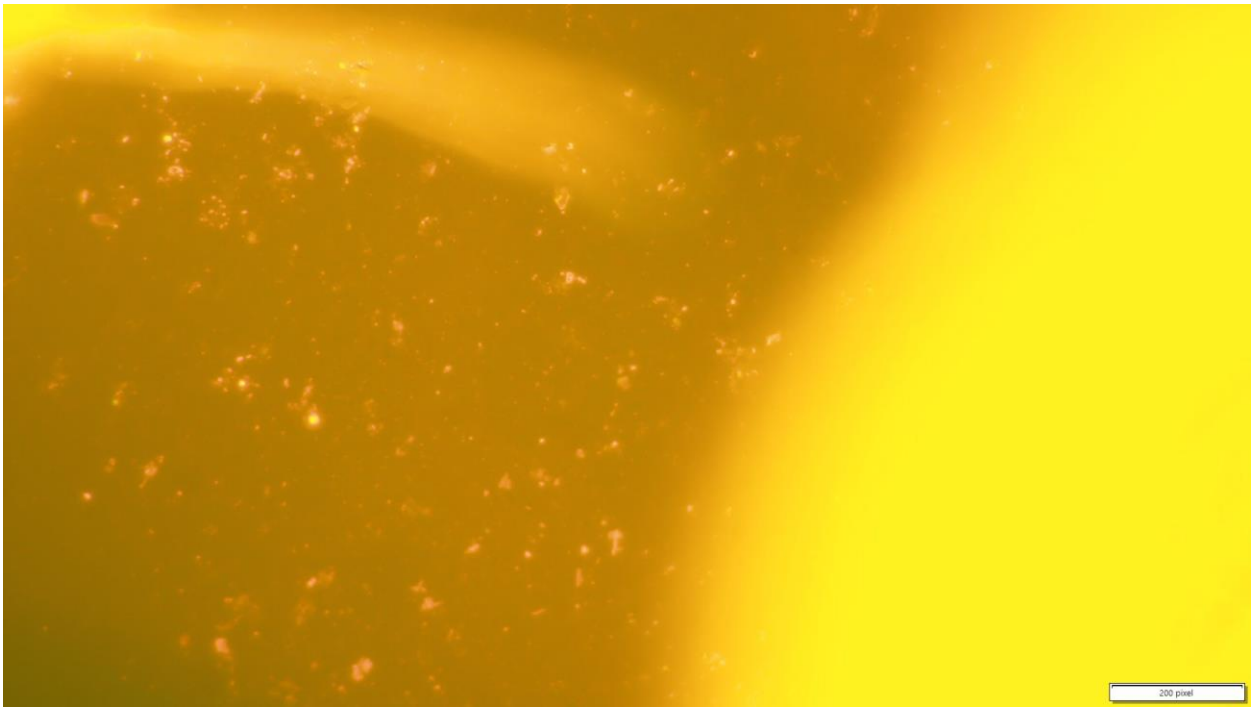

(q)

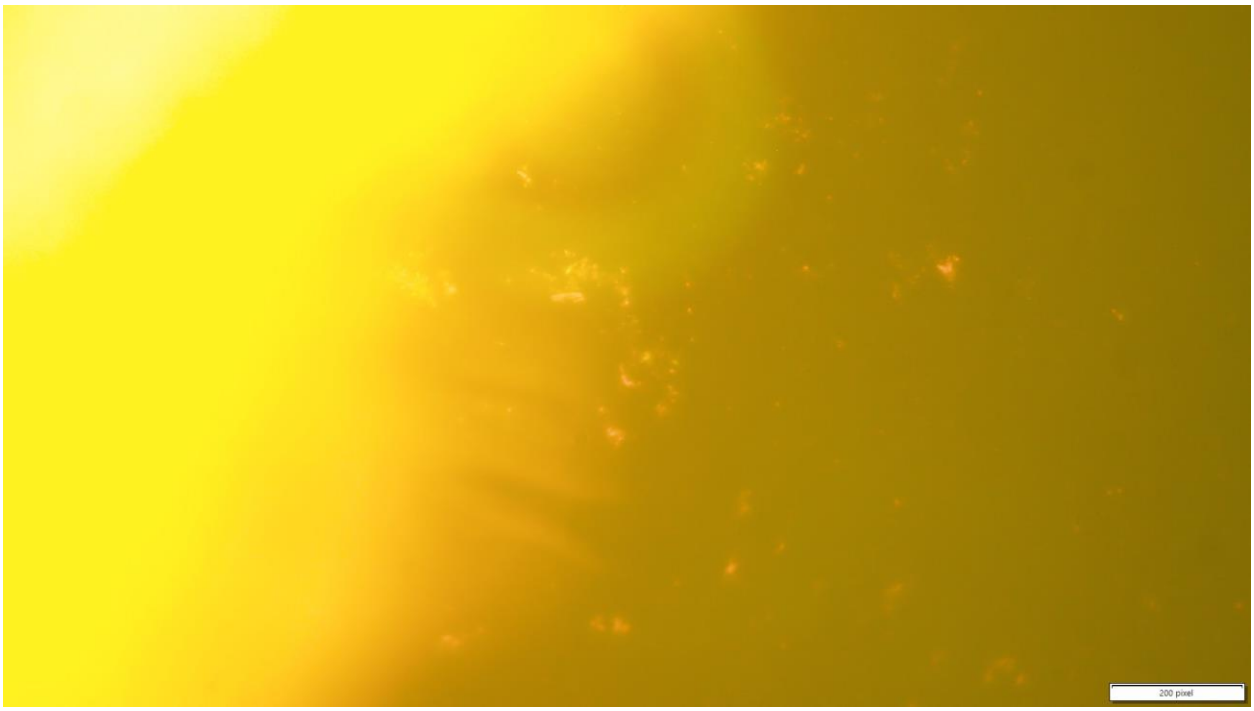

(r)

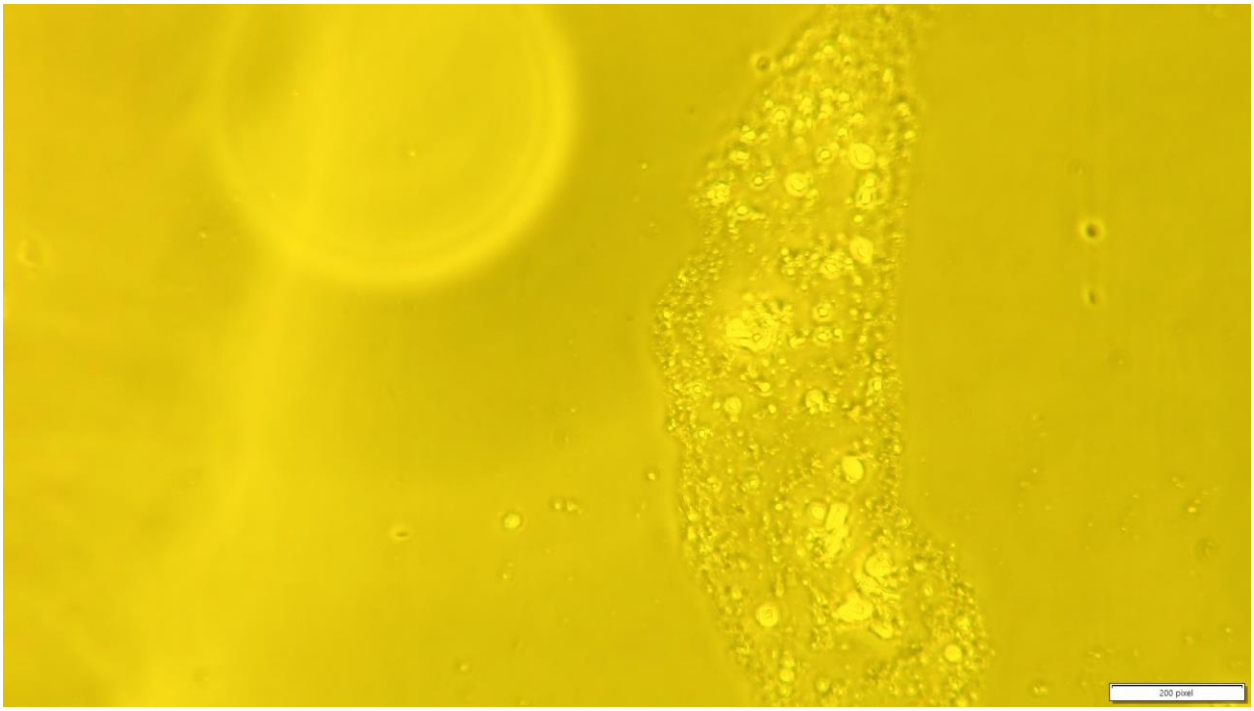

(s)

Figure A-16. *(a-r) Fluorescence images obtained from lentil seedling roots and the surrounding bacteria. (s) This picture was taken by using phase contrast microscopy combined with fluorescence illumination. The yellow glowing parts are microbial aggregations.*

Figures A-17 (a-k) are also depicting the lentil plant roots imaged using fluorscence microscopy. In this series of figures FilmTracer LIVE/DEAD Biofilm Viability Kit was used as the fluorscent dye and DAPI dilter cube was utilized for the illumination. This approach did not achieve the illumination of the bacterial cells as good as when Sypro Ruby was used. However, it can be regarded as an advantage that it did not illuminate the root structures themselves, but only a portion of the surrounding cells were illuminated as yellow dotted areas, as can be seen in the figures below. Further information of the different fluorscent dyes available for obseerving biofilms is provided in Appendix J.

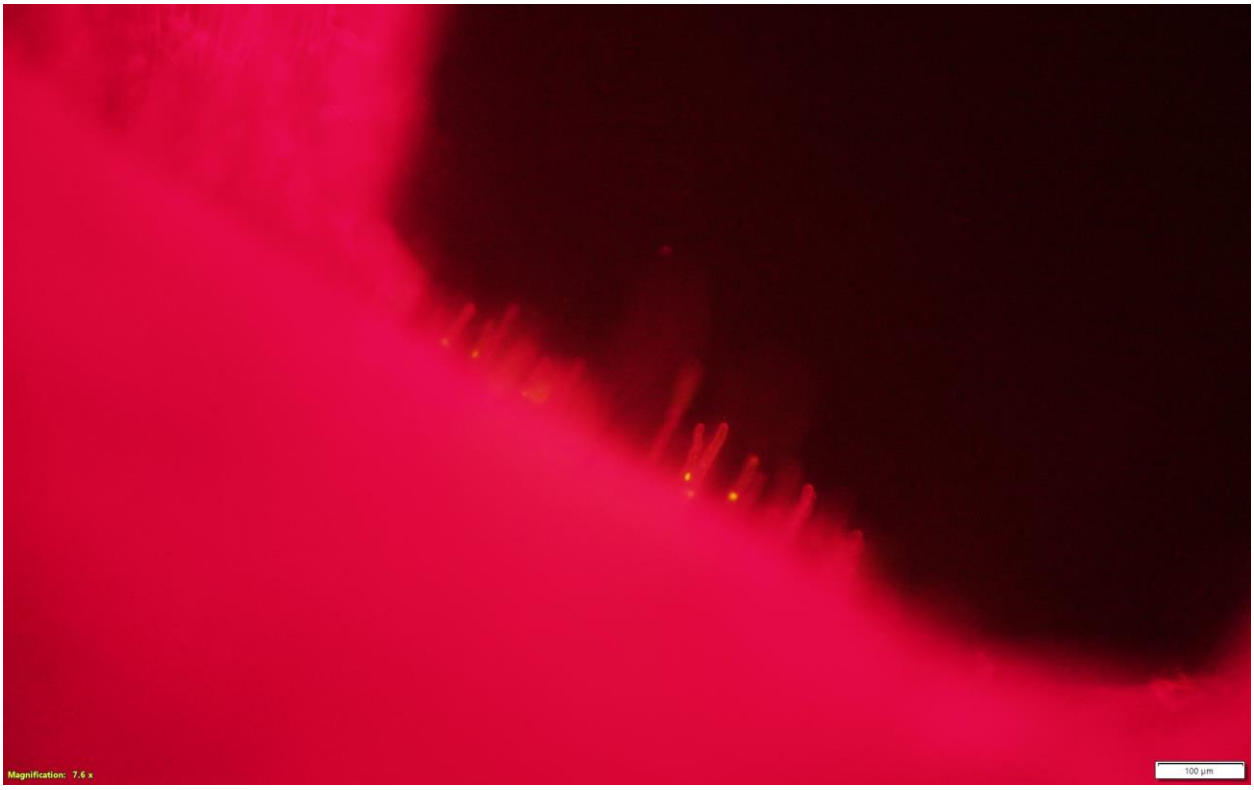

(a)

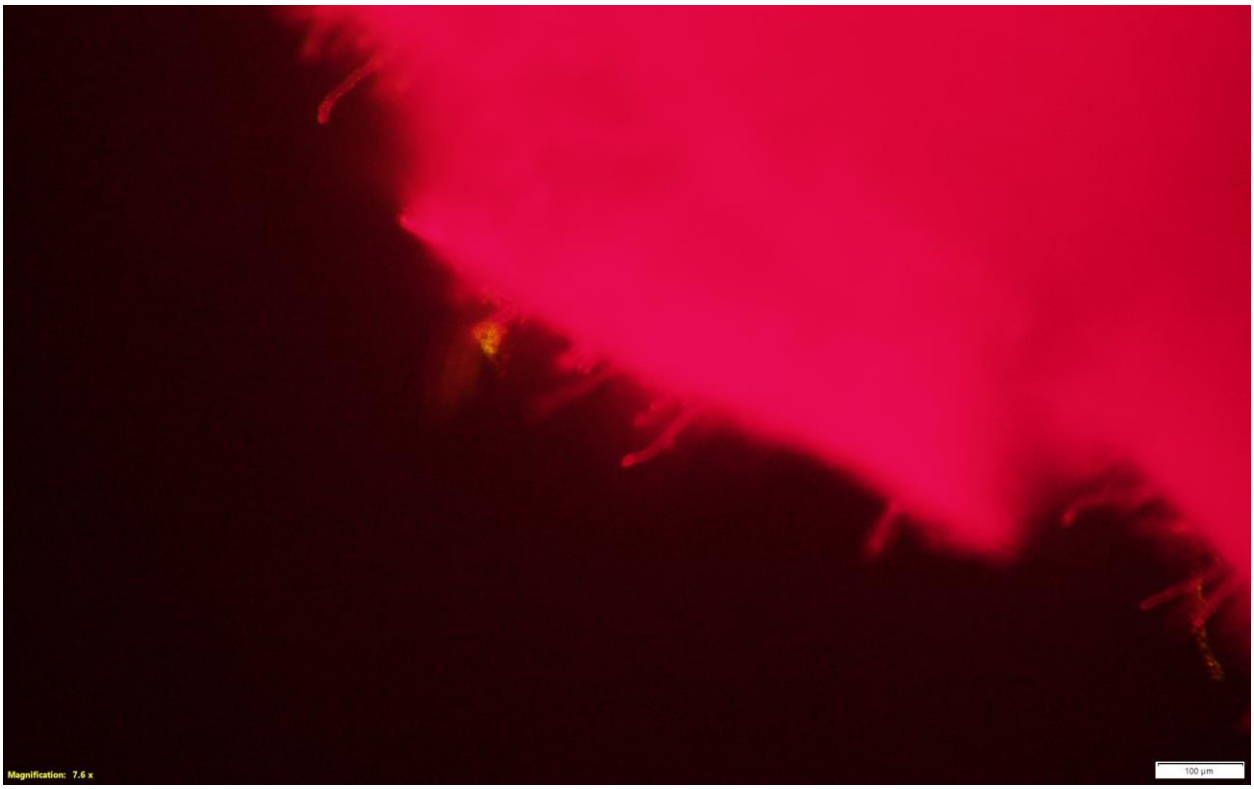

(b)

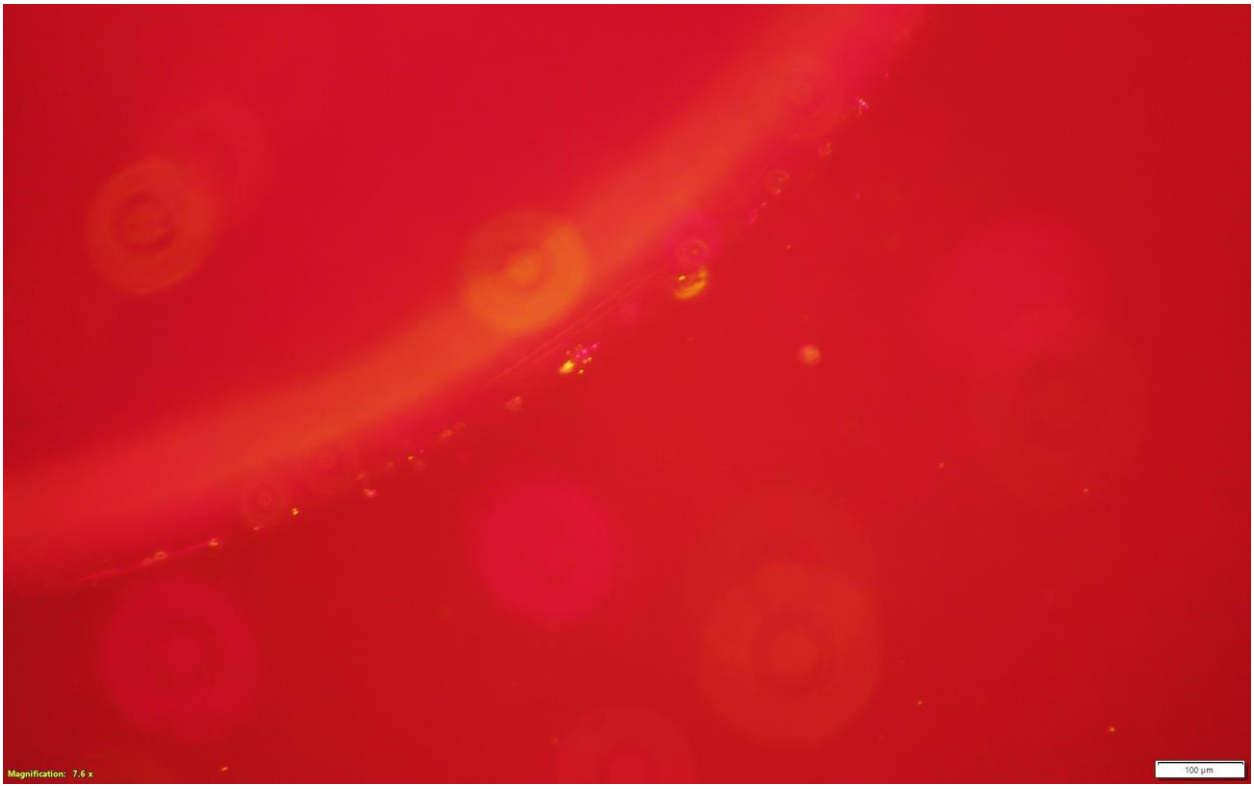

(c)

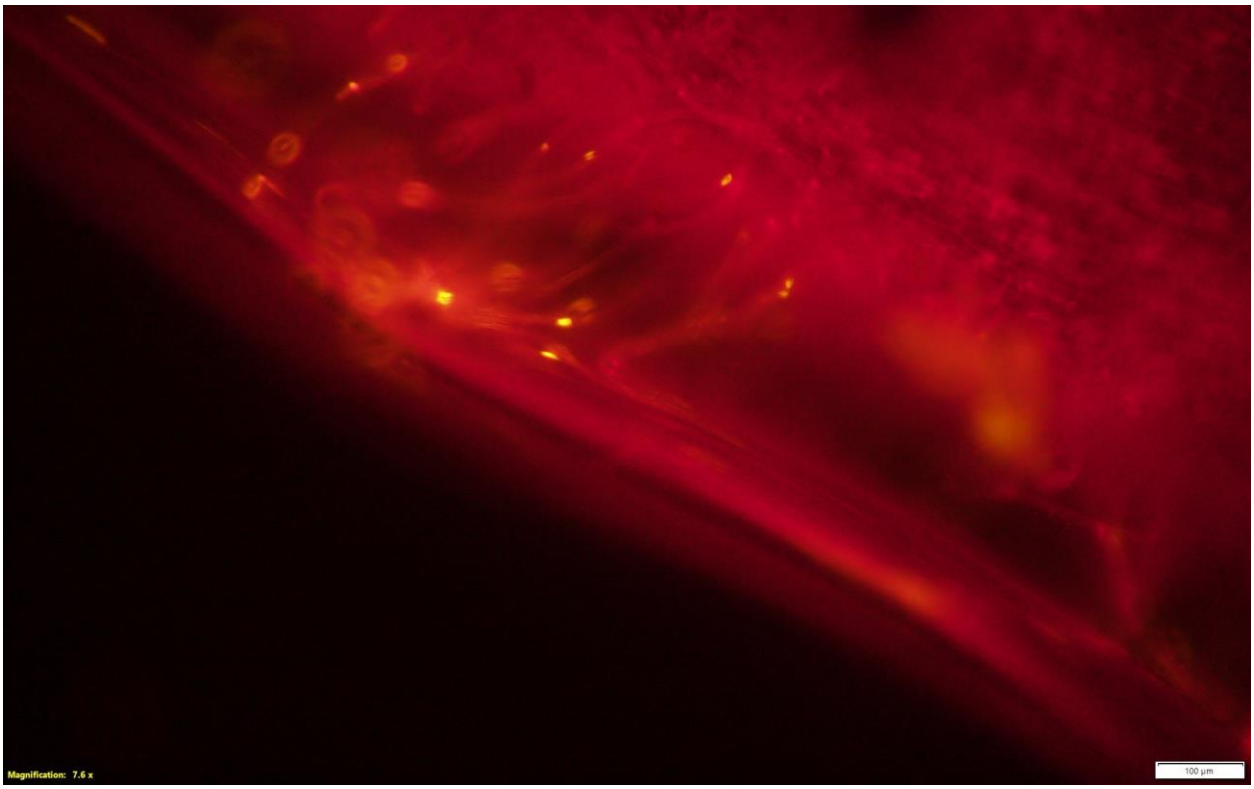

(d)

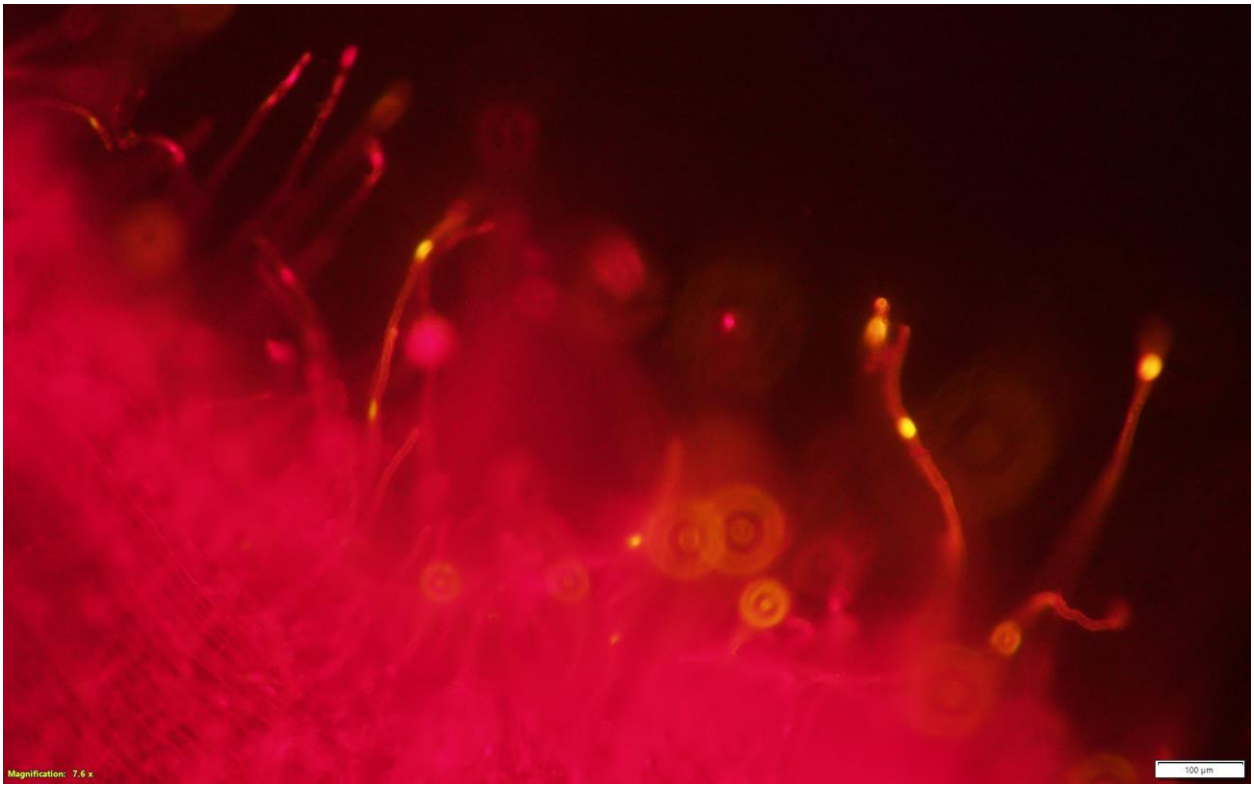

(f)

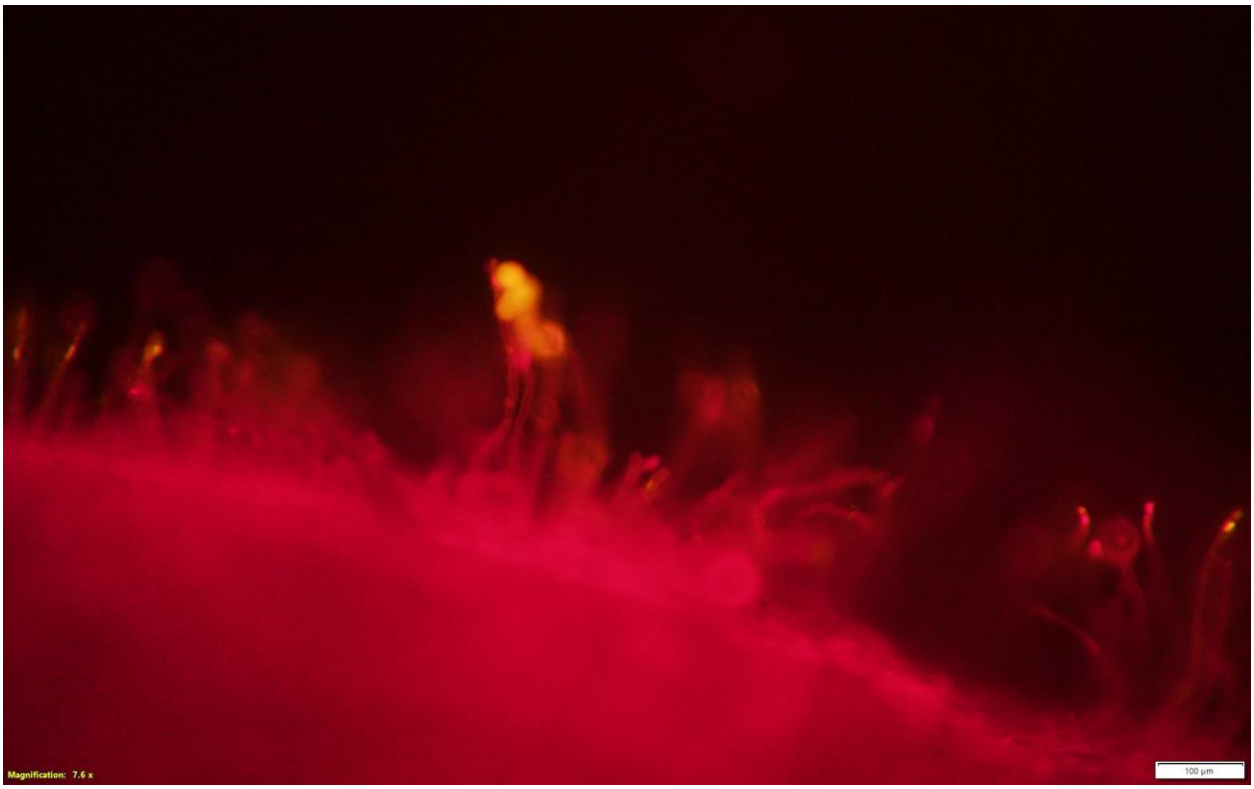

(g)

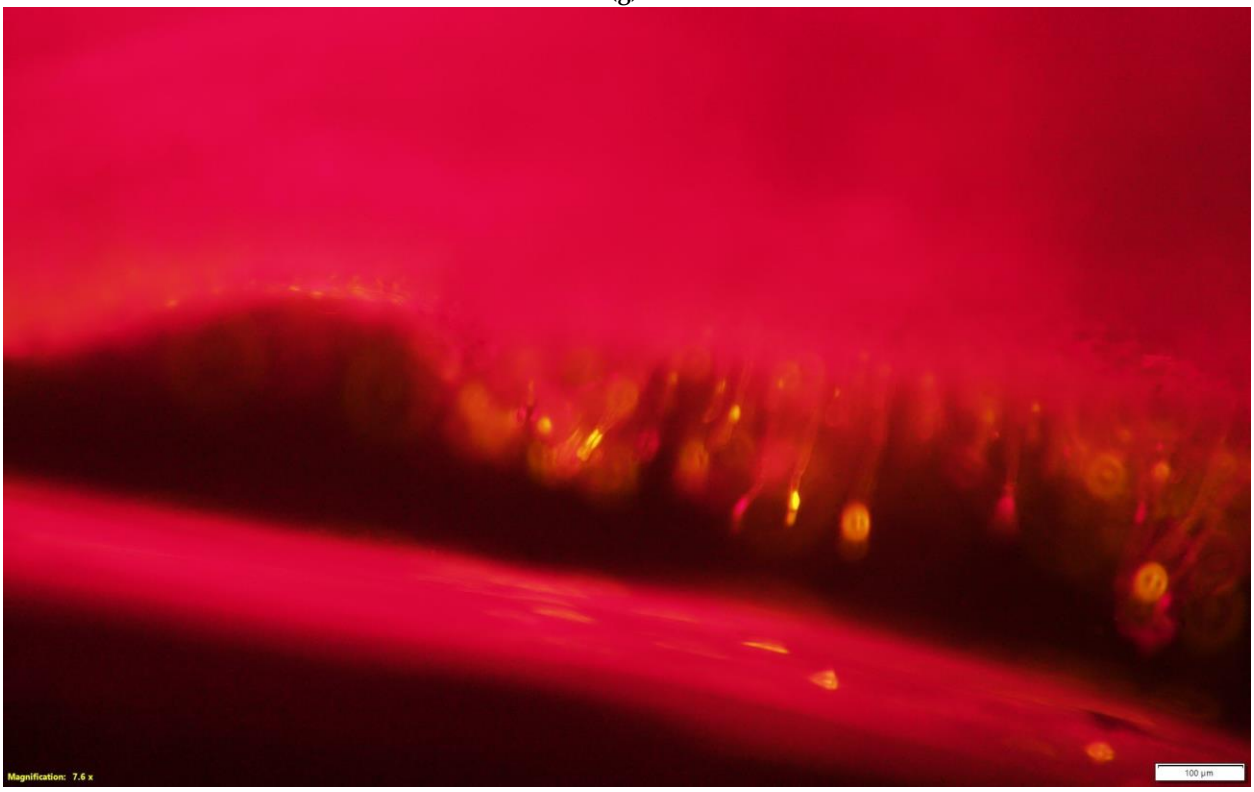

(h)

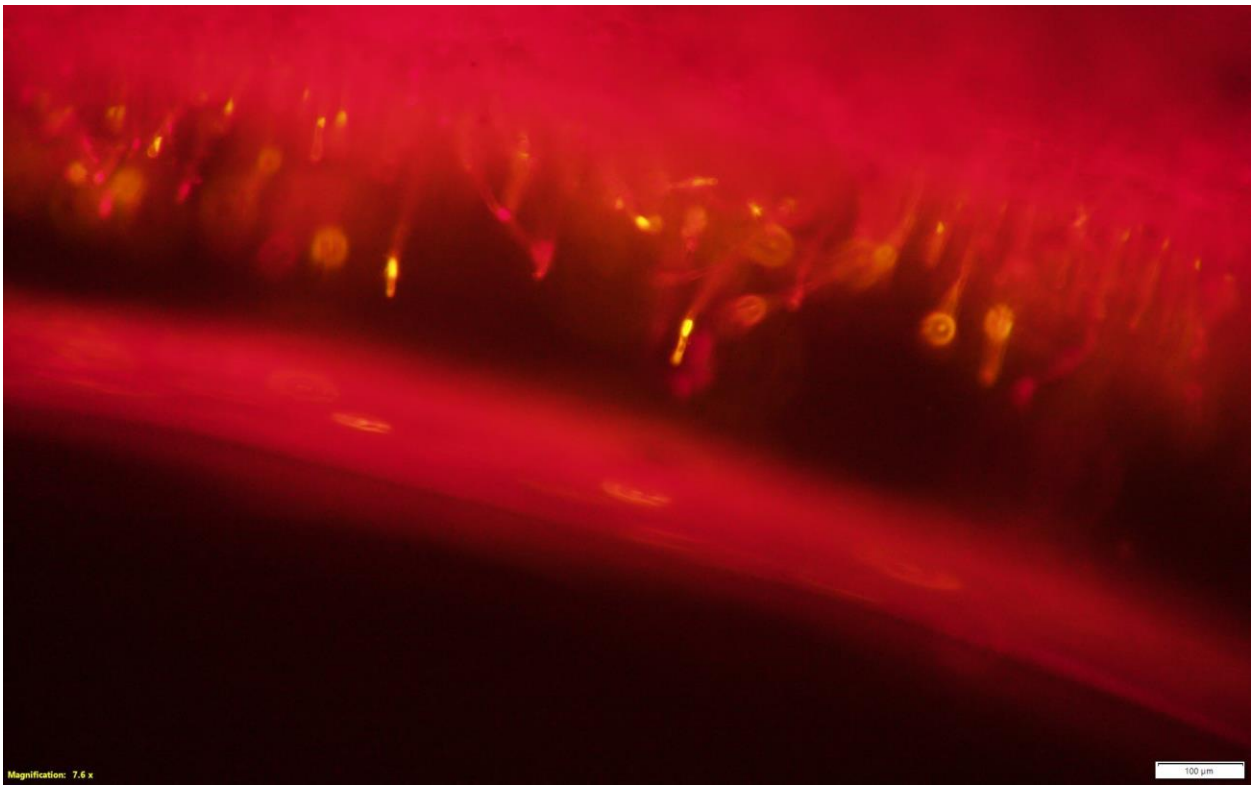

(i)

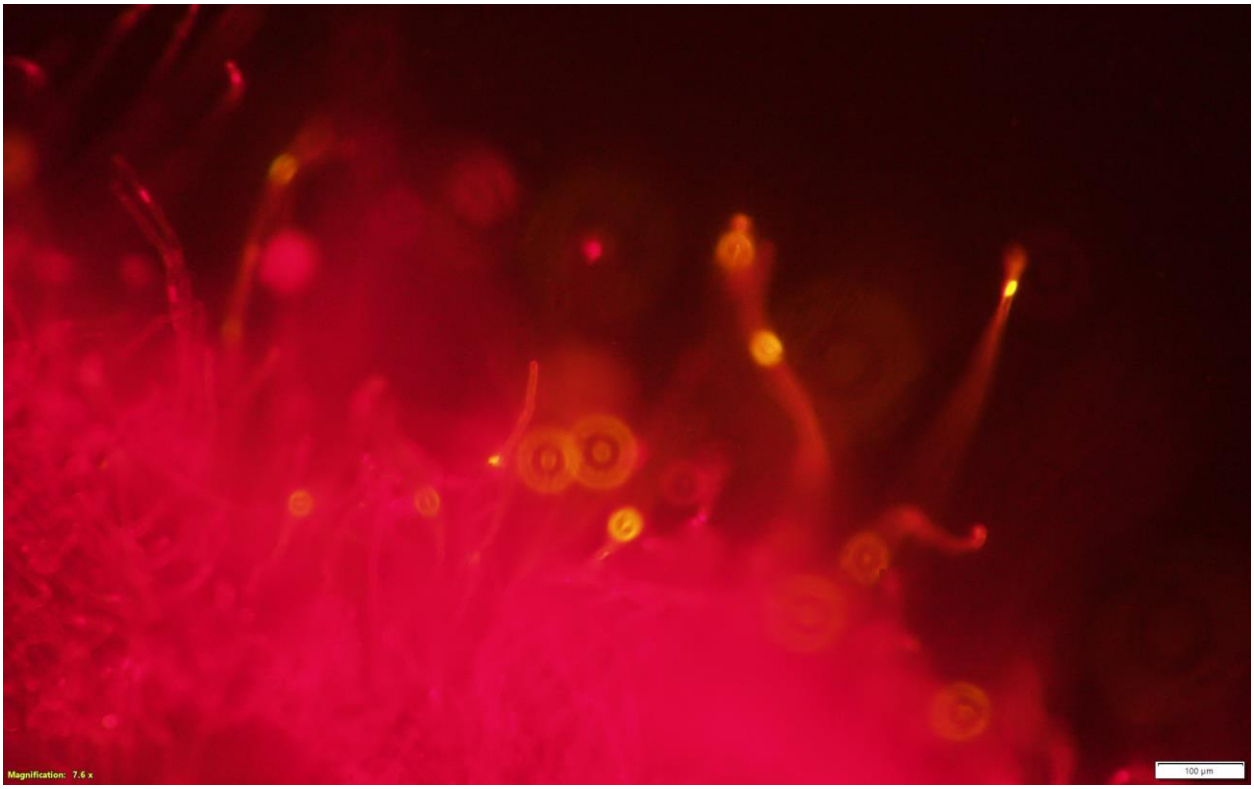

(j)

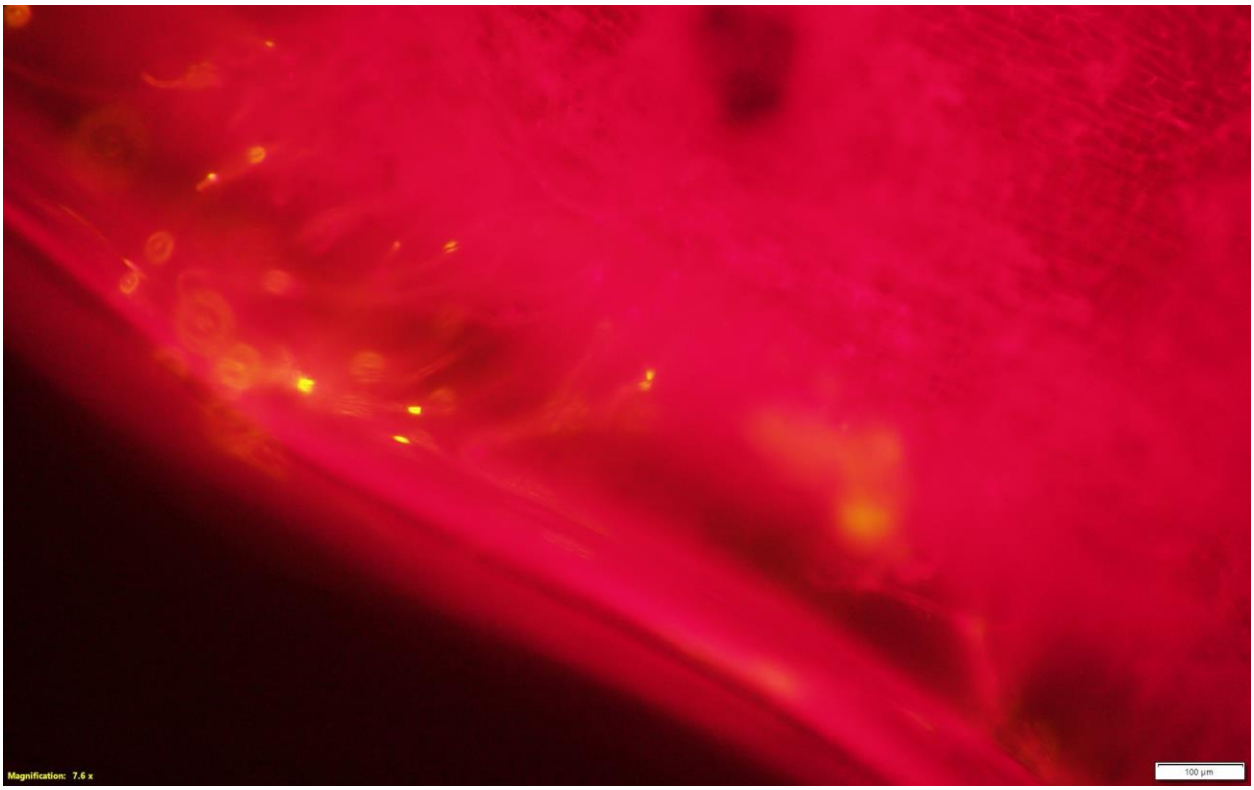

(k)

Figure A-17. *(a-k) Fluorescence images of lentil roots using FilmTracer LIVE/DEAD Biofilm Viability Kit as the fluorscent dye and DAPI dilter cube. The yellow glowing areas are the stained microbiota exisitng near the roots.*

Figure A-18 depicts an image of root surface using Sypro Ruby but DAPI filter cube. As can be seen the sample is illuminated to an extreme extent and the image obtained is not informative of bacterial formations.

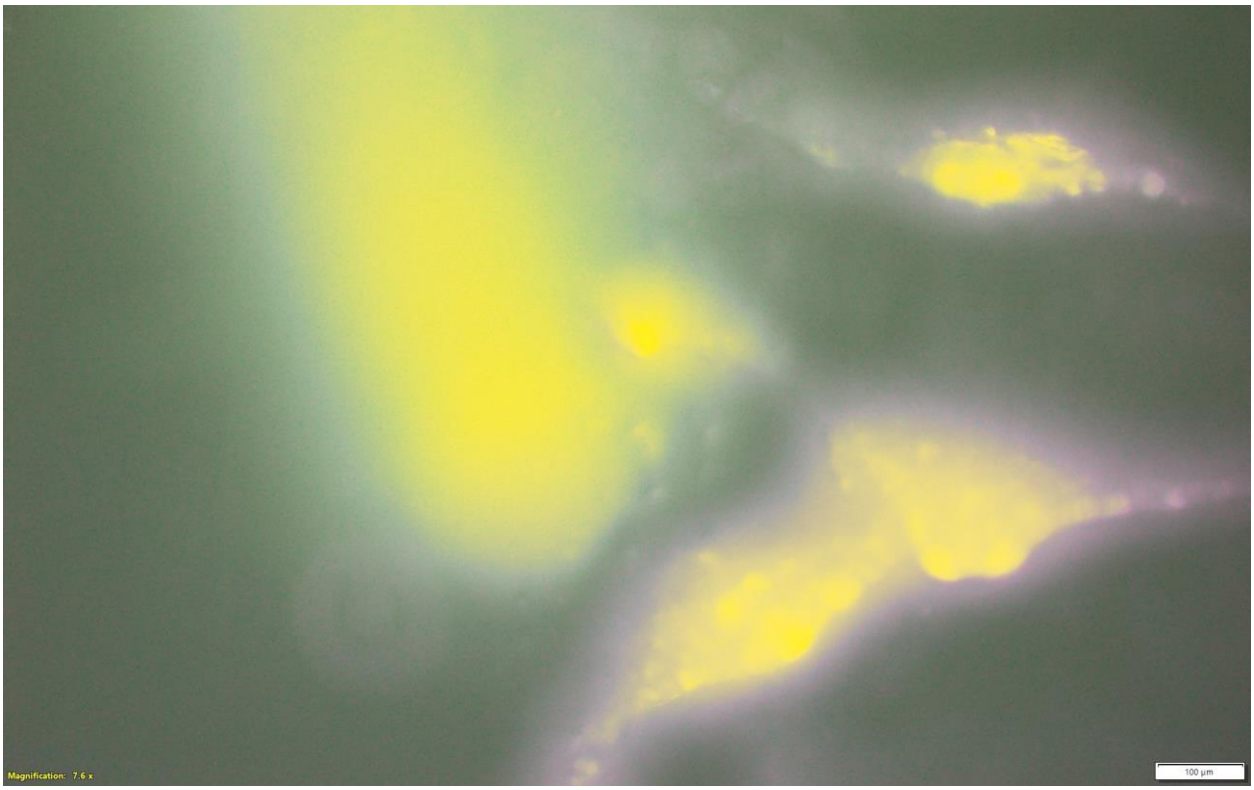

Figure A-18. *Fluorescence image of lentil plant root using Sypro Ruby dye and DAPI filter cube.*

APPENDIX B ROOT PRODUCTION AND GROWTH

As part of the experimental future experimental plan, measuring and characterizing plant roots may be important. Therefore, the production of plants could be conducted in lab-scale to allow for such studies. Legumes are easy and fast to grow, and are known to be suitable hosts for bacterial biofilm. *Rhizobium leguminosarum* for instance has been named as such because t is isolated from legumes. Unprocessed legume seeds can be purchased from nurseries and placed in petri dished filled with water for a couple of days. Then, the seeds can be transferred to solid or sand container filled with sand or soil. The container can be made out of 1/8" plexiglass sheets at the machine shop of Mechanical Engineering Department using the laser cutting machine. Figure below is a drawing of the different faces of a small and narrow soil container that was made using the same method.

As for the growth procedure, good soil, lighting, and watering of the seeds could lead to desirable results. Red/blue LED grow lights have been used to grow seeds and seemed to be effective when utilized for 12-hour on/off cycles.

The process of growing seedlings is easy:

- Place the seeds in a petri dish filled with water for two days.
- After two days transfer the seeds to the soil or sand container that is prepared.
- Leave them at the surface of the sand/soil for one day, keeping them watered, Figure B-2.
- Once the seedlings came out of the seeds' skin, top the seeds up with 0.5 to 1 inch of soil or sand, Figure B-3.
- Water everyday and keep the light source on for at least 12 hours a day.

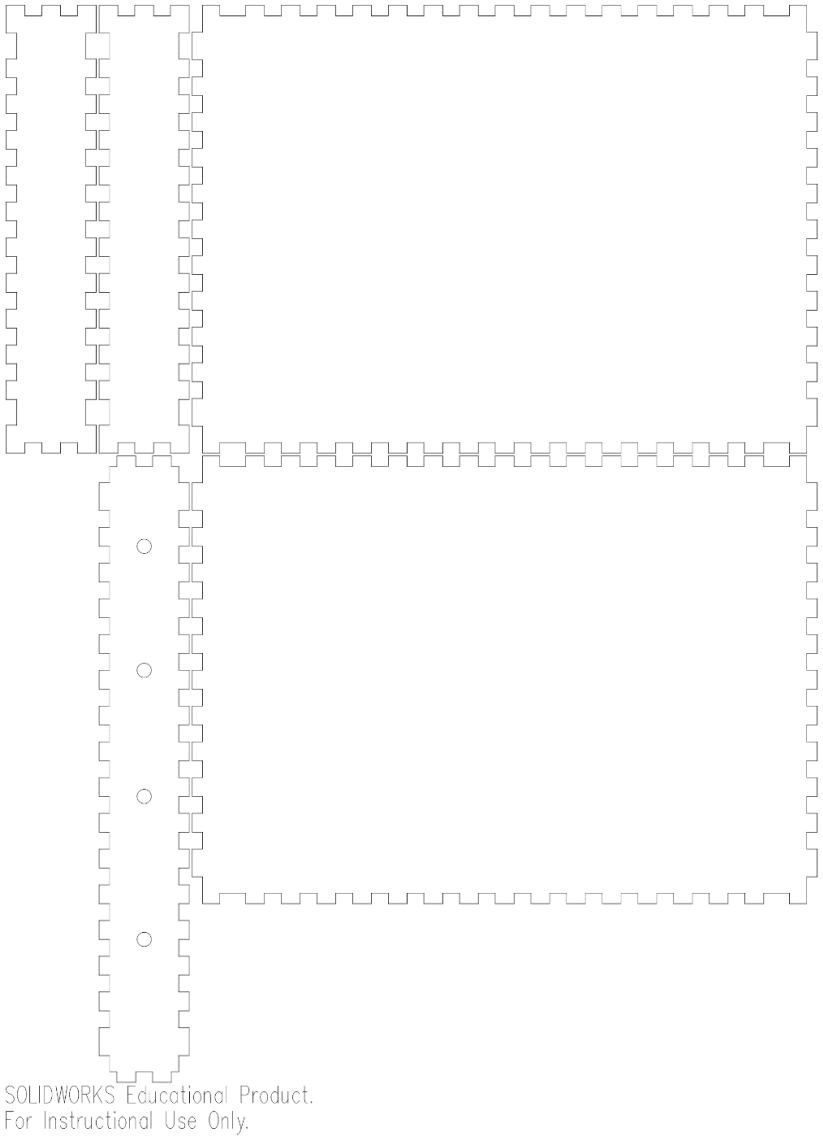

Figure B-1*. Drawing of a soil container used for growing seedlings. It is made narrow and from plexiglass to be transparent and roots could be visually observed. The holes are included for the bottom face for proper drainage. The drawing in this figure is not equal to the actual size.*

Figure B-2. *Lentil seeds being placed on sand.*

Figure B-3*. Image of lentil seedlings one week after planting the seeds.*

Figure B-4. *Well-grown lentil seedlings imaged two weeks after planting. The roots, as can be seen through the plexiglass have achieved a vast growth and are ready to be exploited and studied.*

APPENDIX C ROOT PULLOUT FOR MICROSCOPIC OBSERVATION

1. Saturate the container by pouring just enough amount of water in the container, in which the roots are grown. The water helps reducing the soil-root friction and eventually easier root pullout. If too much water is added, loss of biological sample may occur.
2. Gently take out the root nodules by making sure the root is not going to break.

Figure C-1. *Lentil roots just pulled out of sand environment. Th grains of sand are attached to the roots.*

3. Gently submerge the root in a beaker containing water
4. Shake the root for a minute until the adhered sand, dirt, and soil is removed off the surface of the root

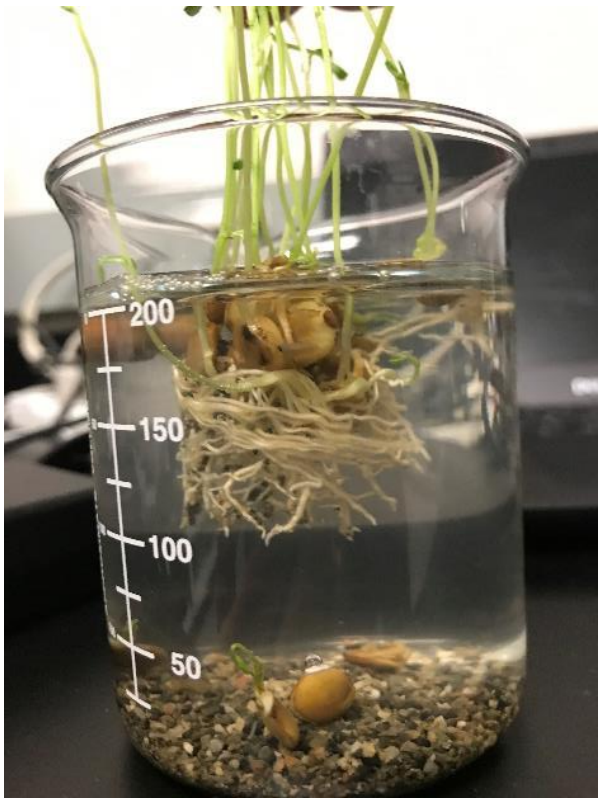

Figure C-2. *Removing the sand grains off the surface of the roots by gentle shaking in Tween 20 solution.*

Figure C-3. *Cutting a small piece from the roots for microscopy.*

5. Using a razor blade (or a microtome) cut thin layers of the plant or sever the root plants
6. Place the slices on a microscope slide
7. Conduct the staining method of interest
8. Place the cover slips on the sample and attach it to the slide using Vaseline (Petroleum Jelly)
9. The sample is ready for microscopy

For the detachment of the available rhizospheric biofilm from the roots Follow the same procedure as the Root Pullout until step 5. Place the root in Tween 20 solution, and then use gentle vortex mixing and/or low speed (~4,000 g) and for 10 minutes, some researchers suggest using sonication, but since it may cause the live bacterial cells to break open and die, this step can be skipped.

APPENDIX D COMMONLY USED FLUORESCENT DYES FOR BIOFILM OBSERVATION

Fluorescent dyes are most useful when used with the suitable filter cube. There are currently two fluorescence filter cubes available in the laboratory. One is a FITC (or B) that has an excitation range of 450-480 nm and an emission range of wavelengths of over 515 nm. The second one is a DAPI filter cube that provides an excitation range of 360-390 nm and an emission range of 435-485 nm. Therefore, using these filter cubes, a wide range of wavelengths can be covered, and the commonly available dyes should work. The table below introduces the commonly used fluorescent dyes for environmental biofilm monitoring:

Table D. *List of popular fluorescent dyes used for microbial studies.*

Fluorescent dye name	Excitation/Emission (nm)
SYTO 9 Green Fluorescent Nucleic Acid Stain	485/500
FilmTracer SYPRO Ruby Biofilm Matrix Stain	450/610
DAPI (4′,6-diamidino-2-phenylindole)	350/470
SYTO 13 Green Fluorescent Nucleic Acid Stain	488/509
LIVE/DEAD™ BacLight™ Bacterial Viability Kit (Includes (a) SYTO 9 and (b) Propidium Iodide)	a: 480/500 b: 490/635
Green Fluorescent Protein (GFP)	460/510
Fluorescein (FITC)	490/525
Calcofluor white	440/500-520
FM 1-43 Dye (N-(3-Triethylammoniumpropyl)-4-(4-(Dibutylamino) Styryl) Pyridinium Dibromide)	479/598

APPENDIX E BACTERIAL SOLUTION PREPARATION

In this section, the inoculation of bacterial cells in liquid growth media using isolated cells streaked on agar plates, such that of Figure E-1 is reviewed.

Figure E-1. *Streaked pseudomonas putida cells on solid agar medium. Grown and ready to be transferred to liquid medium.*

- Prepare the LB broth solution and sterilize at 121°C for at least 15 minutes. LB broth comes in two different forms, powder and liquid. The advantage of using the powder over the liquid is that it can be made fresh before every usage and does not require cold temperatures for storage, while the liquid broth needs to be stored in the fridge after opening the bottle.
- Turn on the Bunsen burner and sterilize the smear loop on top of the flame until red color can be observed on the loop. Let the inoculation loop cool down.
- Open the petri-dish containing the bacterial colonies. Gently take some of the bacterial cells from the surface of the agar.

- Transfer to the beaker containing the growth media (e.g. LB broth) and stir for one minute.
- Cover the beaker or transfer to a lidded container.
- Place in the incubator and set to desired temperature.
- Depending on the bacteria, allow one or two days for the growth. This amount of time is enough for the bacterial cells to reproduce and saturate the media.

LB broth is a clear and pale yellow solution when has few to no amounts of bacteria, but will become cloudy as it reaches a stationary phase in the growth of bacterial cells, as imaged in Figures E-2.

Figure E-2*. Picture on the left-hand side shows clear LB broth with the bacterial cells that are just transferred to the container. Bacterial pellets can be seen at the bottom of the glass. Picture on the right-hand side shows the same growth media after one day of incubation, cloudy and saturated of bacteria.*

APPENDIX F COMPUTER CODES USED FOR INTEGRATION AND AUTOMATION OF TESTING INSTRUMENTS

F.1 C++ code for the switching of 8 channels

The program ran on the nRF52 kit (in SEGGER Embedded Studio):

```
/** @brief Function for testing UART loop back.
 *  @details Transmitts one character at a time to check if the data received
from the loopback is same as the transmitted data.
 *  @note  @ref TX_PIN_NUMBER must be connected to @ref RX_PIN_NUMBER)
 */
static void uart_loopback_test()
{
    uint8_t * tx_data = (uint8_t *)("\r\nLOOPBACK_TEST\r\n");
    uint8_t   rx_data;

    // Start sending one byte and see if you get the same
    for (uint32_t i = 0; i < MAX_TEST_DATA_BYTES; i++)
    {
        uint32_t err_code;
        while (app_uart_put(tx_data[i]) != NRF_SUCCESS);

        nrf_delay_ms(10);
        err_code = app_uart_get(&rx_data);

        if ((rx_data != tx_data[i]) || (err_code != NRF_SUCCESS))
        {
            show_error();
        }
    }
    return;
}
#else
/* When UART is used for communication with the host do not use flow
control.*/
#define UART_HWFC APP_UART_FLOW_CONTROL_DISABLED
#endif


/**
 * @brief Function for main application entry.
 */
int main(void)
{
    uint32_t err_code;
    bsp_board_init(BSP_INIT_LEDS);
    nrf_gpio_cfg_output( 22 );
    nrf_gpio_cfg_output( 23 );
    nrf_gpio_cfg_output( 24 );
    nrf_gpio_cfg_output( 25 );
```

```
    const app_uart_comm_params_t comm_params =
      {
          RX_PIN_NUMBER,
          TX_PIN_NUMBER,
          RTS_PIN_NUMBER,
          CTS_PIN_NUMBER,
          UART_HWFC,
          false,
#if defined (UART_PRESENT)
          NRF_UART_BAUDRATE_115200
#else
          NRF_UARTE_BAUDRATE_115200
#endif
      };

    APP_UART_FIFO_INIT(&comm_params,
                       UART_RX_BUF_SIZE,
                       UART_TX_BUF_SIZE,
                       uart_error_handle,
                       APP_IRQ_PRIORITY_LOWEST,
                       err_code);

    APP_ERROR_CHECK(err_code);

#ifndef ENABLE_LOOPBACK_TEST
    printf("\r\nUART example started.\r\n");
  #define PIN17 17
  #define PIN18 18
  #define PIN19 19
  #define PIN20 20
    while (true)
    {
        uint8_t cr;
        while (app_uart_get(&cr) != NRF_SUCCESS);
        while (app_uart_put(cr) != NRF_SUCCESS);
        if (cr >= '0' || cr <= '7')
        {
          cr -= 0x30;
          writeGpioOuts17to20( cr );
          printf("\r\nOK\r\n");
        }
        if (cr == 'q' || cr == 'Q')
        {
            printf(" \r\nExit!\r\n");

            while (true)
            {
                // Do nothing.
            }
        }
    }
#else

    // This part of the example is just for testing the loopback .
    while (true)
    {
```

```
        uart_loopback_test();
    }
#endif
}

static void writeGpioOuts17to20( uint8_t i )
{
  if( i > 15 )
  {
    return;
  }

  for( uint8_t j=0; j<4; j++)
  {

    if( ( i % 2) != 0 )
    {
      nrf_gpio_pin_clear(17+j);
      nrf_gpio_pin_set(22+j);
    }
    else
    {
      nrf_gpio_pin_set(17+j);
      nrf_gpio_pin_clear(22+j);
    }
    i = i/2;
   }
}

/** @} */
```

F.2 Master code used for the operation of the impedance measurements (in Python):

```
#Sweep measurement

import visa
from time import sleep
import csv
import time
from string import maketrans
import string
import sys

import serial

def SwitchMuxChannel( sPort, channelNumber ):
    if( channelNumber > 7 ):
        print "Ch out of range"
    try:
        sPort.write(str(channelNumber))
    except KeyboardInterrupt:
        "keyboard interrupt, closing ser port"
        sPort.close()
```

```
    except SystemExit:
        "system exit, closing ser port"
        sPort.close()
    except:
        "Unexpected error:", sys.exc_info()[0]
        "close and reopen serial port, retry SwitchMuxChannel"
    raise
        sPort.close()
        time.sleep(1)
        sPort.open()
        SwitchMuxChannel( sPort, channelNumber )

ser = serial.Serial('COM4', baudrate=115200)  # open serial port


rm = visa.ResourceManager()
rm.list_resources()
('USB0::0x2A8D::0x2F01::MY54306069::0::INSTR')
LCRM = rm.open_resource('USB0::0x2A8D::0x2F01::MY54306069::0::INSTR')
print LCRM.query("*IDN?")
sleep(3)
LCRM.write("*rst; *cls")
LCRM.write(":APERture LONG,1")

#print LCRM.query(":VOLTage[:LEVel]?")
print LCRM.query("*TST?")

LCRM.write(":Frequency:CW 20")
#print LCRM.query("*Frequency:CW?")
LCRM.write(':VOLTage:LEVel 0.1')
LCRM.write('Frequency:CW?')
print(LCRM.read())

LCRM.write(":CORRection:LENGth 1")

myfile = open("Test 13_Dec 25.csv", 'wb')
wr = csv.writer(myfile, delimiter=',',quoting=csv.QUOTE_NONE,
escapechar="\\")
myfile.write("StartTS,Freq,Ch0R,Ch0X,Ch1R,Ch1X,Ch2R,Ch2X,Ch3R,Ch3X,Ch4R,Ch4X,
Ch5R,Ch5X,Ch6R,Ch6X,Ch7R,Ch7X,EndTS\n")

List1 =
[20,100,250,500,1000,2500,5000,10000,25000,50000,75000,100000,200000,300000]
while True:
    try:
        for frq in List1:
            LCRM.write("Frequency:CW "+     str(frq))
            for chNum in range(8):

                SwitchMuxChannel( ser, chNum )
                LCRM.write("INIT")
                sleep (2)
                LCRM.write("TRGger:Imm")
                sleep (2)
                impedance = LCRM.query("Fetch:Impedance:Corrected?")
                print "freq="+str(frq)+"ch"+str(chNum)+"impedance = " +
str(impedance)
```

```
            if (chNum == 0):
                myfile.write(str(time.time())+","+str(frq)+",")

            impedance = str(impedance)
            tbl = string.maketrans('\n' , ',')
            impedance = impedance.translate(tbl)

            myfile.write(str(impedance))

            if (chNum == 7):
                myfile.write(str(time.time())+"\n")
            sleep (2)
    #delay for next set of measuements
    time.sleep(60)
except (KeyboardInterrupt, SystemExit):
    myfile.close()
```